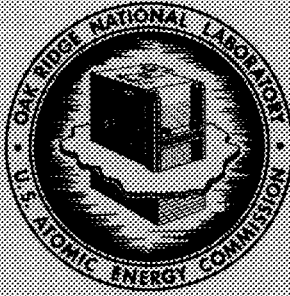




3 4456 0513992 6



# OAK RIDGE NATIONAL LABORATORY

operated by

UNION CARBIDE CORPORATION

for the

U. S. ATOMIC ENERGY COMMISSION



ORNL - TM - 2748

## LMFBR FUEL CYCLE STUDIES

PROGRESS REPORT FOR SEPTEMBER, NO. 7

OAK RIDGE NATIONAL LABORATORY  
CENTRAL RESEARCH LIBRARY  
DOCUMENT COLLECTION

### LIBRARY LOAN COPY

DO NOT TRANSFER TO ANOTHER PERSON

If you wish someone else to see this document, send in name with document and the library will arrange a loan.

**NOTICE** This document contains information of a preliminary nature and was prepared primarily for internal use at the Oak Ridge National Laboratory. It is subject to revision or correction and therefore does not represent a final report.

#### LEGAL NOTICE

This report was prepared as an account of Government sponsored work. Neither the United States, nor the Commission, nor any person acting on behalf of the Commission:

- A. Makes any warranty or representation, expressed or implied, with respect to the accuracy, completeness, or usefulness of the information contained in this report, or that the use of any information, apparatus, method, or process disclosed in this report may not infringe privately owned rights; or
- B. Assumes any liabilities with respect to the use of, or for damages resulting from the use of any information, apparatus, method, or process disclosed in this report.

As used in the above, "person acting on behalf of the Commission" includes any employee or contractor of the Commission, or employee of such contractor, to the extent that such employee or contractor of the Commission, or employee of such contractor prepares, disseminates, or provides access to, any information pursuant to his employment or contract with the Commission, or his employment with such contractor.



3 4456 0513992 6

ORNL-TM-2748

Contract No. W-7405-eng-26

CHEMICAL TECHNOLOGY DIVISION  
METALS AND CERAMICS DIVISIONLMFBR FUEL CYCLE STUDIES PROGRESS REPORT FOR SEPTEMBER, NO. 7

## I. AQUEOUS FUEL REPROCESSING

W. E. Unger, R. E. Blanco, D. J. Crouse, A. R. Irvine, C. D. Watson

## II. FUEL MATERIAL PREPARATION

R. G. Wymer, R. E. Brooksbank, R. E. Leuze, J. P. McBride  
W. D. Bond, P. A. Haas

## III. FUEL FABRICATION AND EVALUATION

A. L. Lotts, C. M. Cox, J. D. Sease, T. N. Washburn

NOVEMBER 1969

OAK RIDGE NATIONAL LABORATORY  
Oak Ridge, Tennessee  
operated by  
UNION CARBIDE CORPORATION  
for the  
U. S. ATOMIC ENERGY COMMISSION

Note: Previous issues of this report are identified as:

1. ORNL-TM-2552
2. ORNL-TM-2585
3. ORNL-TM-2624
4. ORNL-TM-2650
5. ORNL-TM-2671
6. ORNL-TM-2710

## CONTENTS

	<u>Page</u>
ABSTRACT . . . . .	1
HIGHLIGHTS . . . . .	1
I. AQUEOUS FUEL REPROCESSING	
1. Shipping (Task 1).. . . . .	4
2. Receiving and Storage (Task 2) . . . . .	13
3. Head-End Processing of LMFBR Fuels (Task 3) . . . . .	17
4. Volatile Fission Product Removal (Task 4) . . . . .	25
5. Dissolving (Task 5) . . . . .	26
6. Feed Preparation (Task 6) . . . . .	27
7. Solvent Extraction (Task 7) . . . . .	28
8. Plutonium Purification (Task 8) . . . . .	35
9. Waste Treatment and Storage (Task 9) . . . . .	35
10. Off-Gas Treatment (Task 10) . . . . .	35
11. Radiation and Shielding (Task 11) . . . . .	45
12. Criticality (Task 12) . . . . .	48
13. Engineering Studies (Task 13) . . . . .	51
II. FUEL MATERIAL PREPARATION	
1. Conversion Studies . . . . .	52
2. Sol-Gel Processes for Preparation of LMFBR Recycle Fuel. . . . .	61
III. FUEL FABRICATION AND EVALUATION	
1. Fabrication Development . . . . .	74
2. Fuel Evaluation . . . . .	78



LMFBR FUEL CYCLE STUDIES PROGRESS REPORT FOR SEPTEMBER, NO. 7

## ABSTRACT

This report continues a series outlining progress in the development of methods for the reprocessing and fabrication of LMFBR fuels. Development work is reported on problems of irradiated fuel transport to the processing facility, the dissolution of the fuel and the chemical recovery of the  $\text{PuO}_2$ - $\text{UO}_2$  values, the containment of volatile fission products, product purification, preparation of fuel material by the sol-gel process, conversion of fuel processing plant product nitrate solutions to solids suitable for shipping and for fuel fabrication, fuel fabrication of sol-gel materials, and fuel evaluation studies, both in-pile and out-of-pile. Pertinent experimental results are presented for the information of those immediately concerned with the field. Detailed description of experimental work and data are included in topical reports and in the Chemical Technology Division and Metals and Ceramics Division Annual Reports.

---

HIGHLIGHTS

## Division I

A simulated one-sixth-scale steel cask dropped from a height of 30 ft onto an unyielding surface exhibited only superficial damage. Seal leak rate changed from below the level of detection ( $4 \times 10^{-10}$  cc of helium per second) to  $2 \times 10^{-9}$  cc of helium per second at one atmosphere differential pressure. Other simulated cask models ranging to 1/37 scale exhibited roughly proportional damage. A 30 ft drop test with a one-eighth-scale model cask demonstrated that even superficial damage to a cask can be prevented by providing local energy absorbers (cushions) made up of relatively large diameter tubes filled with small diameter tubes. (Sects. 1.3 and 1.4)

Study was begun of the stability of secondary amines which are potentially useful plutonium extractants. It was shown that di(tridecyl)amine is relatively stable in contact with 7 M  $\text{HNO}_3$  but decomposes rapidly if nitrous acid is present in the nitric acid solution. (Sect. 7.2)

In a recent TRU processing campaign in which the irradiated targets were dissolved in nitric acid, about 98% of the iodine was removed from the dissolver solution by air sparging. Decontamination

factors for removing iodine from the off-gas in a test system consisting of two liquid scrubbers in series followed by a Hopcalite bed--charcoal bed system ranged from  $1 \times 10^5$  to  $4 \times 10^5$  for three runs. (Sect. 10.1)

Elemental iodine absorption in mercuric nitrate solution results in disproportionation of the iodine to the iodide and iodate forms. (Sect. 10.1)

## Division II

Uranium-plutonium carbides and carbonitrides have been successfully prepared using methods developed in the course of sol-gel process development. Both microspheres and shards have been prepared. X-ray analyses of both carbides and carbonitrides indicate a product free of oxides, sesquicarbides and dicarbides. Oxygen impurities range from 2000 to 6000 ppm. (Sect. 1.3.1)

Recent experiments on the preparation of CUSP sol have shown that a glass column packed with 1/4-in Berl saddles produces a sol of the same high quality as that prepared by the multiple stage stirred column previously used. The packed column has the advantage of having no moving parts and lending itself more readily to remote operation. (Sect. 2.1)

Over 60 microsphere forming tests with CUSP sol have delineated satisfactory sphere forming conditions with a variety of sphere forming alcohol compositions. An important observation is that a small amount of oxidation caused either by dissolved oxygen in the alcohol or by subsequent exposure of gelled microspheres to air has a very deleterious effect on the fired product. (Sect. 2.3)

## Division III

Fuel rods consisting of two 3-in.-long fueled annuli clad in 3/8-in. OD titanium-modified type 304 stainless steel with a 1/8-in.-diam central thermocouple well of W-25% Re were fabricated for use in the instrumented capsule series in the Oak Ridge Research Reactor (ORR). The fuel pins contained sol-gel microspheres and pellets for comparative study of their thermal behavior. (Sect. 1.2.2)

The thermodynamic studies which are concerned with the distribution of oxygen in the fission products have indicated that  $\text{Pu}^{3+}$  is oxidized to a state effectively between +3 and +4 in the solid solution in which the principal component is  $\text{UO}_2$ . This could have a significant effect on the behavior of fuels since such a phenomenon would provide an additional sink for oxygen which is released upon fissioning of the fuel. (Sect. 2.1.3)

Hazards analysis, test specifications, and operating manual for the Series I TREAT experiments which are to compare the transient value of the unirradiated sol-gel-derived Sphere-Pac and pelletized (U,Pu)O<sub>2</sub> fuels were submitted to the TREAT staff and accepted with minor revisions. (Sect. 2.2.4)

Five fuel rods containing Sphere-Pac fuels being irradiated in the EBR-II in Subassembly X050 have been exposed to 5906 Mwd of operation. The rod having the highest burnup has accumulated a calculated 3.1% FIMA. (Sect. 2.2.5)

A proposal for "Approval-in-Principle" for the Series II unencapsulated EBR-II tests, the objective of which is to establish the performance characteristics and limitations of (U,Pu)O<sub>2</sub> fuels fabricated by different processes, was submitted to the USAEC. (Sect. 2.2.5)

## I. AQUEOUS FUEL REPROCESSING

(W. E. Unger, R. E. Blanco, D. J. Crouse, A. R. Irvine, C. D. Watson)

## 1. SHIPPING (TASK 1)

(A. R. Irvine, J. D. Rollins, R. S. Lowrie,  
D. C. Watkin, J. H. Evans)

The objective of Task 1 is to assure that an economic and safe method of shipment of LMFBR spent fuel will be available when needed for transport of fuel from the demonstration and early commercial LMFBR's. The work involves analytical studies of the various facets of the problem; design, construction, and test of components, and of assemblies; and preliminary design of prototype casks.

The bulk of the effort on this task is directed toward expanding the store of information on the effectiveness of sodium as a primary coolant and of cask design features which can assure containment of coolant (and fission products) within the cask fuel cavity. Other coolants (including gases, liquids, and solids) have been considered, but they do not appear to be as attractive as liquid sodium.

Work performed during this report period was almost entirely in the areas of Tasks 1.1 through 1.4, which deal with evaluation and test of heat dissipation methods and of cask integrity. Indeed, the preponderance of effort performed to date in this task area has related to heat dissipation and cask integrity. Such information as has been and will be collected relating to these two items will be useful regardless of what coolant is employed (provided it is a liquid) and regardless of size. While rough estimates of the largest reasonable shipping batch have been prepared, these estimates have required little effort and in no way control the line of development effort.

Reportable accomplishments include the following:

## 1.2 Heat Dissipation Tests (Task 1.2)

- A. Operation of the reduced scale cask mockup (with mercury as the heat transfer medium) continued as additional tests and temperature measurements were made to determine the extent that the baffles interfere with the thermal convective flow within the fuel cavity. Data from these tests are being analyzed.
- B. The second startup of the electrically heated mockup of an Atomic International Reference Oxide Reactor fuel assembly has been further delayed due to additional tube heater failures as well as a slippage in the delivery schedule of the heater manufacturer. Arrival of replacement heaters is now scheduled for the middle of October 1969.

- C. Fabrication of components for the full-scale, half-length, 37-subassembly, sodium-cooled, electrically-heated cask mockup is nearing completion. Startup of operation which was previously scheduled for November 1969 has been delayed.

1.3 and 1.4 Cask Integrity Studies and Tests  
(Tasks 1.3 and 1.4)

- D. Work on the "bird cage" crash frame design for cask protection has been discontinued due to budget restrictions and the necessity for a more economical approach. Fabrication of the test specimen discussed in the previous monthly report (ORNL-TM-2710) has been cancelled.
- E. Construction drawings, fabrication, and impact testing were completed for a 1/8 scale cask plus three energy absorbing systems for one end of the cask. The three energy absorbers were of the tube-in-tube design, made of 9-in.-long sections of pipe, sched 40, and of three different sizes; viz., 1-1/4-in., 2-in., and 3-in. They contained 9, 22, and 52 type 304 stainless steel tubes (3/8 in. OD and 0.065 in. wall), respectively. In Fig. 1-1 these absorbers are shown detached from the cask which was essentially undamaged following a 30-ft corner drop onto each of the absorbers. Attachment of the energy absorbers to the bottom of the cask is illustrated in Fig. 1-2.
- F. Parametric studies and tests were continued on energy absorbers of the tube-in-tube design. Test specimens 3 in. in length with the outer tube made of 2, 2-1/2, and 3 in. sched 40 pipe, respectively, were deformed under the impact of drop hammers ranging in weight from 313 lb to 482 lb dropped from a height of 30 ft. The pipe specimens contained 22, 33, and 52 tubes (3/8 in. OD, 0.065 in. wall), respectively. All material was type 304 stainless steel. These tests provided data which can be used to determine the size of a tube-filled pipe (i.e., the number of tubes) necessary to absorb a given amount of impact energy.

Additional tests were performed with 2-in. pipe specimens 3-in. long and filled with 22 tubes wherein the wall thickness of the 3/8-in. tubes ranged from 0.032-in. to 0.125-in. Specimens were deformed under the impact of a 310 lb hammer which was dropped from a height of 30 ft. Results of these tests are illustrated in Fig. 1-3 which indicates that the 0.065-in. wall thickness (center specimen) utilized in all 3/8 in. OD tubes tested to date represents a reasonable choice of thickness to diameter ratio. The thinner wall tubing was relatively weak and thus collapsed with minimal energy absorption whereas the thick walled tubing was so strong that the 2-in. sched 40 pipe could not exert sufficient

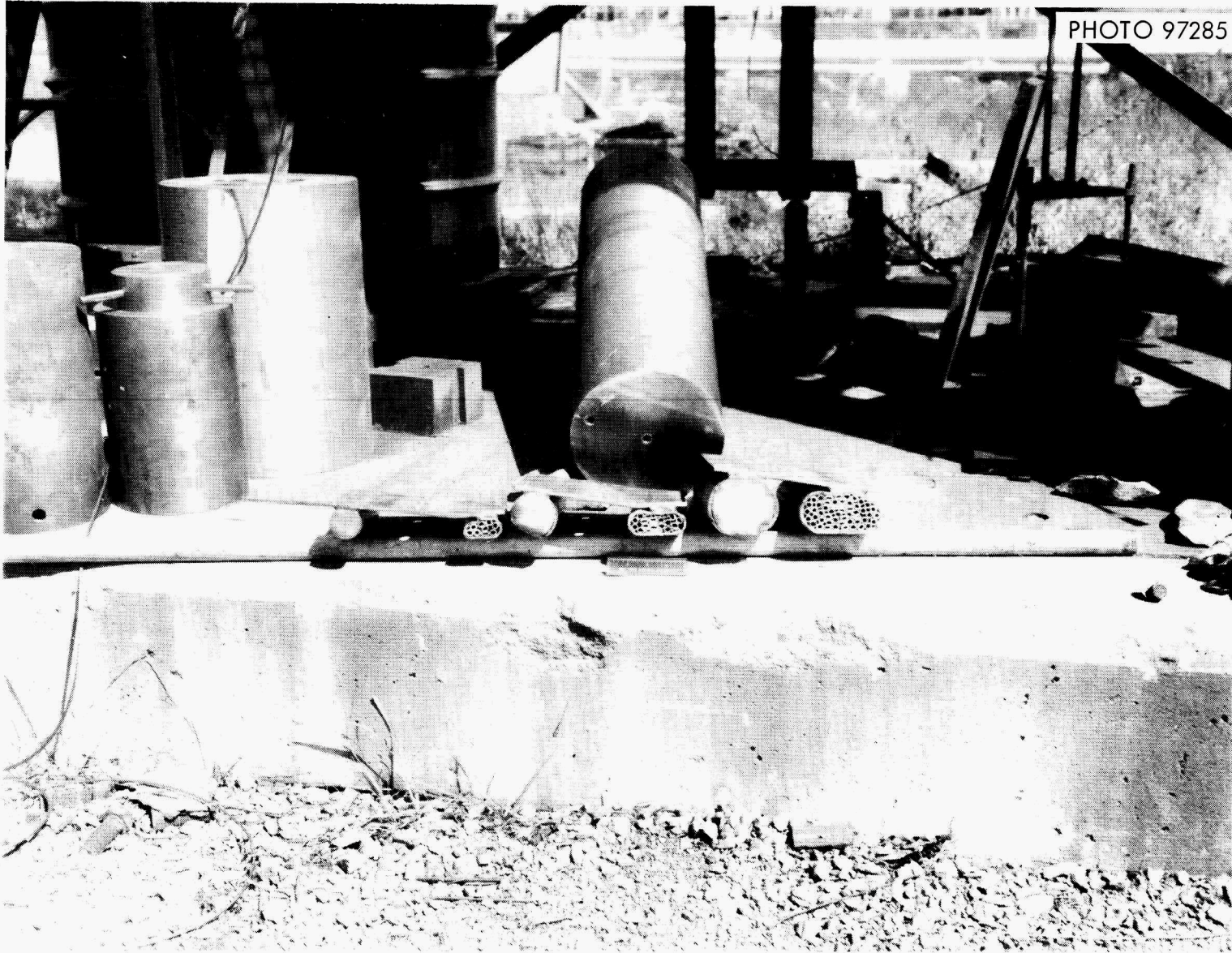


Fig. 1-1 Tube-in-Tube Energy Absorbers Along with 1/8-Scale Model Cask Following 30-Ft Drop on Corner.

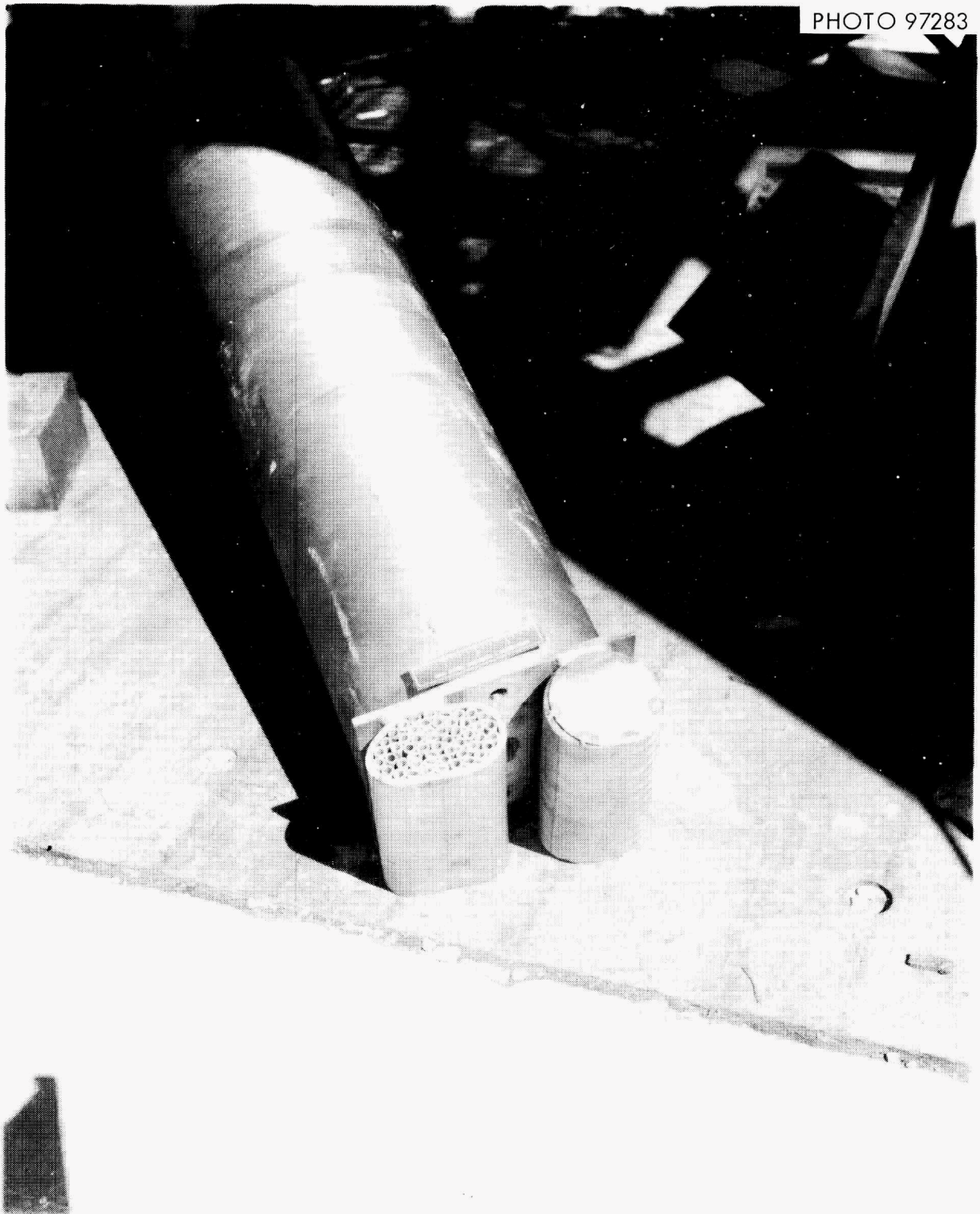


Fig. 1-2 Orientation of Cask-End Crash Frame Assembly (3-in Pipe Section Shown Following 30-Ft Corner Drop).

PHOTO 97260

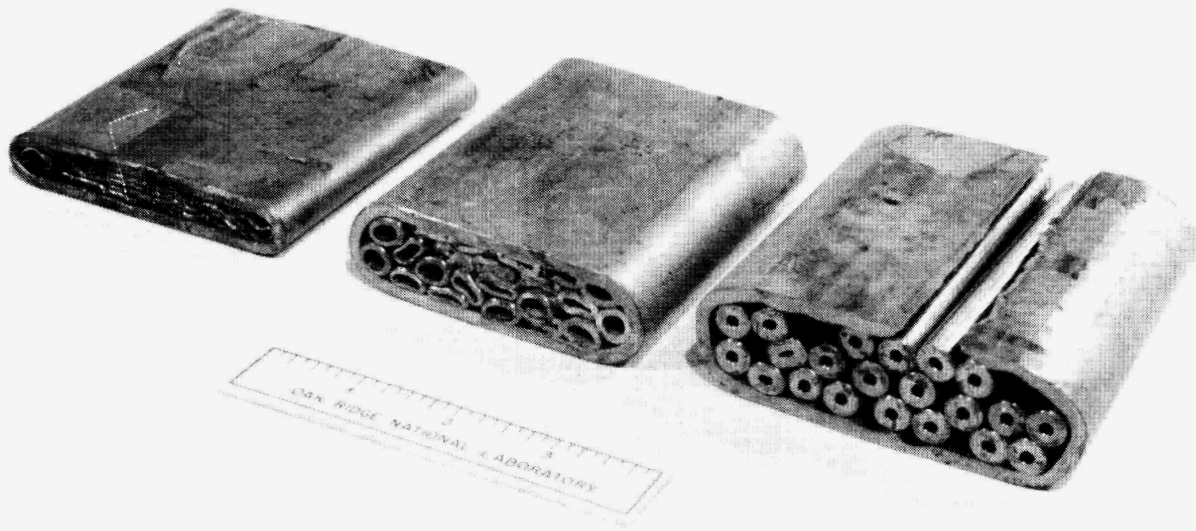


Fig. 1-3 Tube-in-Tube Energy Specimens Following Impact with a 310-lb Hammer Dropped from 30-Ft.

retaining force to hold them within its perimeter upon imposition of a heavy external force. Most of the impact energy was thus transmitted to the pipe wall (tube envelope) which failed under tension.

- G. Cask modeling tests were initiated on impact specimens of 1/9.38, 1/18.7, and 1/37.5 scales. Results of the first series of drop tests are shown in Fig. 1-4. Pertinent physical dimensions associated with the deformed sections of the above three cask models as well as a 1/6 scale model (see paragraph (H) below) are listed in Table 1-1. In addition to these measurements, force-time data were recorded during impact by means of a load cell and electrically connected oscilloscope-camera assembly. Figure 1-5 is a reproduction of a photograph (oscilloscope image) produced from load cell transmission during impact of a 1/18.7 scale specimen. The straight line connecting the end points of the S-shaped force-time curve (Fig. 1-5) was used as an approximation\* to facilitate construction of the force-deformation curve shown in Fig. 1-6. Data of the latter type will be used to construct curves of average load per unit area versus deformed area which are essential in predicting the response of a full-scale cask during impact.

Table 1-1. Pertinent Dimensions of Deformed Sections<sup>a</sup> of Cask Scale Specimens

Scale	Cask Weight (lb)	Vertical Deformation (inches)	Subtended Angle of Deformed Area (°)	Angle of Inclination <sup>b</sup> (°)
1:37.5	4.7	0.14	65	30
1:18.7	37.9	0.2	77.5	20
1:9.34	300	0.415	76	27
1:6	1150	0.52	77.5	15

<sup>a</sup>See Fig. 1-4 and Fig. 1-7.

<sup>b</sup>All specimens were dropped at an inclined angle of 15°.

\*More refined calculations will entail the use of a numerical integration technique such as Simpson's Rule or the trapezoidal rule.

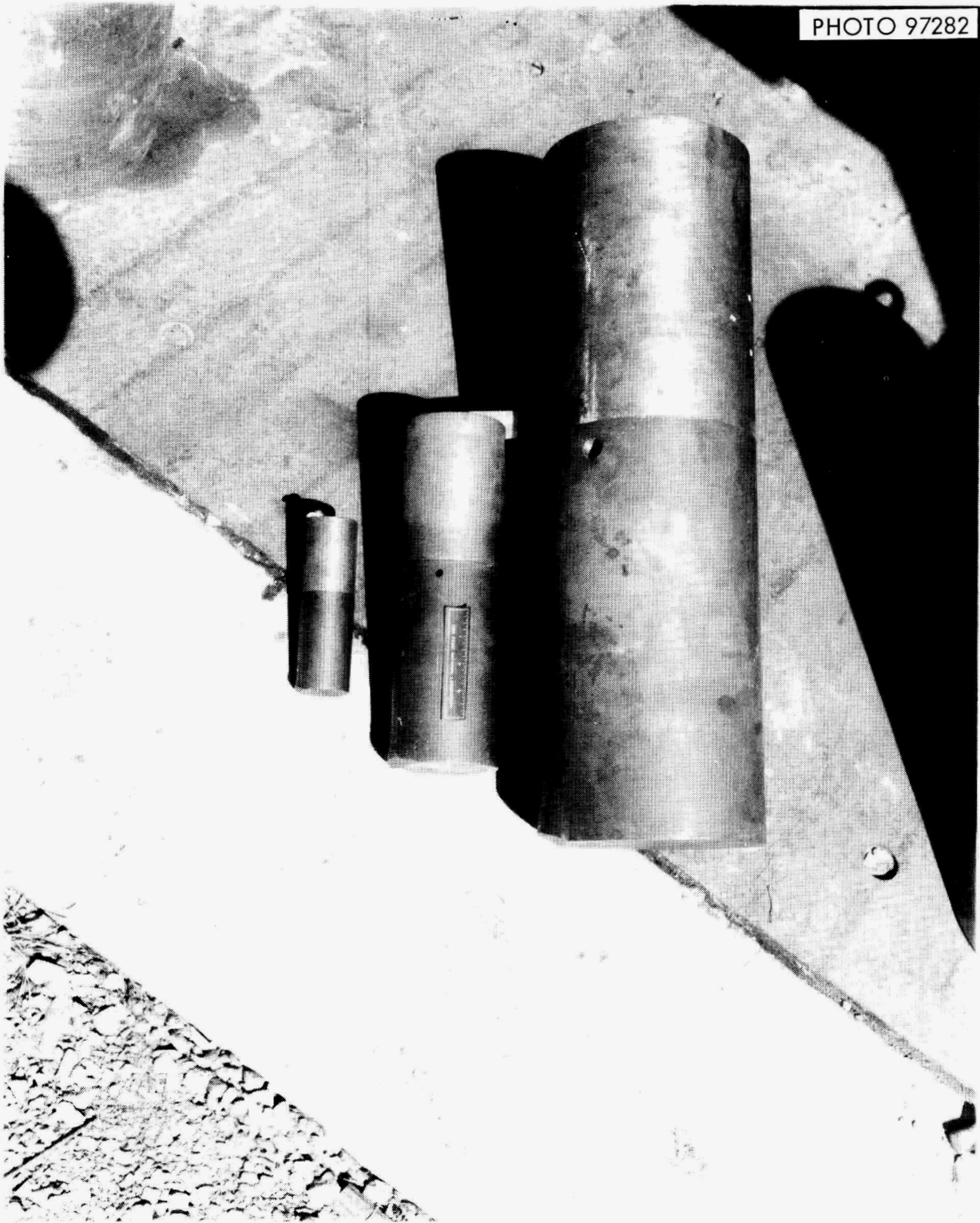


Fig. 1-4 Cask Scale Model Specimens Following 30-Ft Corner Drop Tests.

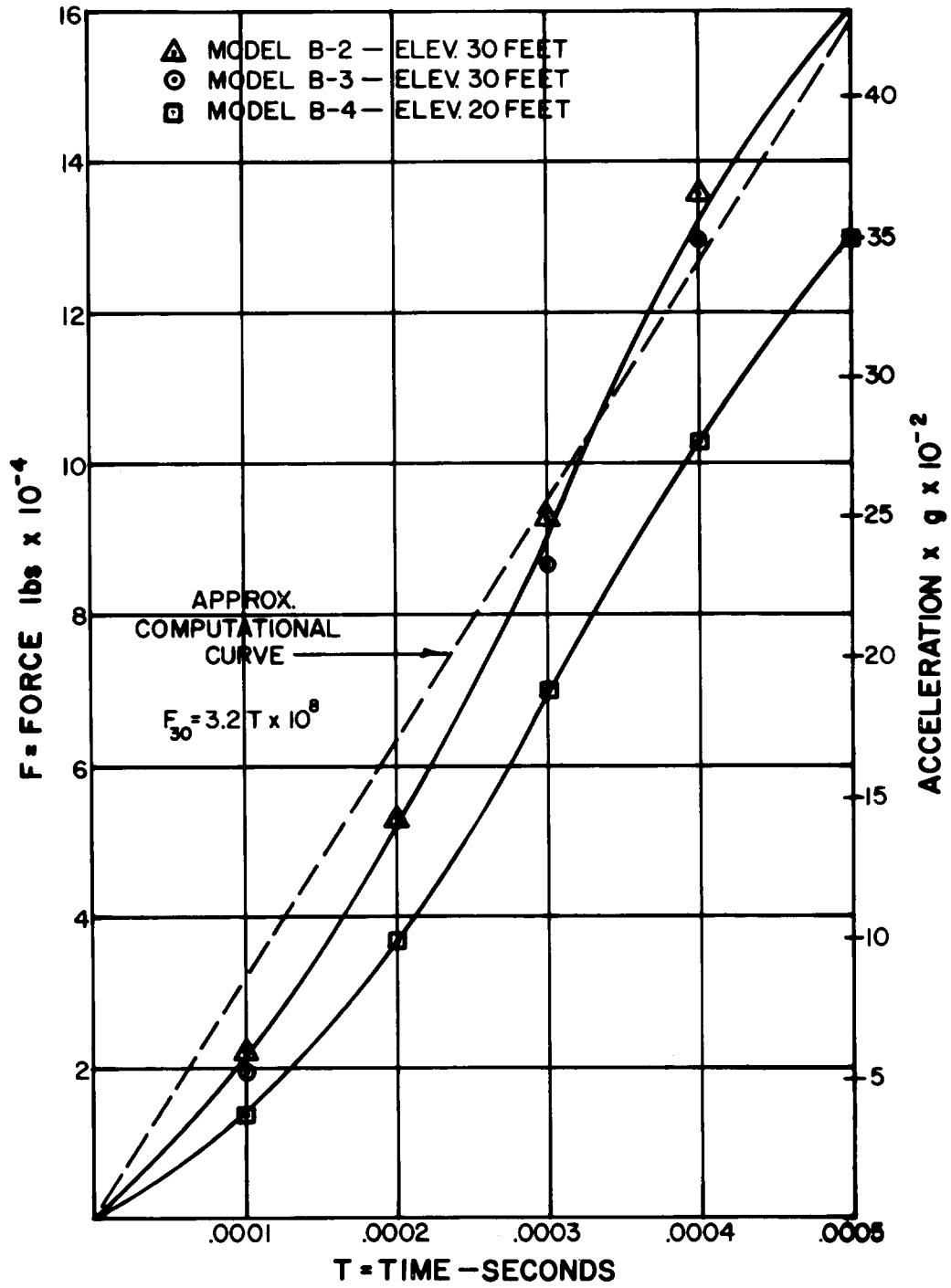


Fig. 1-5 Force vs Time Data for Cask Scale (1:18.7) Specimen as Recorded with Load Cell-Oscilloscope Equipment.

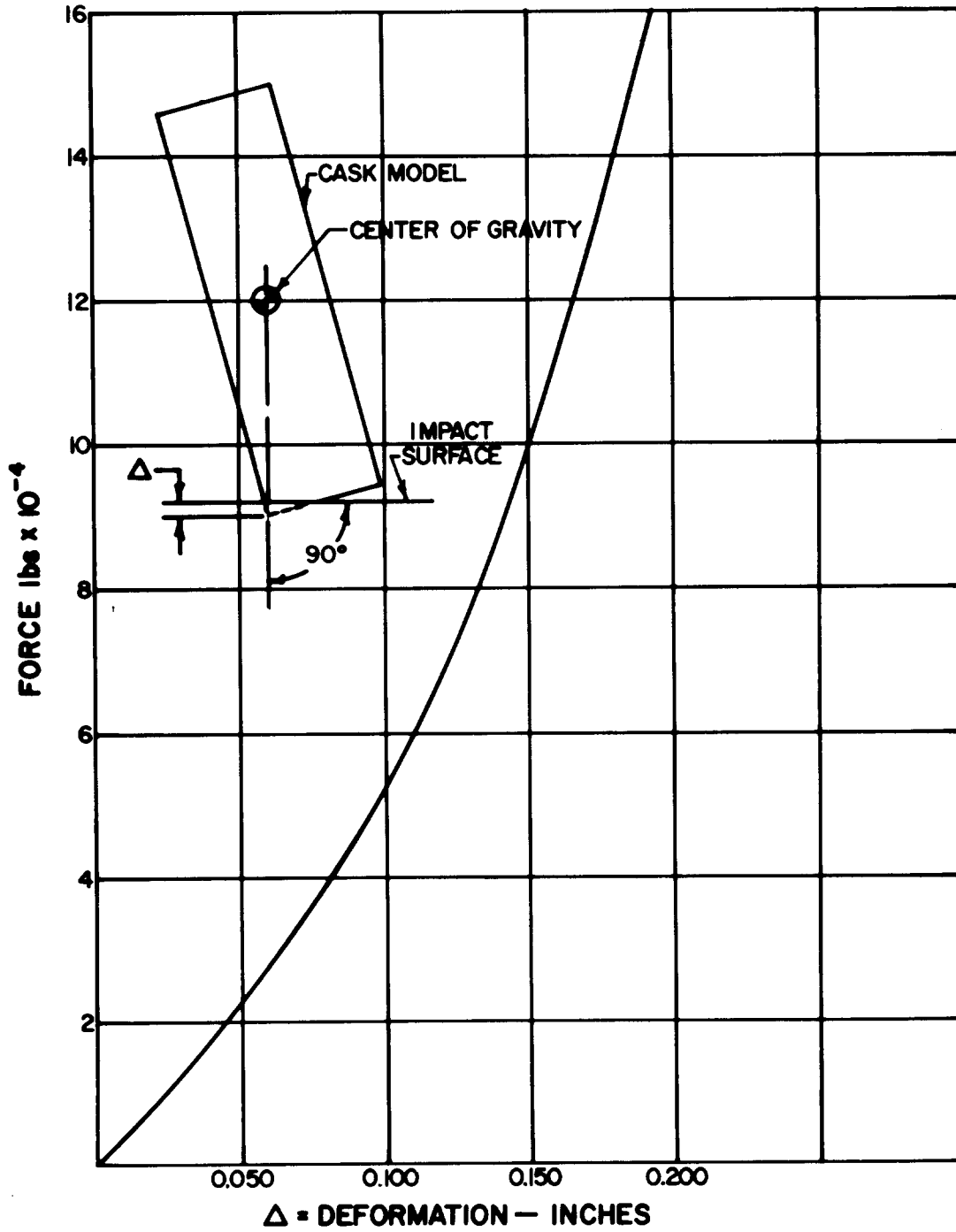


Fig. 1-6 Force vs Deformation Data Obtained from Double Integration of the Computational Curve in Fig. 1-5.

Fabrication was initiated on a load cell capable of handling loads up to  $2 \times 10^6$  lb. This cell will be used to obtain force-time data on the 1/9.38 and (possibly) larger scale model casks similar to those obtained thus far on the smaller models discussed above.

- H. A 1/6 scale model cask which incorporated a Grayloc type seal (positioned within the cask as shown in Fig. 1.5 of ORNL-TM-2552) was dropped from a height of 30 ft onto an essentially unyielding surface. A subsequent He leak check indicated that negligible ( $2.3 \times 10^{-9}$  cc/sec of He) leakage occurred as a result of the drop test. The He leak rate prior to the test had been recorded at  $4.08 \times 10^{-10}$  cc/sec. Figures 1-7 and 1-8 illustrate the respective external (see Table 1-1) and internal (no visual damage) conditions of the cask following the drop test. The photographed hollow section of the cask was attached to a solid (hammer) section during the test in order to simulate the total weight (1150 lb) of a 1/6 scale model cask.

Work during the following report period will continue along the same general lines. Additional test data on impact deformation and post-test seal integrity will be obtained from tube-in-tube type energy absorbers and scale-model cask specimens, respectively. Limited heat dissipation work is anticipated based on the scheduled arrival of replacement electrical heaters.

## 2. RECEIVING AND STORAGE (TASK 2) (A. R. Irvine and C. D. Watson)

This task is concerned with the means for rapid, effective, economical, and safe operation of receiving and storage facilities for LMFBR fuels. The character of the work to be performed under this task will be determined largely by the outcome of investigations performed for the shipping and for the head-end processing tasks. Conversely, these other two tasks will be required to take into consideration the effect of variables in their area on the task of receiving and storage. This work will take cognizance of related work on fuel handling and sodium removal that will be performed under Elements 3 and 5, respectively, of the LMFBR program plan.

Initial conceptual work was done on a receiving-sodium removal facility for either a system used exclusively for LMFBR fuel reprocessing or a system which is added to an existing facility to permit reprocessing of LMFBR fuel in a system originally designed for reprocessing of LWR fuels. While the concept is in its earliest stages, it involves (1) receiving the fuel into an inert gas cell; (2) removal of external sodium via reaction with steam mixed with inert gas followed by a water spray; (3) testing for gross fuel leaks by analysis



Fig. 1-7 External View of 1/6-Scale Model Cask Following 30-Ft Corner Drop (Showing Plug Above Seal Housing).

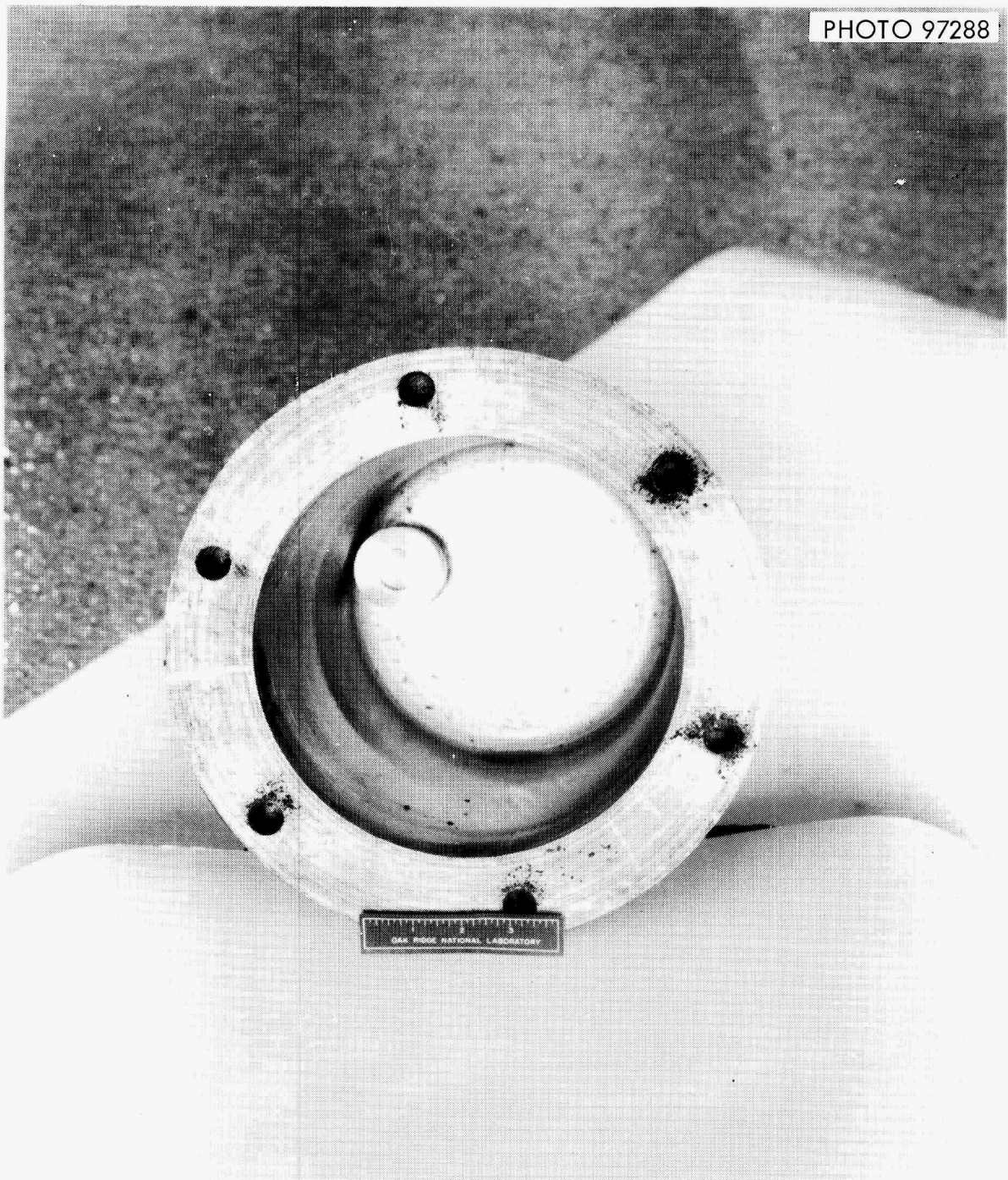


Fig. 1-8 Internal View of 1/6-Scale Model Cask Following 30-Ft Corner Drop (Showing Seal Housing).

of water in which the "cleaned" subassembly is immersed; and, (4) canning of grossly defective subassemblies in temporary, easily closed and opened, containers. Those fuel subassemblies having no, or small, defects could be removed and stored without canning.

Two informal, undocumented reports dealing with storage of LMFBR fuels in water have been reviewed. One was issued by APDA in 1960 and the other by Westinghouse in 1969. Both of these informal reports indicate that stainless steel clad oxide fuel which has been cleaned of external sodium probably can be stored satisfactorily in a water pool, even though the fuel rods may have small defects and contain sodium.

The work on sodium deactivation equipment construction is reported under Task 3.5.

### 3. HEAD-END PROCESSING OF LMFBR FUELS (TASK 3) (C. D. Watson)

The objective of this task is to develop economic head-end processing steps, in preparation for Purex recovery methods, for long- and short-decayed fuels.

In this report period: HEX calculations of new black body and gray body view factors using some very recent data were begun; modifications to the ORNL assembly or bundle shear and the multirod shear were completed; drawings of an experimental single rod shear were completed but fabrication has been delayed; preliminary design of an in-cell fuel assembly dismantling unit for multitubular fuel assemblies was completed; the ability of a plasma-arc torch to cut off (melt) the corner of the shroud without damaging the contained fuel rods was successfully demonstrated; melt-decladding still appears promising although the desired high degree of separation of molten cladding and core material has not been attained.

In general all experimental work is being deferred pending completion of a Head-End Engineering Evaluation Study which is now under way.

Reportable accomplishments include:

#### 3.1. Decay Heat Dissipation (Task 3.1) (R. L. Cox)

The writing of an ORNL report to document the theoretical calculations of the temperature profile in LMFBR hexagonal fuel rod arrays has been temporarily halted for the purpose of calculating new black body and gray body view factors. These view factors are necessary for the accurate calculation of the temperature distributions in irradiated fuel rod assemblies under conditions in which radiation is an important mode of heat dissipation. Previously, reference 1 has been used as a source for these values. However, the method of calculation used in the reference is an approximate one, making it difficult to ascertain the accuracy of the final results. Hence, it is proposed to employ more exact methods now available in the literature to redetermine these view factors for inclusion in the ORNL report. Work on the report will be continued next month using the new view factors. Also as part of a Head-End Engineering Evaluation Study, an analysis of heat dissipation problems will be started and calculations (linear power, fission products, etc.) using computer code, ORIGIN, for the AI and GE advanced fuel concepts begun.

Experimental confirmation of the theoretical calculations made by HEX continues to be delayed by lack of replacement heaters for the AI reference oxide reactor subassembly test device. Please see (B.) of subsection 1.1, page 3 of the August<sup>2</sup> report.

### 3.2. Dismantling of Multitubular Assemblies (Task 3.2) (R. S. Lowrie, G. A. West)

In this report period, the preliminary design of an in-cell fuel assembly dismantling unit for AI reference oxide fuel was completed. The two principal problems involved in this design were: (1) a method of cropping the end hardware from the assembly, and (2) the removal of the fuel rods from the shroud. As previously reported<sup>3</sup> abrasive disc sawing was selected for cropping because it appeared to be the best way of cutting such dissimilar configurations as the shroud, unfueled tubing, solid steel rods, ceramic-filled tubing, nickel reflector rods, springs, etc., which are associated with the fuel assembly. Originally, it was proposed to slit the shroud of the cropped fuel assembly, then push out the loose fuel rods into the singulator. Because the length of a dismantling unit using this scheme was excessively long (over 45 ft), it was decided to use a dual slitting saw approach in which the first and third corners of the hexagonal shroud are cut (see Fig. 3-1). The section of the shroud thus cut loose is lifted off, and the fuel rods dumped by rotating the remaining trough-like shroud section 180 degrees. The present conceptual dismantling unit functions as follows:

1. The fuel assembly is pulled into the machine and clamped in place on the work table.
2. Two abrasive saws are used to simultaneously cut off the end hardware which is then discarded to waste. This leaves a bundle of loose rods contained in the hexagonal shroud.
3. The dual slitting saw with its own motor and feed mechanism, cuts corners 1 and 3 the full length of the shroud.
4. The loose section of the shroud is lifted off and discarded to waste.
5. The trough-like shroud section is rotated 180 degrees, allowing the loose fuel rods to fall out.
6. The remaining section of the shroud is discarded to waste.

Feasibility of both the abrasive saw cropping method and the dual slitting saw concept remains to be proven. Equipment components for the cropping test on the end fittings have been fabricated and will be installed on the Ty-Sa-Man saw as soon as craft time is available, hopefully in October. Components for the slitting test have been fabricated. Performance of these tests now depends on the availability of a milling machine in the ORNL shops.

As reported last month,<sup>4</sup> a plasma-arc torch has been suggested as an alternative method for cutting off the corners of the hexagonal shroud. During the month, a series of scoping-type tests were made to ascertain the feasibility of this method. The test equipment used consisted of a commercial Linde plasma-arc torch (using argon as the

ORNL DWG. 69-10378

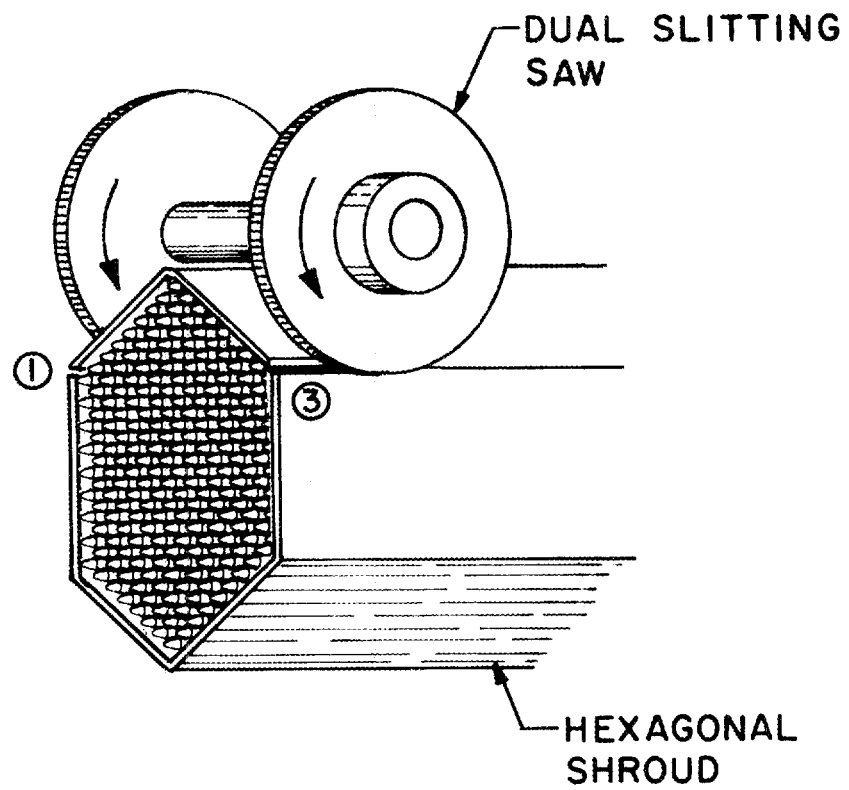


Fig. 3-1 Dual Saw Concept for Slitting LMFBR Fuel Assembly Shroud.

cover gas) attached to a traveling carriage and aligned to cut off the corner of a test piece, see Fig. 3-2. A wire-wrapped fuel rod was positioned in the corner of the test piece to ascertain if the arc was precise enough to cut the corner without damaging the fuel rods. Carriage speed was 25 in./min. In four tests made, the plasma-arc torch successfully cut off (melted) the corner of the test assembly without damaging in any way the fuel rods positioned inside the corner. Very little of the metal removed was blown away by the arc, most of it melted and ran down the side of the test piece, see Fig. 3-3. The success of these tests establishes the plasma-arc as a definite contender for slitting the shroud, although more precise testing is obviously needed. Further, the use of a plasma-arc torch for cropping the end sections should also be evaluated.

### 3.3. Shearing (Task 3.3) (G. A. West, R. S. Lowrie, C. H. Odom)

Assembly or Bundle Shear. - Modifications to the 250-ton shear to increase its stroke from 10-3/16 in. to the maximum possible length of 12-1/2 in. were completed. The new hydraulic lines and valves and electrical control changes checked out satisfactorily. The increase in the shear stroke was necessary to evaluate the new shear blades which are designed to break up a shrouded fuel bundle into discrete pieces. The proposed blades are about 11.75 in. long compared to the 5.75-in. length of the old blades. Elongated stepped blade and "shark's" tooth type blades<sup>5</sup> are proposed in order to break the stainless steel hexagonal fast breeder fuel shroud into pieces small enough to pass through the process lines. However, the purchase of the shear blade material has been deferred and the evaluation testing will be delayed. Modifications to the gags and feed envelope to accommodate fast breeder fuel bundles is continuing. Delivery of the material for special gags is presently scheduled for November. Fabrication of these parts will also be delayed until later in the fiscal year.

The gag forces required to compress a can and the fuel rod assembly contained therein is to be determined on prototype sections. A test fixture was designed and fabrication is 50% completed. However, completion of the test fixtures will also be delayed similarly to the gags.

Multirod-Shear. - Our present efforts on the development of a multirod shear are being concluded until the end of the fiscal year. The unit has been installed for demonstration purposes by providing larger hydraulic supply lines (1-1/2 in. IPS) and two double-solenoid control valves. In trial tests with prototype fuel rods, the electrical controls operated very satisfactorily. The unit appears to be capable of making about 120 shear strokes/min. Extensive testing will be necessary to define the exact limits of the shear capacity and reliability of the design.

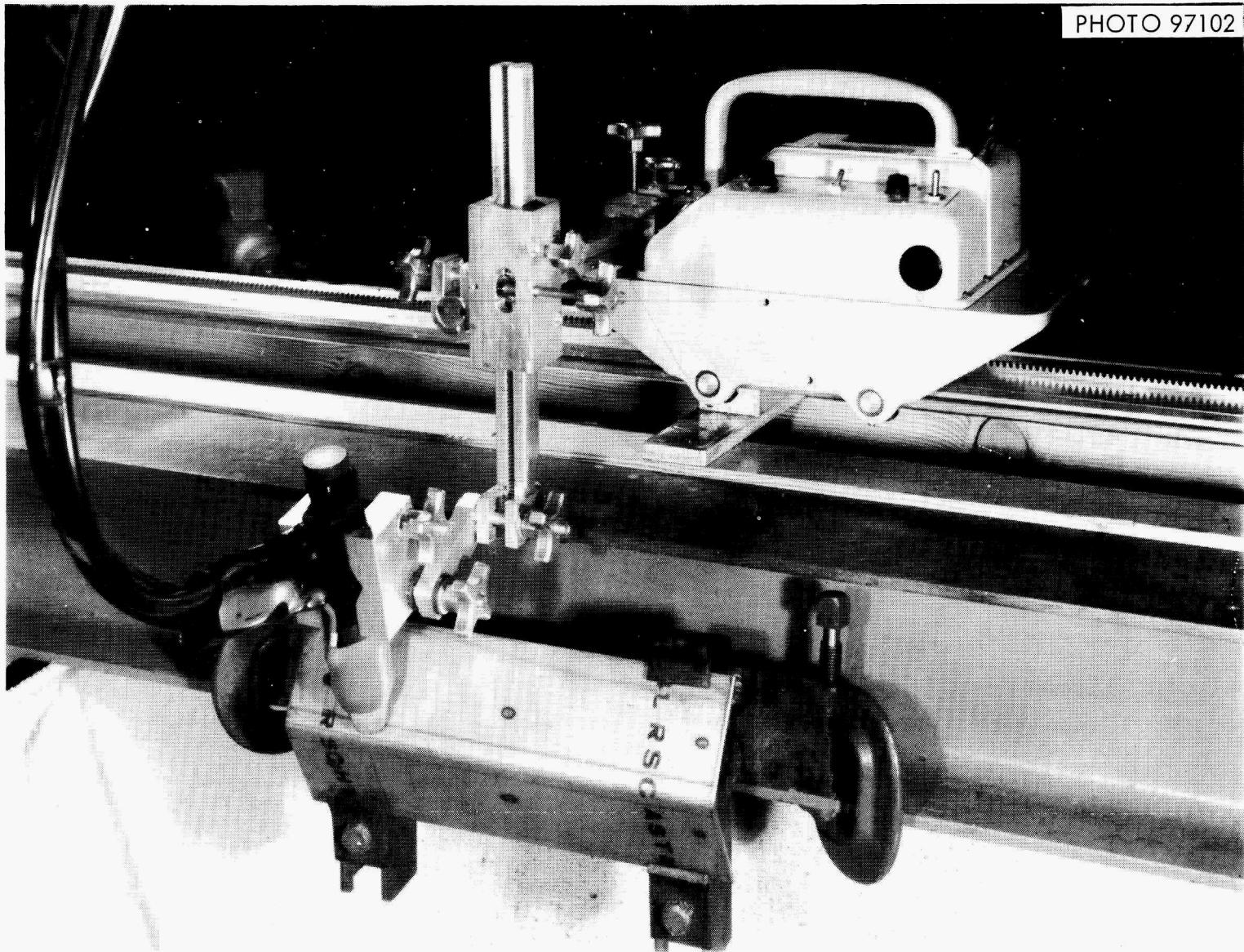


Fig. 3-2 Plasma-Arc Test Facility.

PHOTO 97103

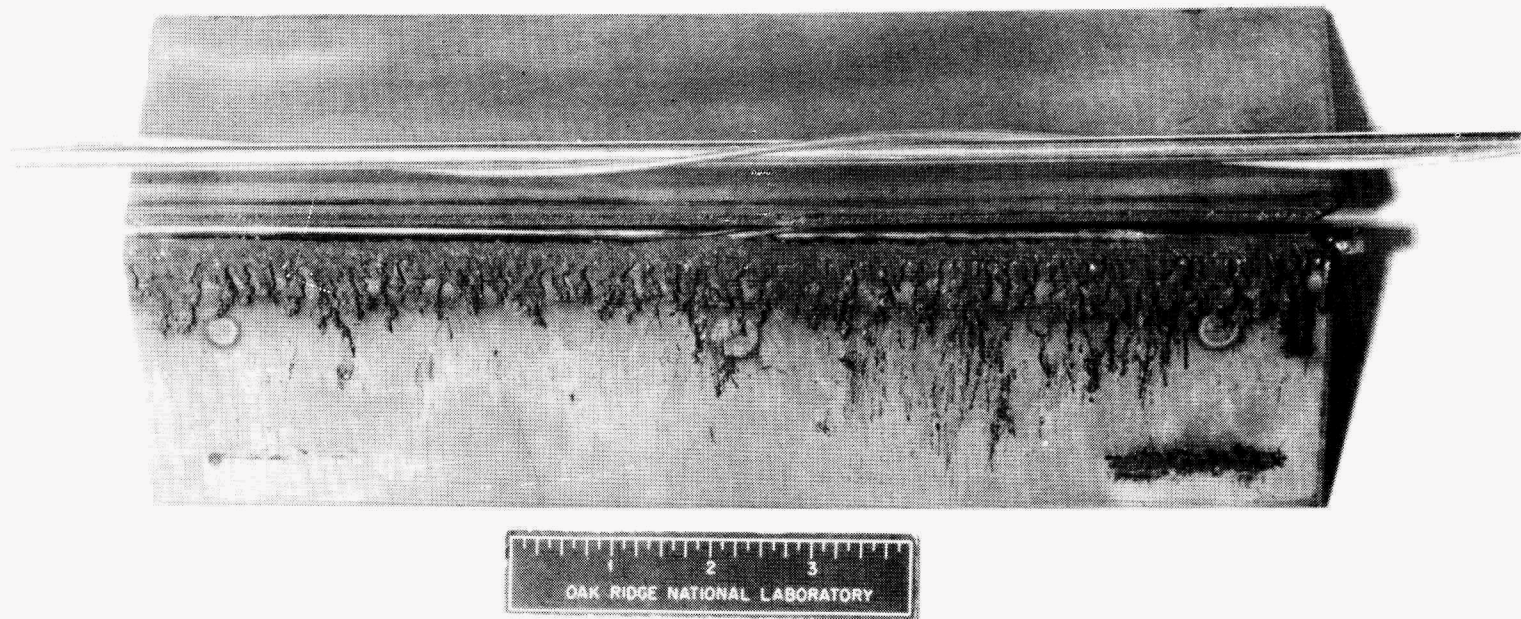


Fig. 3-3 Plasma-Arc Test Piece.

Experimental Single Rod Shear. - Design concept revisions and detail (fabrication) drawings for an experimental single rod shear was completed. However, the fabrication and purchase of parts has been deferred until the end of the fiscal year.

During the next report period, an analysis and updating of the various shearing operations will be started as part of an Engineering Evaluation Study.

3.4 Isolation of Shearing Operations (Task 3.4)  
(R. S. Lowrie, C. H. Odom, G. A. West)

Vacation and illness of the principal investigator, C. H. Odom, prevented a review and analysis of interstage sealing and valving devices as indicated in the August report (ORNL-TM-2710). Now the review will be included as part of an Engineering Evaluation Study.

3.7. Alternative Head-End Processes (Task 3.7)  
(S. D. Clinton, A. R. Irvine)

Melt-decladding is being considered as a backup process for the shear-leach head-end. By heating the fuel assemblies above the melting point of stainless steel (1450°C) it may be possible to volatilize iodine, xenon, krypton, and tritium and to separate the molten cladding from the urania-plutonia core material.

A test was made in an induction furnace at 1540°C with 0.270-in.-diam urania pellets enclosed in 5-in. lengths of 304-L stainless steel tubing. Nine specimens were stacked longitudinally in a triangular array and tack welded together. The array was then inserted in a 2.5-in.-diam cylindrical alumina crucible inclined at an angle of 10 degrees with the horizontal. A zirconia disc with a 0.25 in. high segment removed was positioned below the specimens to skim urania fragments from the surface of the flowing molten stainless steel. As the cladding melted from the array, about 76 wt % of the stainless steel (total of 245 g) separated from the pellets and collected at the lower end of the crucible. There was no apparent indication that urania fragments had been carried by the molten steel, however, the determination of the actual urania loss to the steel will have to await a chemical analysis. In a previous similar run at 1550°C, about 94% of the stainless steel was separated from the pellets. The reason for the increased holdup of steel between and around the layers of pellets in this latest run has not been established.

During the next month, a melt declad run will be made with one or more stainless steel pins containing crushed and sized urania particles to determine the feasibility of separating molten cladding from fragmented oxide fuels. In the initial test, the urania particles will be in the size range of 300 to 600 microns.

References

1. O. H. Klepper, Radiant Interchange Factors for Heat Transfer in Parallel Rod Arrays, ORNL-TM-583 (Dec. 1963).
2. W. E. Unger, R. G. Wymer, A. L. Lotts, et al., LMFBR Fuel Cycle Studies Progress Report for August, No. 6, ORNL-TM-2710, p. 3.
3. W. E. Unger, et al., Aqueous Processing of LMFBR Fuels, Progress Report, April 1969, No. 2, ORNL-TM-2585, p. 8.
4. W. E. Unger, R. G. Wymer, A. L. Lotts, et al., LMFBR Fuel Cycle Studies Progress Report for August, No. 6, ORNL-TM-2710, p. 8.
5. W. E. Unger, R. G. Wymer, A. L. Lotts, et al., LMFBR Fuel Cycle Studies Progress Report for August, No. 6, ORNL-TM-2710, p. 10.

#### 4. VOLATILE FISSION PRODUCT REMOVAL (TASK 4) (D. J. Crouse, C. D. Watson)

The objective of Task 4 is to develop a head-end processing method for removing iodine, xenon, krypton, and tritium from the fuel prior to aqueous processing. Early removal of these gases from the fuel into a relatively small volume of gas would greatly facilitate off-gas treatment. This is of particular importance with respect to iodine control because of the very high plant retention factors that will be required for  $^{131}\text{I}$  when treating short-cooled fuels.

This month accumulation and interpretation of the data from the recent processing of four short-cooled LMFBR fuel rod specimens was continued.

##### 4.1 Volatilization from Oxide Fuels (Task 4.1) (V. C. A. Vaughen, J. H. Goode, L. A. Byrd, G. D. Davis, W. B. Howerton, O. L. Kirkland, R. C. Lovelace)

Analysis of the data from the hot cell experiments on the shearing, oxidation, and dissolution of four short-cooled (30 to 60 days) stainless steel-clad fuel rods, containing sol-gel 15%  $\text{PuO}_2$ --85%  $\text{UO}_2$  microspheres, was continued. Most of the analyses have been completed, and permit some observations on the volatility of certain fission products.

Tritium. -- Because of analytical problems associated with the high radiation levels in the short-decay fuel solutions and because of greater interest in  $^{131}\text{I}$  and other fission products, no special effort was made to completely determine the fate of tritium in these experiments. Analysis of the nitric acid leaches of the fuel rods indicated that about 0.01% of the calculated yield of tritium was in the solution. This was expected since voloxidation removes the tritium from the fuel oxide.

In the near future we will analyze the noble gases collected during shearing of the fuel rods to determine if any free tritium was in the gas plenum.

Tellurium. -- We found little or no segregation of  $^{129}\text{Te}$  during the irradiation, oxidation, or dissolution of the fuel rod in Run FR-44 (3/4-in.-cuts, 750°C). Leaches of the plenum and end plugs, burner head and body, and of the fuel and cladding showed essentially the same amount of  $^{129}\text{Te}$  per gram of fuel in each case.

Noble Gases. -- Burnup calculations for each fuel rod are not complete, so we do not yet have exact fission gas release values. Qualitative observations indicated a greater fraction of  $^{85}\text{Kr}$  than  $^{133}\text{Xe}$  was released during the shearings, and that oxidation at 750°C released about twice the percentage of Xe-Kr as did oxidation at 450°C. The total quantities of  $^{133}\text{Xe}$  and  $^{85}\text{Kr}$  in each rod appear to be proportional to the estimated burnups.

<sup>131</sup>Iodine. - Data on the volatilization of <sup>131</sup>I will be reported next month since interpretation of the data is incomplete.

5. DISSOLVING (TASK 5)  
(D. J. Crouse, C. D. Watson)

The objective of Task 5 is to ensure that LMFBR fuels can be dissolved in nitric acid with high metal recoveries. Since the dissolution characteristics of the fuels can vary widely depending on their plutonium content, method of preparation, and irradiation histories, extensive leaching data are being obtained to define the effects of the many variables. A thorough understanding of iodine chemistry in the dissolver system is needed as a guide for providing effective iodine control. The dissolver equipment must be designed and operated within rather narrow limitations imposed by criticality control and off-gas considerations. It appears that satisfactory solution of these problems can best be accomplished using a continuous dissolver and this approach is being emphasized. Evolution of a successful dissolver will require development of equipment for dependably moving the sheared stainless steel hulls and other solids through the system, and development of seals for isolating the system to prevent excessive in-leakage of diluent gases.

Analysis of the leaching data from the recent hot cell tests with short-cooled fuel rod specimens indicates that thermal diffusion of the ThO<sub>2</sub> insulator pellets into the fuel during irradiation was responsible for the poor plutonium recoveries obtained in leaching in some tests.

5.1 Dissolution Data (Task 5.1)  
(V. C. A. Vaughen, J. H. Goode, L. A. Byrd, G. D. Davis, W. B. Howerton,  
O. L. Kirkland, R. C. Lovelace)

The leaching data on the four short-cooled fuel rods described in Task 4.1 is still being analyzed. Thermal diffusion of the ThO<sub>2</sub> insulator pellets into the (U, Pu)O<sub>2</sub> fuel column (and vice versa) occurred during irradiation. Oxidation and sintering at 450 to 750°C of ThO<sub>2</sub>-PuO<sub>2</sub> or ThO<sub>2</sub>-UO<sub>2</sub> is known to cause disproportionation of a solid solution into a U<sub>3</sub>O<sub>8</sub> phase and a stable fluorite lattice.<sup>1</sup> Either or both mechanisms interfered with the nitric acid dissolution of the plutonia in our fuel rods; HF catalyst was necessary for complete dissolution of the specimens that had been oxidized.

Although the rods were sheared in a manner calculated to exclude the ThO<sub>2</sub> insulator pellets from the fuel, we found an average of 39% of the total thorium in the fuel column. A 0.5-in. long segment from the center of the 3-in.-long fuel column contained no ThO<sub>2</sub>, and dissolved completely in 8 M nitric acid (12-hr leach).

Reference

1. J. M. Leitnaker, Metals and Ceramics Division of ORNL, personal communication.

## 6. FEED PREPARATION (TASK 6) (D. J. Crouse)

The aqueous feed discharged from the dissolver will contain solids (undissolved fission products, corrosion products, etc.) and will probably require clarification prior to solvent extraction. Preparation of the feed for solvent extraction also will include adjustment of the plutonium valence and the nitric acid concentration and a treatment to remove iodine. This task also covers feed preparation for subsequent process cycles.

This month additional data were obtained on sparging of iodine from nitric acid in the temperature range of 50 to 70°C.

### 6.2 Iodine Control (Task 6.2) (G. I. Cathers, C. J. Shipman)

The removal of essentially all of the iodine from the nitric acid dissolver solution prior to solvent extraction is necessary to prevent iodine contamination of the solvent extraction system and to simplify the iodine off-gas treatment problem. A study of the partial pressure of iodine over nitric acid solutions is, therefore, being conducted with the objectives of determining the optimum conditions for the sparging of iodine from the dissolver solution and examining those factors that hinder iodine volatilization.

The transpiration technique is being used to study the partial pressure of free iodine ( $I_2$ ) over  $I_2$ - $HNO_3$  solutions. This is basically just a sparging process in which the amount of iodine carried from the sparged liquid is related to the volume of sparge gas employed.

An  $I_2$  carrier concentration ranging from  $5 \times 10^{-4}$  to  $5 \times 10^{-2}$  M was usually employed in the test solutions along with sufficient  $^{131}I$  activity to permit measurement of the concentration as sparging proceeded. This solution was usually prepared by premixing KI with  $^{131}I$  activity in a 0.01 M sulfite solution, then adding this to the nitric acid solution. Our present equipment consists of a 300-ml flask held in an air thermostat so that the freeboard surface and the 250-ml volume of sparged liquid are at the same temperature. In most tests the air sparging rate was 43 ml/min. The exit gas tube was heated above 100°C to prevent moisture condensation. In most of the tests in which nitrite additions were made, the  $NaNO_2$  solution was introduced through a stainless steel capillary tube from a precision motor-driven syringe. The latter was actuated by a cycle timer in some tests.

A total of about thirty runs have been made with 4 M nitric acid at temperatures of 50, 60, and 70°C. Although the first-order relationship,  $dc/dt = -kc$ , was followed in many of the tests, it was not possible to obtain reproducibility. Deviations from the first-order relationship were frequent but unreproducible. Runs made at different initial iodine concentrations did not give overlapping semilogarithmic plots. The

addition of  $\text{NaNO}_2$  solution, either at the beginning of a run or periodically during a run, to generate some nitrous acid did not eliminate the variability of the data. Nevertheless, the results of these tests have established the volatility of iodine from 4 M nitric acid to within an order of magnitude. In 15 tests at  $50^\circ\text{C}$ , the first-order constant  $k$  varied over the range of 0.00094 to 0.0046; in 2 tests at  $60^\circ\text{C}$ , the range was 0.0045 to 0.0061 and in 10 tests at  $70^\circ\text{C}$ , the range was 0.0020 to 0.011.

In an effort to improve the reproducibility of the data in future tests,  $\text{N}_2\text{O}_3$  gas will be fed continuously into the air stream rather than adding sodium nitrite periodically for the generation of nitrous acid. Nitrogen gas will probably be used in place of air in order to minimize the possibility of converting some of the  $\text{N}_2\text{O}_3$  or  $\text{HNO}_2$  to  $\text{NO}_2$  and  $\text{N}_2\text{O}_4$  and, hence, to  $\text{HNO}_3$  and  $\text{NO}$ .

## 7. SOLVENT EXTRACTION (TASK 7) (D. J. Crouse, C. D. Watson)

The objective of Task 7 is to establish that LMFBR fuels can be processed successfully by solvent extraction methods. Initial emphasis is on development of solvent extraction flowsheets suitable for interim processing of LMFBR fuels in existing plants. Present Purex flowsheets are being modified where necessary to provide for the high plutonium content of these fuels. The wide solvent extraction experience accumulated at production sites is being assessed and factored into these studies. Particular emphasis is being given to experimental evaluation of iodine behavior in solvent extraction and to the effect of solvent damage on process performance, especially when processing short-cooled fuels. Different solvent extraction contactors are being evaluated with respect to their relative merits for processing LMFBR fuels.

This month the effect of temperature on the distribution of plutonium and uranium in the TBP extraction system was studied and studies were continued on TBP degradation in nitric acid. Also, investigation of the stability of secondary amines in the nitric acid system was started.

### 7.1 Flowsheet Development (Task 7.1) (D. E. Horner, J. R. Collins)

We are obtaining data concerning the effect of temperature on the TBP extraction process at the high plutonium concentrations that will be typical of LMFBR fuels processing. In batch tests with a simulated first-cycle feed containing 7 g of Pu and 58 g of U per liter, the plutonium extraction coefficient increased from about 0.5 to 1.2 and the uranium coefficient decreased from about 1.7 to 1.0 when the extraction temperature was increased from 23 to  $60^\circ\text{C}$  (Fig. 7-1). In these tests the aqueous nitric acid concentration was 3 M, the TBP concentration was 15%, and the phase ratio was 1/1. Under these conditions, the plutonium and

ORNL DWG 69-10384

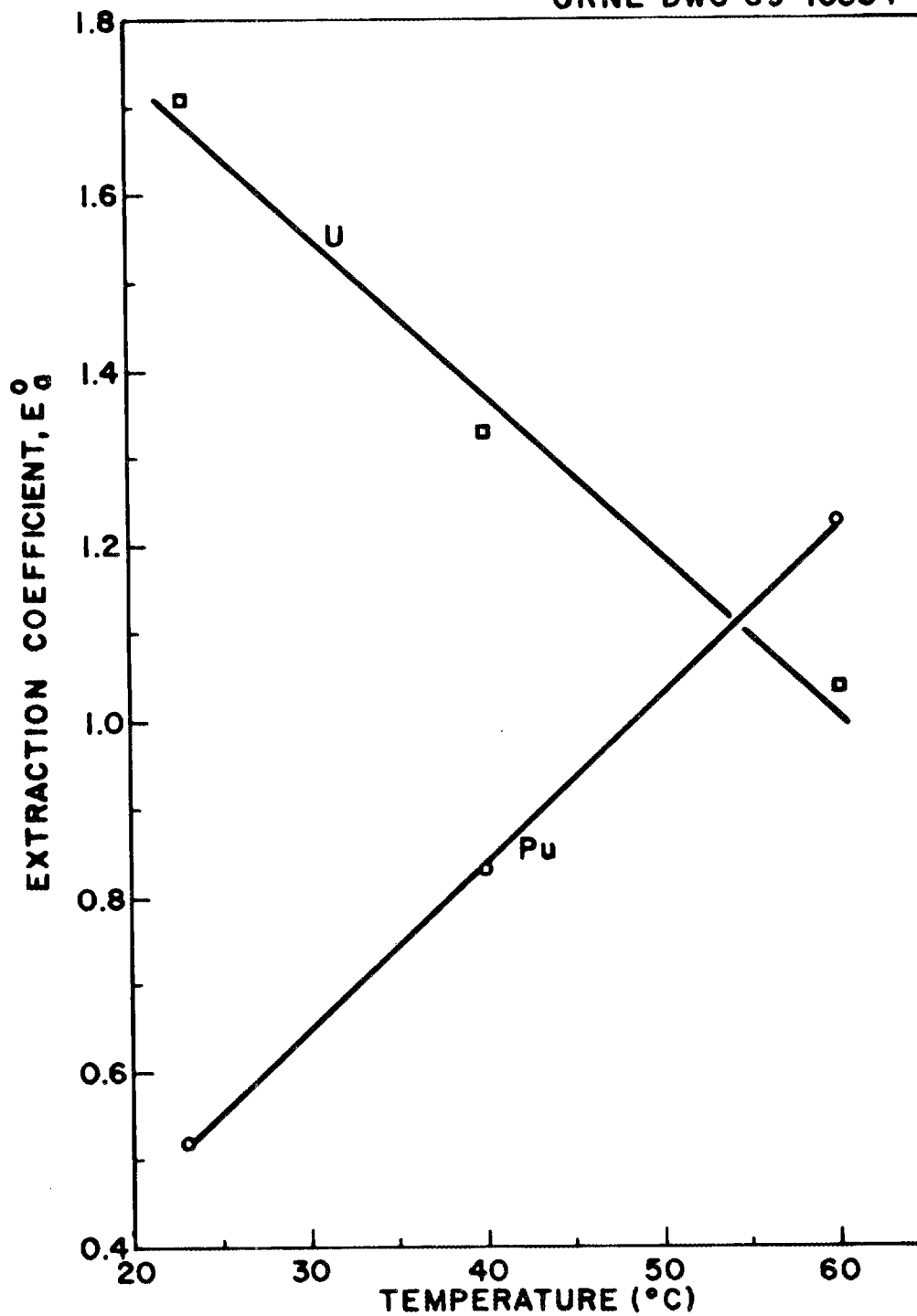


Fig. 7-1 Effect of Temperature on Plutonium and Uranium Extraction with 15% TBP-85% n-Dodecane. Aqueous phase: 3 M  $\text{HNO}_3$ , 7 g of Pu and 58 g of U per liter. Phase ratio: 1/1.

uranium extraction coefficients were approximately equal at 55°C.

Operating at an elevated temperature in the first-cycle extraction step would result in more efficient plutonium extraction, requiring fewer stages for recovery. The advantage of this must be balanced against the potential disadvantages of possible poorer decontamination from zirconium<sup>1</sup> and increased solvent degradation at the higher temperature.

We are determining the effect of temperature on the extraction and scrubbing of plutonium under second-cycle conditions where uranium would not be present.

### Computer Simulation of the TBP Extraction System (W. Davis, Jr.)

Groenier<sup>2</sup> recently summarized some of the pertinent factors concerning computer simulation of the TBP extraction system. Two of the most useful goals of such simulation are the optimization of the extraction process with a computer and assuring that concentrations of fissionable materials in the extractor will be within limits defined by criticality considerations. Groenier demonstrated that empirical analysis of data of J. G. Moore<sup>3</sup> can yield correlation coefficients that lead to reasonably good agreement between calculated and experimental (batch countercurrent) uranium and plutonium distribution data for a particular set of conditions. Unfortunately, there are other experimental distribution data, obtained under somewhat different conditions, that cannot be represented by these same correlation coefficients. While it is possible to rationalize some of the disagreements in terms of analytical difficulties and the presence of some Pu(VI), instead of only Pu(IV), yet we must recognize that correlation equations used to date, for example, in the report of Baumgartel, *et al.*,<sup>4</sup> were chosen for their simplicity and because there do not yet exist the additional data that are needed to permit formulation of more complicated, and more accurate, equations. These additional data include densities of aqueous and organic phases and the water content of the organic phase. They also include activity coefficients of the various species in the 5-component aqueous system H<sub>2</sub>O-HNO<sub>3</sub>-UO<sub>2</sub>(NO<sub>3</sub>)<sub>2</sub>-Pu(NO<sub>3</sub>)<sub>4</sub>-PuO<sub>2</sub>(NO<sub>3</sub>)<sub>2</sub>.

The probability that anyone will measure the activity coefficients in the 5-component aqueous system H<sub>2</sub>O-HNO<sub>3</sub>-UO<sub>2</sub>(NO<sub>3</sub>)<sub>2</sub>-Pu(NO<sub>3</sub>)<sub>4</sub>-PuO<sub>2</sub>(NO<sub>3</sub>)<sub>2</sub> in the near future appears to be very small. For this reason we have chosen to extrapolate our previous studies<sup>5</sup> of the aqueous system H<sub>2</sub>O-HNO<sub>3</sub>-UO<sub>2</sub>(NO<sub>3</sub>)<sub>2</sub> by assuming that the activity of nitric acid can be described by the equation

$$\ln \left[ \frac{a_2(m_2, m_3, m_4, m_5)}{a_2(m_2, 0, 0, 0)} \right] = [m_3 (P_1 + P_2 m_3) + m_4 (\alpha_1 + \alpha_2 m_4) + m_5 (\beta_1 + \beta_2 m_5)] \\ \times (1 + P_3 m_2 + P_4 m_2^2) \quad (1)$$

The term  $a_i$  ( $m_2, m_3, m_4, m_5$ ) represents the activity of species  $i$  as a function of the four concentrations  $m_2, m_3, m_4, m_5$ , any or all of which may equal zero. The subscripts 1, 2, 3, 4, and 5, on  $m$  or  $a$  only, refer, respectively, to  $H_2O, HNO_3, UO_2(NO_3)_2 \cdot 6H_2O, Pu(NO_3)_4,$  and  $PuO_2(NO_3)_2$ ;  $m_i$  is the concentration of component  $i$  in moles per kilogram of water;  $m_1 = 55.509$  moles  $H_2O/kg H_2O$  at  $25^\circ C$ ;  $P_1, P_2, P_3,$  and  $P_4$  are constants with values as previously reported;<sup>5</sup>  $\alpha_1, \alpha_2,$  and  $\beta_1, \beta_2$  are parameters to describe the assumed effects of  $Pu(NO_3)_4$  and  $PuO_2(NO_3)_2,$  respectively, on the activity of  $HNO_3.$  From Eq. (1) and the Gibbs-Duhem equation and the cross-differential equations,<sup>5</sup> we can derive the 4 equations to describe the activities of  $UO_2(NO_3)_2 \cdot 6H_2O, Pu(NO_3)_4, PuO_2(NO_3)_2,$  and  $H_2O.$

With accurate extraction data, densities, water content of the organic phase plus the assumption that the extended Debye-Huckel equation would apply to solutions of  $Pu(NO_3)_4$  in water and  $PuO_2(NO_3)_2$  in water if hydrolysis did not occur, then there is a high probability that we can determine all unknown parameters and, thereby, provide a more accurate basis for the computer simulation of the solvent extraction process.

## 7.2 Solvent Stability (Task 7.2)

(V. C. A. Vaughen, J. H. Goode, L. A. Byrd, G. D. Davis, W. B. Howerton, O. L. Kirkland, R. C. Lovelace)

Solvent extraction feed derived from leaching the short-decay fuel rods (Sect. 5.1) was used in batch cross-current cyclic experiments to study the radiation stability of 15% TBP in  $n$ -dodecane. In two 4-cycle runs the contact time of the organic solvent with the aqueous feed ( $\sim 2.8$   $\beta$ -watts/liter) in the extraction step was varied so as to provide a solvent dose of  $0.2$  whr liter<sup>-1</sup> cycle<sup>-1</sup> in the first run and  $0.6$  whr liter<sup>-1</sup> cycle<sup>-1</sup> in the second run. Data from these tests are incomplete and will be reported later.

## Decomposition of TBP and Precipitation of Butyl Phosphates in Aqueous Nitric Acid Solutions (W. Davis, Jr., A. H. Kibbey)

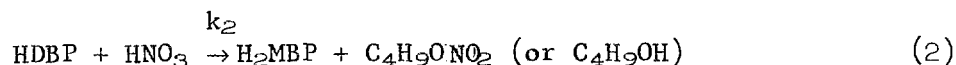
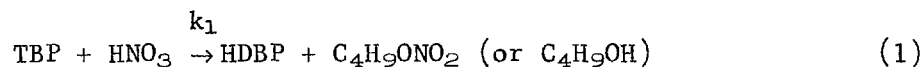
In a one- or two-phase system composed of water, nitric acid, and tributyl phosphate, the latter decomposes into dibutyl-, monobutyl-, and ortho-phosphoric acids. The extent of this decomposition is a function of concentrations, temperature, and time. If zirconium nitrate is added to such a system, the zirconium will form complexes with the phosphates. Depending upon the quantities of these complexes, they will either be dissolved in the TBP phase, if this is present in large amount, or will precipitate as a white solid, if very little TBP is present. Such precipitation apparently does occur in existing Purex solvent extraction plants. We have been primarily interested in determining the rate of

decomposition of TBP in the presence and absence of radiation in the absence of zirconium, on the one hand, and of precipitation of zirconium butyl phosphates in the aqueous phase, on the other, since there is so little information in the literature concerning these aspects of fuel processing. To keep the aqueous phase saturated with TBP, we have maintained enough TBP to form a second phase, typically 1 ml TBP/300 ml aqueous solution.

There are no experimental data on the solubility of TBP in aqueous nitric acid solutions at conditions corresponding to our studies, but we extrapolated data of Higgins, Baldwin, and Soldano<sup>6</sup> to calculate 328, 429, and 562 mg TBP per liter of 1, 3, and 5 M HNO<sub>3</sub>, respectively, at 50°C. Thus, only about 10 to 20% of the TBP in our experiments was in the aqueous phase if the extrapolated solubilities were correct. Using only visual examination we found that the solubility of TBP in 3 and 5 M HNO<sub>3</sub> containing 1 g Zr/liter was less than 300 but more than 150 mg/liter at 50°C. These values are significantly below the extrapolated values for HNO<sub>3</sub> solutions mentioned above.

Previous<sup>7</sup> decomposition experiments with 0.25 to 10 g Zr/liter in 1, 3, and 5 M HNO<sub>3</sub> at 50°C showed a long (approximately 4 days) induction period before precipitation was seen. We have now completed precipitation experiments with 3 and 5 M HNO<sub>3</sub> solutions containing somewhat less than to slightly more than enough TBP to saturate the aqueous phase. In general, we observed the same type of induction period prior to initiation of precipitation of zirconium butyl phosphates from aqueous solutions not saturated with TBP as we had with solutions in contact with a small amount of second-phase TBP.

We are using data on the quantities of dibutyl phosphoric acid (HDBP) and monobutyl phosphoric acid (H<sub>2</sub>MBP), formed during decomposition of TBP dissolved in the aqueous phase and in the absence of zirconium, to evaluate the quantities  $k_1S_0$  and  $k_2$  of the decomposition equations (1) and (2).



Here,  $S_0$  is the solubility of TBP in the aqueous phase, which, as we noted above, has not been measured for our experimental conditions. In most of our earlier experiments<sup>8,9</sup> the number of samples was too small and analyses for H<sub>2</sub>MBP too uncertain for us to calculate  $k_2$  (or  $k_3$ , the rate constant for decomposition of H<sub>2</sub>MBP to H<sub>3</sub>PO<sub>4</sub>). Thus, we have repeated 3 experiments at 1, 3, and 5 M HNO<sub>3</sub> and 50°C during which we took 5 to 7 samples. Rate constants  $k_1S_0$  calculated from these, and earlier experiments (Table 7-1) are in fairly good agreement. In addition, the uncertainties of calculated values of  $k_2$  are small enough to warrant our listing these. However, the large uncertainties (about equal to  $k_2$  itself)

preclude our making any attempt to explain why  $k_2$  decreases (instead of increases) as the nitric acid concentration increases.

Table 7-1. Rate Constants in the Successive Steps of TBP Decomposition

Conditions: Org. Vol. = 0.003 to < 0.05  
Aq. Vol.  
 Temperature = 50°C

HNO <sub>3</sub> Conc. (M)	No. of Points	$10^4 \times k_1 S_0$ and $\pm 10^4 \sigma(k_1 S_0)$ mmoles liter <sup>-1</sup> hr <sup>-1</sup>	$10^4 \times k_2$ and $\pm 10^4 \times \sigma(k_2)$ (hr <sup>-1</sup> )
1 <sup>a</sup>	4	3.4 ± 0.6	--
1	6	3.5 ± 1.8	3.6 ± 3.0
3 <sup>a</sup>	4	8.6 ± 0.6	--
3	7	6.4 ± 2.2	2.0 ± 2.7
5 <sup>a</sup>	4	9.9 ± 1.0	--
5	5	8.9 ± 4.8	1.7 ± 1.2

<sup>a</sup>Data previously reported.

#### Chromatographic Studies of Solvent Degradation Products (J. G. Moore)

Studies were started to determine the stability of secondary amines in nitric acid systems since these compounds are potentially an attractive alternative to ion-exchange for the final purification of plutonium in the LMFBR fuel processing cycle. For example, with 0.3 M di(tridecyl)amine in diethyl-benzene as the solvent, plutonium can be extracted effectively from 5 M HNO<sub>3</sub> and then recovered by stripping the organic phase with 0.15 M HNO<sub>3</sub>.

In the initial degradation tests, amine solutions were subjected to rather extreme conditions to obtain samples of degraded material for chromatographic studies. French workers have reported rapid degradation of trilaurylamine in the presence of nitrite but avoided this difficulty by adding sulfamate ion to the system. To study the effect of nitrite, we contacted a diethylbenzene solution containing 0.3 M di(tridecyl)amine for 4 hr at 23° and 40°C with an equal volume of 7 M HNO with and without 0.05 M NaNO<sub>2</sub> initially present. After contact, the organic phases were separated, scrubbed for 5 min with an equal volume of 0.15 M HNO<sub>3</sub> and then

converted to free amine by contacting with 0.3 M  $\text{Na}_2\text{CO}_3$ . There was no change in the amine concentration in the 7 M  $\text{HNO}_3$  tests that did not have nitrite present; however, when nitrite was present, the amine concentration decreased 15 and 30% in the 23 and 40°C tests, respectively.

Several stationary phases have been reported as useful for separating amines and their degradation products: SE-30,<sup>10</sup> Apiezon L,<sup>11</sup> Apiezon N,<sup>12</sup> and E 301<sup>11</sup>. Columns will be prepared with each of these materials using Corning GLC 110 Textured Surface Beads as the solid support. This support is 100 to 120 mesh and has been silanized with DMCS. Aliquots of the organic and aqueous phases used in the aforementioned tests will be chromatographed using each of these columns under various temperature conditions.

### References

1. D. G. Karraker, "Temperature Effects on TBP Solvent Extraction Processes," *Progress in Nuclear Energy - Process Chemistry*, **3**, 188, Pergamon Press, N. Y. (1961).
2. W. E. Unger, *et al.*, Aqueous Processing of LMFBR Fuels Progress Report June 1969, No. 4, ORNL-TM-2650.
3. J. G. Moore, The Extraction of Plutonium(VI) from Nitric Acid--Uranyl Nitrate Solutions by Tri-n-Butyl Phosphate, ORNL-4348 (January 1969).
4. G. Baumgartel, W. Ochsenfeld, and H. Schieder, The Distribution of Metal Nitrates in the System  $\text{Pu}(\text{NO}_3)_4\text{-UO}_2(\text{NO}_3)_2\text{-HNO}_3\text{/TBP-Dodecane}$ , Kernforschungszentrum Karlsruhe, Institute for Hot Chemistry, OLS 48/68, KFK 680, Eur 3707d.
5. W. Davis, Jr., P. S. Lawson, H. J. deBruin, and J. Mrochek, "Activities of the Three Components in the System Water--Nitric Acid--Uranyl Nitrate Hexahydrate at 25°C," *J. Phys. Chem.* **69**, 1904 (1965).
6. C. E. Higgins, W. H. Baldwin, and B. A. Soldano, "Effects of Electrolytes and Temperature on the Solubility of Tributyl Phosphate in Water," *J. Phys. Chem.* **63**, 113 (1959).
7. W. E. Unger, *et al.*, Aqueous Processing of LMFBR Fuels Progress Report August 1969, No. 5, ORNL-TM-2671.
8. W. E. Unger, *et al.*, Aqueous Processing of LMFBR Fuels Progress Report April 1969, No. 1, ORNL-TM-2552.
9. Chem. Technol. Div. Ann. Progr. Rept. May 31, 1969, ORNL-4422.
10. R. Narvaez, Curium Process Development III-I. Analytical Techniques for Characterizing Solvent, DP-1010 (July 1966).

11. G. Grossi and R. Vece, "The Gas Chromatographic Analysis of Primary, Secondary, and Tertiary Fatty Amines, and of Corresponding Quaternary Ammonium Compounds," J. Gas Chromatograph 3: 170(1965).
12. M. H. Campbell, "Gas Chromatographic Analysis of Solvent Used in Reactor Fuel Reprocessing and Fission Product Recovery", Anal. Chem. 38, 237 (1966).

#### 8. PLUTONIUM PURIFICATION (TASK 8) (D. J. Crouse)

This task covers the process steps in purifying plutonium, starting with the plutonium product solution from the first Purex cycle and continuing through preparation of a product solution of adequate purity and concentration for delivery to the fuel refabrication operation.

Plutonium chemistry is reasonably well-known although the high plutonium content of LMFBR fuels makes some process revisions desirable. The large amounts of plutonium to be handled provide strong incentive for improving the efficiency of the plutonium purification processes since the cost of these operations will represent a much larger fraction of the total reprocessing costs than previously. In particular there appears to be a need for a higher capacity process than ion exchange for final decontamination of the plutonium.

This month additional tests were run to define the limits to which the TBP solvent can be loaded with plutonium without formation of a third liquid phase. Data from the tests are not sufficiently complete to allow reporting at this time.

#### 9. WASTE TREATMENT AND STORAGE (TASK 9)

Progress on this task is reported separately.

#### 10. OFF-GAS TREATMENT (TASK 10) (D. J. Crouse, C. D. Watson)

Retention of iodine is the major problem in treating the off-gas from processing of short-cooled LMFBR fuels since plant retention factors of  $10^7$  and  $10^8$  would be required. Retention of most of the xenon and krypton, and eventually tritium, also may be required for future large processing plants. Logic diagrams illustrating alternative processing methods, based on present knowledge, for removing the gases from off-gas streams were presented previously.<sup>1</sup> All promising methods will be evaluated and additional chemical and engineering data developed where necessary. Studies are active in the areas of (1) scrubbing iodine species

from gas streams with mercuric nitrate--nitric acid and alkaline solutions, (2) decomposition of organic solvent vapors and organic iodides by catalytic oxidation, and (3) testing of solid iodine adsorbents.

This month (1) an iodine removal system was tested in the TRU facility at ORNL, (2) additional tests with silver zeolite showed that the presence of dodecane in the gas stream decreased the  $\text{CH}_3\text{I}$  trapping efficiency with this effect being greatest at  $350^\circ\text{C}$ , (3) reaction rate constants were determined for reaction of methyl-, ethyl-, n-propyl-, and n-butyliodides with mercuric nitrate solutions, and (4) the reaction of elemental iodine with acidic mercuric nitrate solutions was shown to involve disproportionation of the iodine into the iodide and iodate forms.

### 10.1 Iodine (Task 10.1)

#### Results of Iodine Evolution and Iodine Trapping Experiments at the TRU Facility (O. O. Yarbrow, G. I. Cathers, TRU personnel)

The transuranium processing plant at ORNL processes plutonium and curium targets after decay times of only 5 to 10 days for the recovery of short-lived transcurium elements. Such target processing campaigns (two or three a year) provide an excellent opportunity for demonstrating iodine handling techniques, applicable to LMFBR processing, on a significant scale and under actual plant conditions. In the processing campaigns, completed in September, three separate experiments were conducted to demonstrate (1) removal of iodine from the dissolver solution, and (2) trapping of iodine from the off-gas. Iodine was driven from the nitric acid dissolver solution, by air sparging at elevated temperatures. The amount of iodine removed ranged from 97 to 98.5% in the three runs. Iodine removal equipment on the dissolver off-gas stream consisted of two liquid scrubbers in series, followed by a Hopcalite bed--charcoal bed system. This removal system demonstrated iodine decontamination factors ranging from  $1 \times 10^5$  to  $4 \times 10^6$  for the three runs.

The arrangement of the dissolver and dissolver off-gas iodine removal system is shown in Fig. 10-1. The aluminum in the targets was first dissolved in caustic-sodium nitrate solution and the dejacketing solution was disposed of by pumping it from the dissolver. The remaining actinide oxides were dissolved by digesting in 2.5 liter of 10 M nitric acid for 2 hr at  $110^\circ\text{C}$ . The dissolver was sparged at 200 cc/min with no additional gas purge to the vapor space during this part of the run. Following the 2-hr dissolution period, the dissolver solution was cooled to 80 to  $90^\circ\text{C}$  and diluted to 5 liters. This solution was digested for 8 to 10 hr while sparging at 2 to 3 liter/min and purging the vapor space with air at about 8 liter/min. Sodium nitrite was added at a rate of 0.02 moles/hr. After six hours of digesting at 80 to  $90^\circ$ , a batch addition of 0.05 moles of potassium iodide was made to the dissolver solution. Iodine removal during the two hour digest at  $110^\circ\text{C}$  averaged about 85% corresponding to a removal half-life of about  $3/4$  hr. Iodine removal half-lives for the

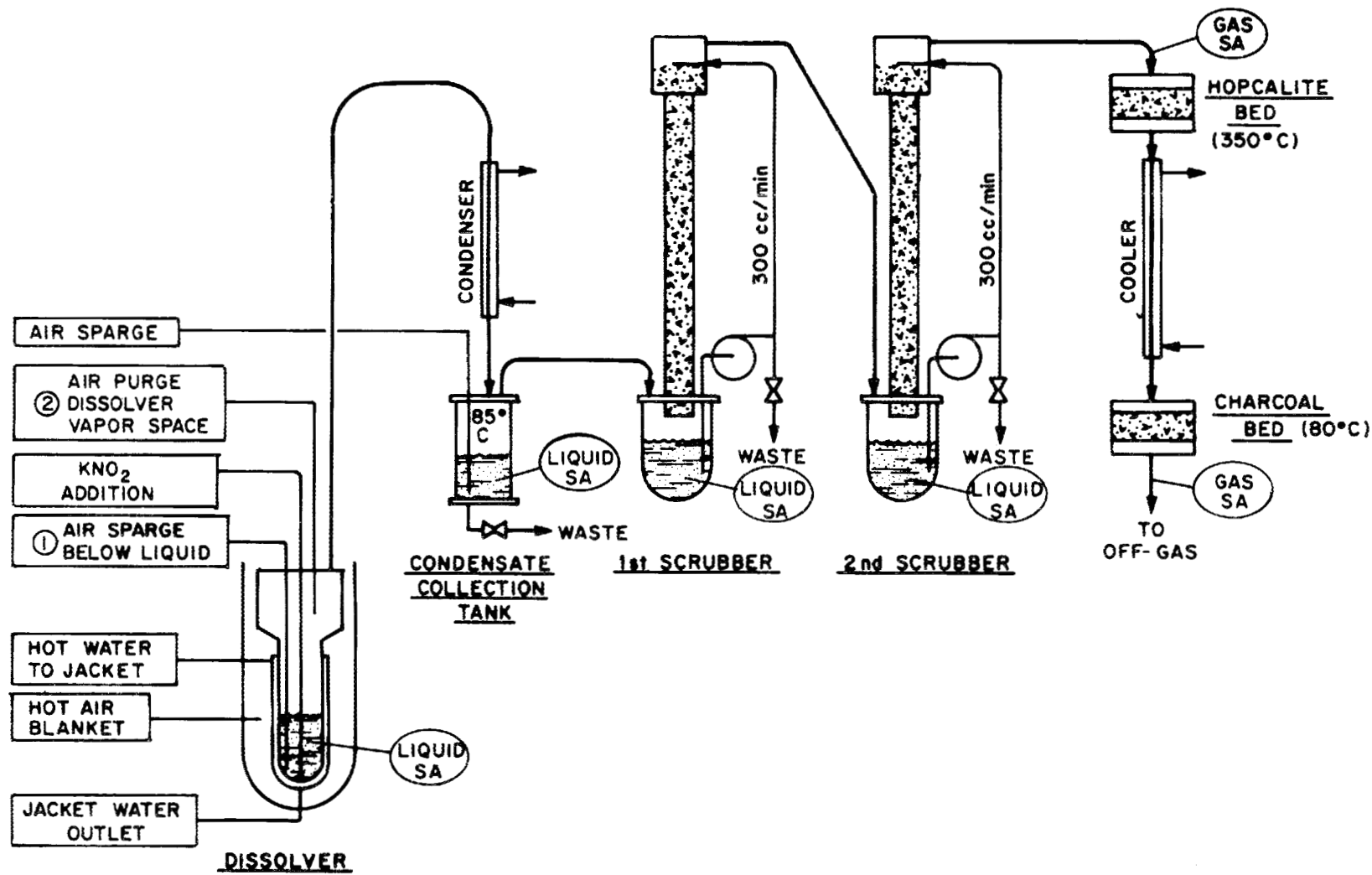


Fig. 10-1 Dissolver and Iodine Removal System Flowsheet TRU Campaign No. 13.

second part of the digest period were 3.5 hr for the first run and about 2.5 hr for the second and third runs. The batch addition of potassium iodide had no measurable effect on the iodine evolution rate in any of the three runs. Total iodine removal ranged from 97 to 98.5% for the three runs. There was strong evidence of iodine accumulation in the gas space of the dissolver during the final run as the iodine was evolved from the dissolver solution at a normal rate throughout the run, but showed up in the off-gas treatment equipment eight hours after the start of the run. The removal half-lives for iodine evolution from the dissolver were much longer than would be predicted from laboratory tests under ideal conditions, and reflux of iodine in the top of the dissolver is the probable cause.

The equipment in the dissolver off-gas removal system (Fig. 10-1) included a condensate catch pot, two liquid scrubbers, a heated Hopcalite bed, a cooler, and a charcoal bed. It was intended that the bulk of the vapors from the dissolver would be condensed and collected in the condensate catch pot. A leak developed at the bottom of this pot at the start of the second run making it necessary to run the condensate pot dry and route the vapors from the dissolver directly into the first scrubber during the second and third runs. This leak grew progressively worse during the third run, until excessive air inleakage made it necessary to leave off the air purge to the dissolver gas space.

The two scrubbers were identical in construction and consisted of a 1-5/8-in.-diam by 44-in.-long packed section filled with 1/4-in. Intalox Saddles. An initial charge of 3 liters of solution was added to the scrubber at the start of each run and solution was recirculated through the column at the rate of 200 cc/min throughout the run. Gas and liquid flowrates through the scrubber averaged 100 and 2000 lb hr<sup>-1</sup> ft<sup>-2</sup>, respectively. The first scrubber was operated with 0.1 M mercuric nitrate--0.1 M nitric acid in the first two runs and with 1 M sodium hydroxide--0.05 M sodium thiosulphate in the third run. The second scrubber was operated with caustic-thiosulphate in all three runs. Decontamination factors for the scrubber are tabulated in Table 10.1. The iodine decontamination factor of 20 to 30 for a single mercuric nitrate scrubber is in line with expected values from laboratory studies. In this campaign a single caustic scrubber outperformed a single mercury scrubber by a significant margin. (DF of 160 for caustic versus 25 for mercuric nitrate.) This may present a biased picture, however, as a series of mercuric nitrate scrubbers will progressively increase the overall DF's, while as shown in run No. 3, additional caustic scrubbers add little to the overall decontamination factor.

Gases from the second scrubber were passed through a catalytic burner (Hopcalite) operated at about 330°C to oxidize any organic compounds in the gas and then were cooled to about 80°C and passed through a 2-in.-depth of KI-treated charcoal for iodine removal. The gas residence time in both the Hopcalite bed and the charcoal bed was about 10 sec. Decontamination factors across the charcoal bed were about 2 x 10<sup>4</sup> for the first two runs, but dropped to 270 for the final run. In this run moisture was observed in the gas samplers before and after the charcoal bed, and the high

humidity possibly accounts for the loss in DF. Overall iodine decontamination factors for the iodine removal system were about  $3.5 \times 10^6$  for the first two runs, dropping to  $1 \times 10^5$  for the last run due to the relatively low DF across the charcoal bed.

Table 10-1 Iodine Decontamination of  
Off-Gas in TRU Test Facility

(Charcoal bed temp. was 70°C in all tests)

Run No.	Gas Flow (ft <sup>3</sup> min <sup>-1</sup> )	Hopcalite Bed Temp. (°C)	Iodine Decontamination Factor			
			First Scrubber	Second Scrubber	Hopcalite- Charcoal	Overall
1	9.1	340-370	18 <sup>a</sup>	9 <sup>b</sup>	$2 \times 10^4$	$3 \times 10^6$
2	3.1	340-370	29 <sup>a</sup>	13 <sup>b</sup>	$1 \times 10^4$	$4 \times 10^6$
3	8.2	300-350	160 <sup>b</sup>	2 <sup>b</sup>	270	$1 \times 10^5$

<sup>a</sup>0.1 M Hg(NO<sub>3</sub>)<sub>2</sub>--0.1 M HNO<sub>3</sub> solution.

<sup>b</sup>1 M NaOH--0.05 M Na<sub>2</sub>S<sub>2</sub>O<sub>3</sub> solution.

Trapping of Radioactive Iodine by Silver Zeolite (R. E. Adams, R. D. Ackley, Zell Combs)

The primary objective of our studies is to develop information to aid in the design of an extremely efficient iodine removal system for LMFBR fuel reprocessing plants. Most of the attention thus far has been given to methods of trapping methyl iodide since trapping of iodine in this form appears to represent one of the more difficult aspects of the iodine retention problem. Recently, the applicability of AgNO<sub>3</sub>-treated Linde Molecular Sieves, Type 13X, (referred to as silver zeolite or Ag-13X) has been under investigation,<sup>2,3</sup> and this agent efficiently trapped CH<sub>3</sub>I from flowing air when the operating temperature was in the range of 100 to 400°C. The Ag-13X adsorber is a development at Idaho Nuclear Corporation reported by Maeck, Pence, and Keller.<sup>4</sup>

Data were obtained at 350 and 450°C for the trapping of CH<sub>3</sub>I on Ag-13X when the air stream contained n-dodecane vapor. In these tests the Ag-13X, in the form of two 1-in. beds in series, was exposed to air containing dodecane vapor for an 18-hr period prior to CH<sub>3</sub>I injection and, also, during the 2-hr period in which CH<sub>3</sub>I was injected. The estimated amount of dodecane introduced into the gas stream was about 20% of the Ag-13X weight. The CH<sub>3</sub>I concentration was 3 ppm, providing (in 2 hr) about 0.5 mg CH<sub>3</sub>I per g of Ag-13X.

The test results, along with data reported previously<sup>3</sup> for tests at 100 and 200°C, are shown in Table 10-2. The decontamination efficiencies for either a 1- or 2-in. depth were highest at 100°C and reached a minimum at about 350°C. We interpret the data as follows: physical adsorption of dodecane (which decreases with increasing temperature) is unimportant; dodecane decomposition in the bed is negligible at 100°C but is appreciable at 200°C and at higher temperatures resulting in deposition of a tar-like material on the Ag-13X that poisons it; at 450°C, the poisoning still occurs but the higher temperature promotes oxidation of the tar and mitigates the poisoning effect. In any event, the Ag-13X may be less susceptible to poisoning than is charcoal which is often used for trapping radioiodine. Passing the gas stream through a catalytic oxidation unit to destroy organic vapors prior to trapping the iodine on a Ag-13X bed should be an effective iodine retention system. The high cost of silver is a potential disadvantage. Although it is assumed that the silver zeolite would be used for removal of the last traces of iodine from the gas rather than for removal of the bulk iodine, its ultimate iodine capacity will be important in evaluating its application. Consequently, we are presently making capacity measurements.

Table 10-2 Effect of Exposure to n-Dodecane Vapor<sup>a</sup> on Efficiency of Ag-13X for Decontaminating Flowing Air Containing Methyl Iodide

Temperature (°C)	Face Velocity (fpm)	Decontamination Efficiency (%)	
		For 1-in. Depth	For 2-in. Depth
100	50	99.56	99.99+
200	63	95.45	99.86
350	84	92.04	99.28
450	97	94.77	99.93

<sup>a</sup> Bed was pre-exposed to flowing air containing dodecane for 18 hr prior to CH<sub>3</sub>I injection; temperature during pre-exposure was the same as during CH<sub>3</sub>I injection.

Measurement of the Reaction Rates of Organic Iodides with Mercuric Nitrate Solutions (R. E. Adams, R. L. Bennett, Ruth Slusher)

The study of the reaction rate of  $\text{CH}_3\text{I}$  with mercuric nitrate--nitric acid solutions was continued and extended to higher molecular weight organic iodides. These other organic iodides are important since they have been detected by gas chromatography in fuel processing off-gas at several installations. We determined the relative reactivity of methyl, ethyl, *n*-propyl, and *n*-butyl iodides with 0.001 M  $\text{Hg}(\text{NO}_3)_2$ --0.005 M  $\text{HNO}_3$  solution. Measurements at higher mercury concentrations were not possible with the presently-used techniques because of the greater reactivity of the higher iodides. The pseudo-first order rate constants obtained at this concentration are listed in Table 10-3.

The rate sequence: methyl < ethyl > *n*-propyl = *n*-butyl may appear to be erratic, but this order is consistent with the results reported from other studies of the reaction of alkyl halides assisted by electrophilic agents such as silver and mercuric nitrates.<sup>5-8</sup> Table 10.4 lists the relative rates obtained in several of these studies and shows this very distinct trend. The relative rates listed have been normalized to the rate of the ethyl halide in each study and apply only to that set of conditions. It is clear that ethyl is the most reactive of the primary low molecular weight halides. This is believed by Benfey<sup>6</sup> to be due to hyperconjugation effects. According to hyperconjugation theory, the more hydrogen atoms on the beta-carbon, the greater is the reactivity. Methyl (with none) is slow, ethyl (with the maximum, 3) is very fast, and *n*-propyl and *n*-butyl (with two) are intermediate in reactivity. However, where branching occurs at the carbon past the alpha-carbon, as with iso-butyl and neopentyl groups, steric effects cause a greatly diminished rate.

If branching occurs on the alpha-carbon, the total number of hydrogens on the adjacent beta-carbons can be large (the secondary isopropyl group has six) and fast rates may be expected. Extremely rapid rates have been observed for secondary and tertiary halides (see Table 10-4). Apparently, then, the reaction rate of most organic iodides, with the exception of branched chain primary iodides such as isobutyl and neopentyl, should be more rapid than methyl iodide. This conclusion applies to reaction in solution and the effects of extremely low solubility of the higher iodides must be considered in the overall removal process.

Table 10-3 Reaction Rate at 30°C of Organic Iodides with 0.001 M  $\text{Hg}(\text{NO}_3)_2$ --0.005 M  $\text{HNO}_3$  Solutions

Alkyl Iodide	Pseudo First Order Rate Constant ( $\text{min}^{-1}$ )
Methyl-	0.13
Ethyl-	0.82
<i>n</i> -Propyl-	0.51
<i>n</i> -Butyl-	0.52

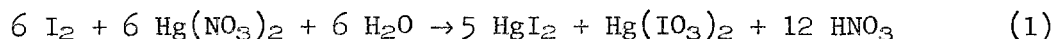
Table 10-4 Relative Reaction Rates of Alkyl Halides in Presence  
of Electrophilic Reagents: Silver and Mercuric Nitrates

	Relative Reaction Rate ( $k_R/k_{C_2H_5}$ )				
	<u>Our Work</u> RI-Hg(NO <sub>3</sub> ) <sub>2</sub> 0.005 M HNO <sub>3</sub>	<u>Dostrovsky and Hughes</u> RBr-AgNO <sub>3</sub> 70% Ethyl Alcohol	<u>Benfey</u> RBr-Hg(NO <sub>3</sub> ) <sub>2</sub> 70% Dioxane	<u>Burke and Donnan</u> RI-AgNO <sub>3</sub> Ethyl Alcohol	<u>Hammond, et al.</u> RI-AgNO <sub>3</sub> Acetonitrile
<u>Primary</u>					
CH <sub>3</sub> -	0.16	0.81		0.43	0.14
CH <sub>3</sub> CH <sub>2</sub> -	1	1	1	1	1
CH <sub>3</sub> (CH <sub>2</sub> ) <sub>2</sub> -	0.62	0.55	0.50	0.45	
CH <sub>3</sub> (CH <sub>2</sub> ) <sub>3</sub> -	0.63				
(CH <sub>3</sub> ) <sub>2</sub> CHCH <sub>2</sub> -		0.08		0.06	
(CH <sub>3</sub> ) <sub>3</sub> CCH <sub>2</sub> -		0.01			
<u>Secondary</u>					
(CH <sub>3</sub> ) <sub>2</sub> CH-			145		
<u>Tertiary</u>					
(CH <sub>3</sub> ) <sub>3</sub> C-					<sup>a</sup>

<sup>a</sup>Tertiary butyl rate was too fast to measure even at 0°C.

Elemental Iodine Adsorption in Mercuric Nitrate Solutions (D. J. Crouse  
J. M. Schmitt, F. G. Seeley)

Recent studies of the reaction of elemental iodine with mercuric nitrate--nitric acid solutions indicate that the iodine disproportionates into iodide and iodate according to the following reaction:



We are able to distinguish between the mercury-complexed iodine and iodate by an extraction method. The iodate is not extracted with diamylamylphosphonate (DAAP) whereas the mercury-complexed iodine is almost completely extracted from 0.1 to 0.2 M HNO<sub>3</sub> in three contacts with 1 M DAAP--dodecane at a phase ratio of 1/1. When elemental iodine was reacted with a mercuric nitrate solution and iodine was then extracted from this solution with DAAP, about one-sixth of the iodine was inextractable, confirming that the reaction shown in equation (1) occurs.

The mercuric iodate is relatively insoluble and separated as a fine white precipitate in some tests. Chemical analysis of the precipitate confirmed that it was mercuric iodate. This low solubility imposes a limit to which the mercuric nitrate solution can be loaded with iodine without precipitate formation that is much lower than the limit dictated by the solubility of mercuric iodide. For example, on titration of 0.05 M Hg(NO<sub>3</sub>)<sub>2</sub>--0.1 M HNO<sub>3</sub> solution with sodium iodide solution, precipitation of mercuric iodide begins at an iodine/mercury mole ratio of about 1/3. When the iodine is added as elemental iodine, however, precipitation of mercuric iodate begins at an iodine/mercury ratio of about 1/70, corresponding to a mercuric iodate solubility in the solution of slightly higher than 0.0001 M.

We considered that iodine present in the scrub solution as iodate might be more subject to release than iodine present as a mercuric iodide complex since the former normally can be reduced in nitric acid to volatile elemental iodine with, for example, nitrite ion. However, in preliminary tests we have not been able to reduce any of the iodate in the scrub solution by adding sodium nitrite, sodium sulfite, or potassium iodide to the solution, indicating that mercuric ion forms strong complexes with iodate ion as well as with iodide ion. Some tests were run in which the scrub solution was sparged with air while intermittently adding sodium nitrite; no release of iodine from the solution was detected. Although nitrite does not reduce the iodate once formed, having nitrite present in the mercuric nitrate solution during reaction with I<sub>2</sub> prevents iodate from forming. Study of this system is continuing.

References

1. W. E. Unger, et al., Aqueous Processing of LMFBR Fuels Progress Report April 1969, No. 1, ORNL-TM-2552.
2. W. E. Unger, et al., Aqueous Processing of LMFBR Fuels Progress Report August 1969, No. 5, ORNL-TM-2671.

3. W. E. Unger, et al., Aqueous Processing of LMFBR Fuels Progress Report October 1969, No. 6, ORNL-TM-2710.
4. W. J. Maeck, D. T. Pence, and J. H. Keller, "A Highly Efficient Inorganic Adsorber for Airborne Iodine Species," in Proceedings of the Tenth AEC Air Cleaning Conference, New York, August 28, 1968, USAEC Report CON-680821, pp. 185-203.
5. I. Dostrovsky and E. D. Hughes, J. Chem. Soc. 169 (1946).
6. O. T. Benfey, J. Am. Chem. Soc. 70, 2163 (1948).
7. K. A. Burke and F. G. Donnan, J. Chem. Soc. 85, 555 (1904).
8. G. S. Hammond, M. F. Hawthorne, J. H. Waters and B. M. Graybill, J. Am. Chem. Soc. 82, 704 (1960).

## 11. RADIATION AND SHIELDING (TASK 11) (J. P. Nichols)

This task consists of analytical studies with the objective of developing information on the radiation properties and shielding requirements of LMFBR fuels outside the reactor. The work involves compilation and correlation of basic nuclear data including decay schemes, nuclear cross sections, radiation sources, and energy spectra, and thermal power (Task 11.1); development of computer programs for calculating transient concentrations of radionuclides in LMFBR fuel (Task 11.2); calculation of dose attenuation kerma for shield materials of interest (Task 11.3); and application of these data to LMFBR fuel cycle processes (Task 11.4).

### 11.2 Concentrations of Nuclides in LMFBR Fuel (M. J. Bell)

The isotopic composition, activity and heat generation rate of the spent fuel discharged from the FFTF has been computed with the ORIGEN code. The calculations were for an average specific power of 100 Mw/MT and 45,000 Mwd/MT burnup and assumed that the fresh fuel contained 78.5% natural U and 21.5% Pu. This information will be used to define the activity and heat generation rate to be expected in shipping and processing spent fast reactor fuels.

### 11.4 Neutron and Capture Gamma Dose Rates from LMFBR Fuels (E. D. Arnold, H. F. Soard)

Calculations are continuing with the ANISN program in the  $S_{16}P_3$  approximation to evaluate the effect of shielding materials on the neutron and capture gamma dose rates from LMFBR spent fuel shipping casks. New 27-neutron group, 20-gamma group  $S_{16}P_3$  cross sections have been generated for B, Pb,  $^{235}\text{U}$ ,  $^{238}\text{U}$ ,  $^{239}\text{Pu}$ ,  $^{240}\text{Pu}$ ,  $^{241}\text{Pu}$ , and  $^{242}\text{Pu}$  to complement the cross sections that are already on hand for most of the materials of potential interest. Cross sections are being generated for lithium.

Figures 11-1 and 11-2 summarizes the calculated neutron and capture gamma dose rates for four shield configurations - iron only, iron plus water, iron plus water containing 1 wt % boron, and iron plus polyethylene. The neutron dose rates are essentially the same for the three hydrogenous materials (water, boronated water, and polyethylene) and there is little difference in the capture gamma dose rates when the hydrogenous material is water or polyethylene. As compared to water, the effect of the 1% boronated water is to reduce the capture gamma dose rate by a factor of approximately 3. In other calculations it was found that the effect of water containing 3 wt % boron was to reduce the capture gamma dose rate by an additional 19%.

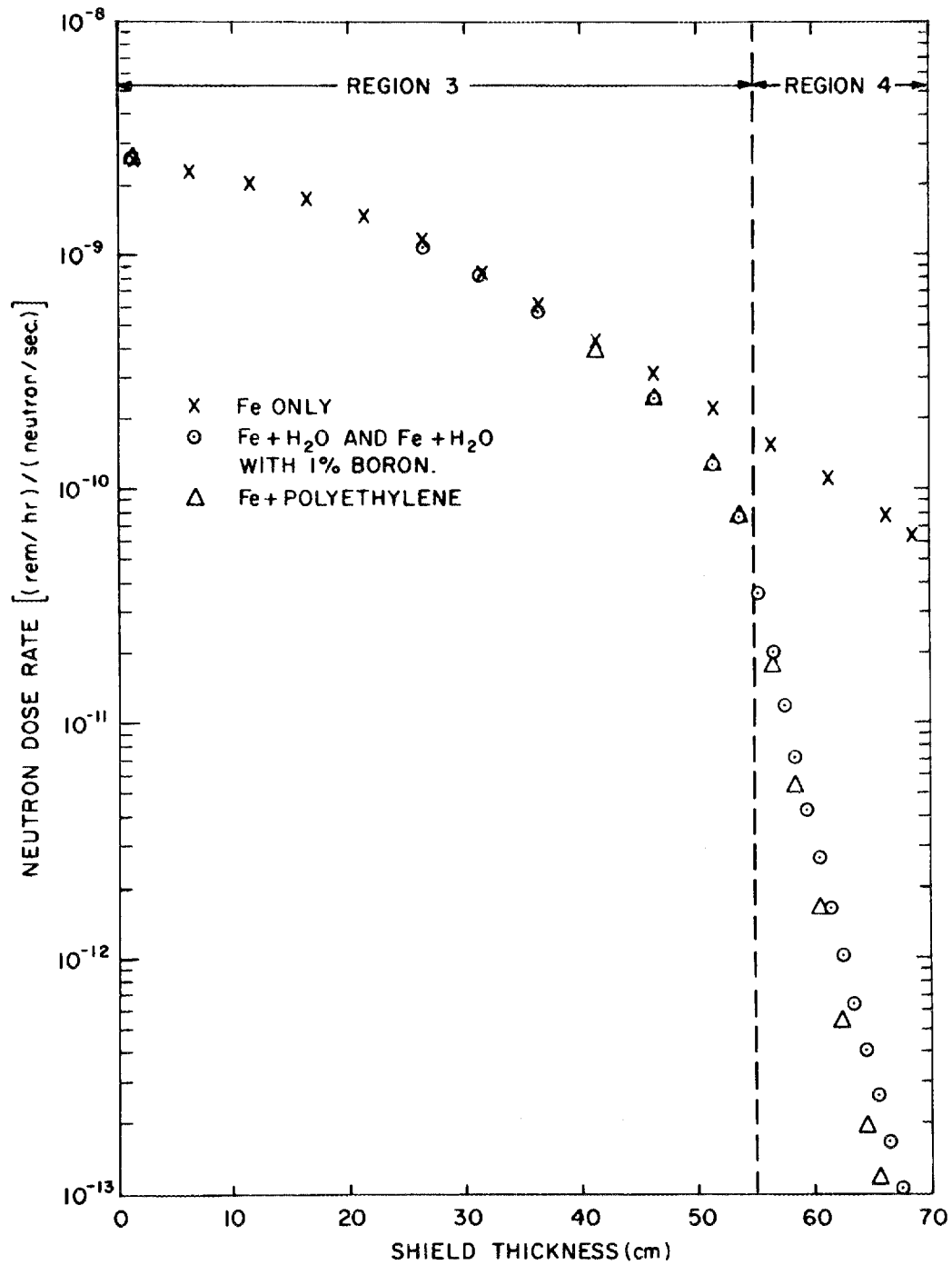


Fig. 11-1 Effect of Shield Composition and Thickness on Neutron Dose Rate from 36 LMFBR Core Elements.

ORNL DWG 69-10352

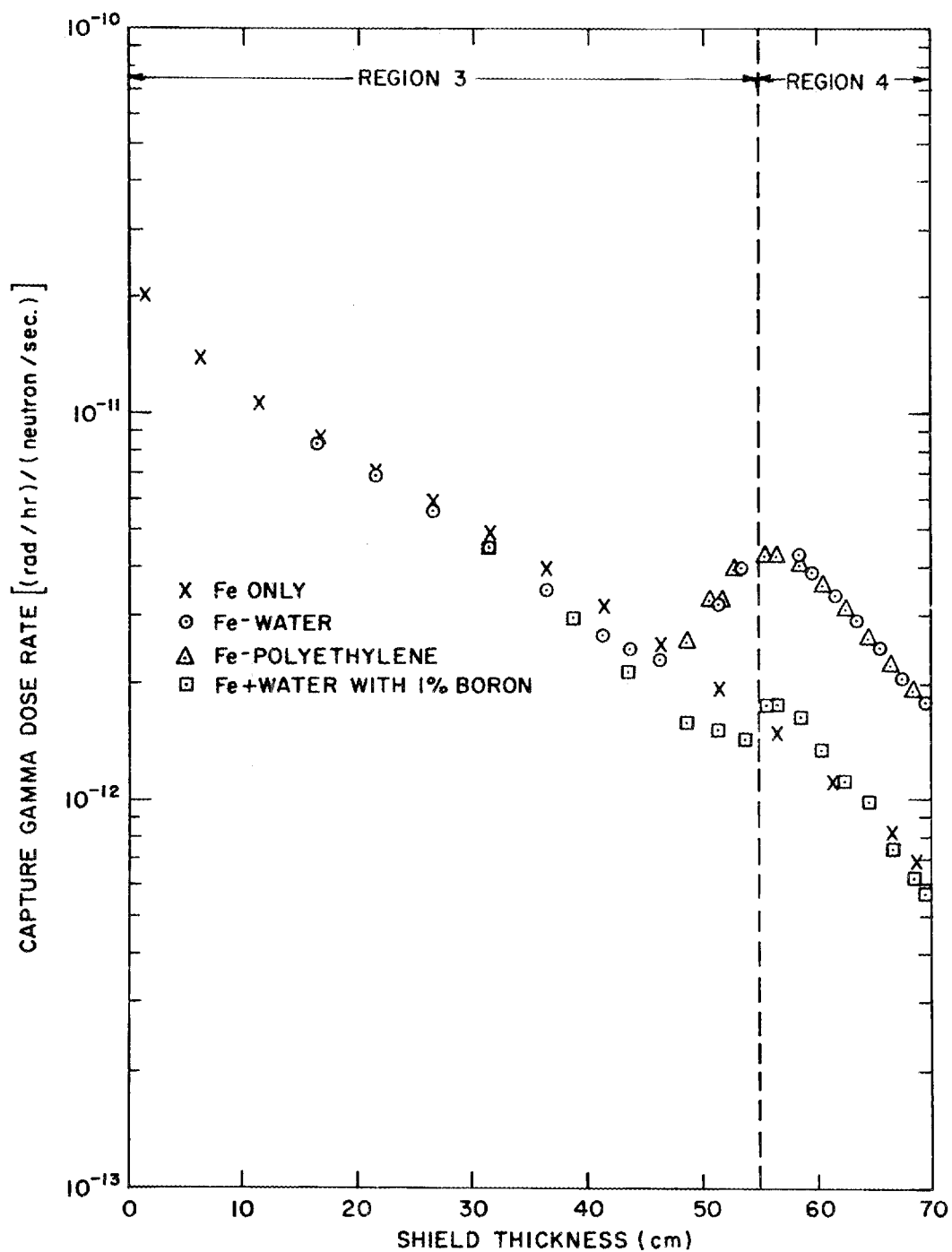


Fig. 11-2 Effect of Shield Composition and Thickness on Capture Gamma Dose Rate from 36 LMFBR Core Elements.

In Figures 11-1 and 11-2 region 3 consists of 55 cm of iron. Region 4 is the homogeneous material except for the all iron calculation where region 3 and region 4 were input as a single region.

## 12. CRITICALITY (TASK 12) (J. P. Nichols)

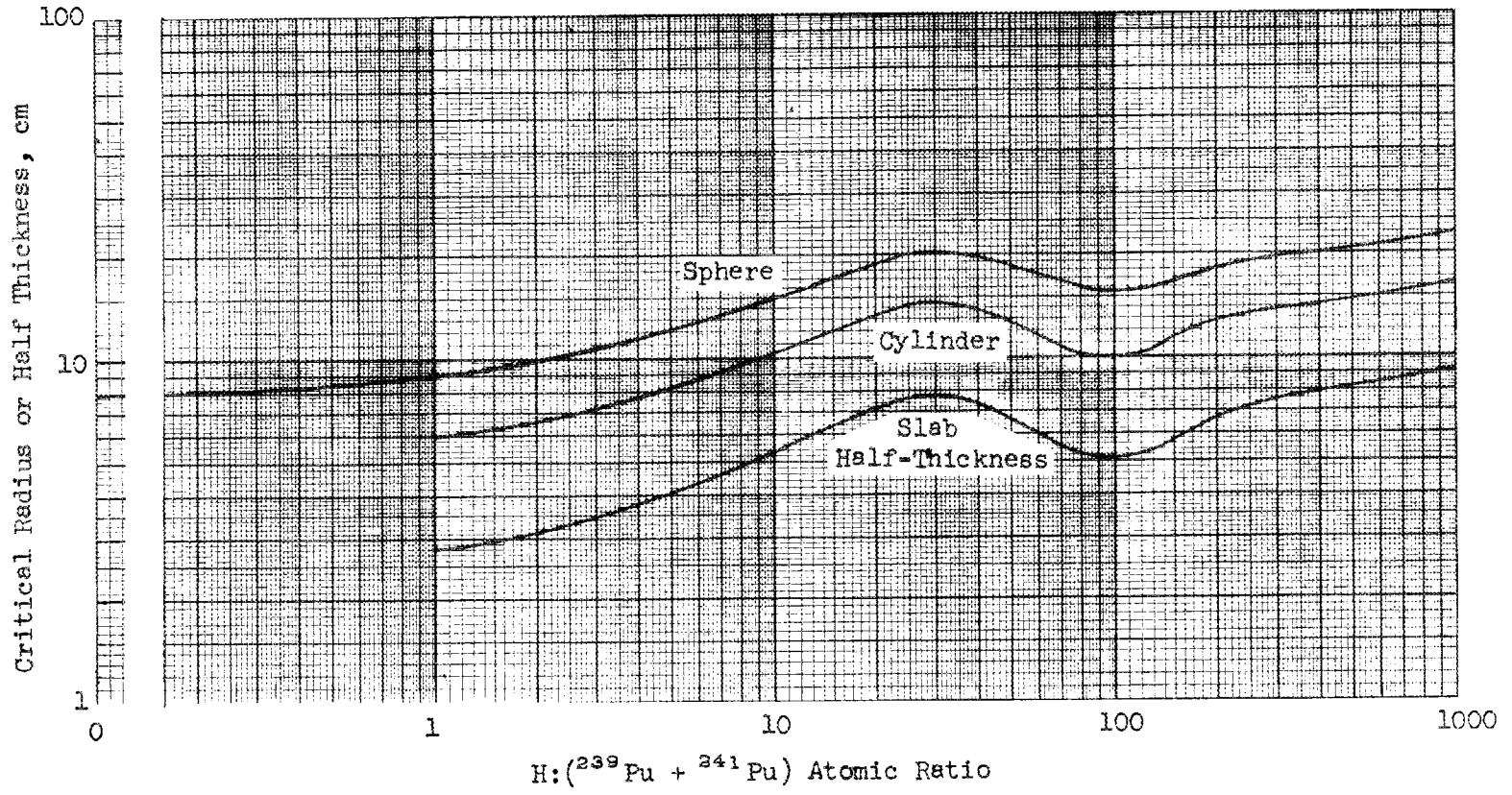
The objective of this task is to develop evaluated criticality data for application to the aqueous processing of LMFBR fuels. The work involves compilation of basic data and liaison with other critical experiment groups (Task 12.1); calculation of basic parameters (Task 12.2); the performance of select critical experiments with systems containing fixed and soluble neutron absorbers (Task 12.3); and the application of the critical data to the design of process equipment (Task 12.4).

### 12.2 Calculation of Basic Parameters (D. W. Magnuson)

Additional survey criticality calculations were made for the critical sizes of LMFBR Discharge<sup>1</sup> PuO<sub>2</sub>-water mixtures in spherical, cylindrical, and slab geometry. These results are given in Table 12-1 and Fig. 12-1, and they augment calculations previously reported.<sup>2</sup> The resonance absorption of neutrons at 1.0 eV by <sup>240</sup>Pu results in peaks in the critical sizes at a moderation ratio of approximately 30. The ANISN transport code in the S<sub>4</sub> approximation was used with Hansen-Roach 16-group cross sections.

We have begun a series of calculations to define the criticality parameters of arrays of LMFBR fuel elements in sodium-filled, steel shipping casks.

- 
1. LMFBR Discharge Plutonium is 62, 31, 5, and 2 wt % <sup>239</sup>Pu, <sup>240</sup>Pu, <sup>241</sup>Pu, and <sup>242</sup>Pu, respectively.
  2. D. W. Magnuson, "Criticality Calculations for Light Water Reactor and Liquid Metal Fast Breeder Reactor Fuels," Y-DR-9, Union Carbide Corporation Nuclear Division, Y-12 Plant (1969).



19

Fig. 12-1 Calculated Critical Radii for Spheres and Cylinders and Slab Half-Thickness for Mixtures of LMFBR Discharge PuO<sub>2</sub> and Water Reflected by 3 cm Stainless Steel.

Table 12-1. Criticality Calculations Using the ANISN S<sub>4</sub> Transport Code with 16-Group Hansen-Roach Cross Sections for LMFBR Discharge PuO<sub>2</sub> and Water Mixtures Reflected by 3 cm Stainless Steel.

H: ( <sup>239</sup> Pu + <sup>241</sup> Pu) Atomic Ratio	(Pu+U)O <sub>2</sub> Volume Fraction	Density <sup>239</sup> Pu + <sup>241</sup> Pu (g/cm <sup>3</sup> )	Calculated Critical Parameter				
			Radius (cm)	Volume (liter)	<sup>239</sup> Pu + <sup>241</sup> Pu Mass (kg)	Infinite Cylinder Radius (cm)	Infinite Slab Thickness (cm)
1	0.79638	5.404	9.03	3.084	16.666	6.03	5.64
3	0.56592	3.840	10.70	5.131	19.705	7.23	6.98
10	0.28115	1.908	15.09	14.393	27.462	10.43	10.72
30	0.11533	0.7826	20.48	35.982	28.159	14.45	15.62
100	0.03764	0.2554	14.54	12.876	3.289	10.04	10.30
300	0.01287	0.0873	19.55	31.299	2.732	13.76	15.00
1000	0.00390	0.0265	23.05	51.298	1.359	16.52	18.68

13. ENGINEERING STUDIES (TASK 13)  
(A. R. Irvine, S. Mann)

The purpose of this task is to examine the overall problem of LMFBR spent fuel recovery plant design and to relate the individual problems involved in fuel recovery to the overall problem and to the other individual problems. The plant design surveys which are to be made include adaptation of existing LWR reprocessing facilities for recovery of fuel from FFTF and initial demonstration reactors, possible adaptation of later LWR reprocessing facilities to accept LMFBR spent fuel from commercial reactors during the first decade (or more) of their existence, and, finally, preparation of a conceptual design for a facility that will be needed when a large number of breeder reactors are in use. Individual problems to be evaluated range from special problems in safety and containment (which are peculiar to reprocessing of LMFBR spent fuel) to equipment design and operational procedures to prevent formation of plutonium polymer.

It is known that ionic plutonium can polymerize, become colloidal, and precipitate from solution. These actions could cause losses of plutonium from solvent extraction equipment and possibly criticality. This problem may be more severe when processing LMFBR fuels than when processing LWR fuels because of the increased plutonium content of LMFBR fuel. A study of the literature is being made to evaluate the magnitude of the problem and to determine what action is indicated.

We are organizing for a study of existing commercial facilities to determine their suitability for processing of early LMFBR fuels. Personnel who are specialists in chemical development and in equipment development will be used along with design engineers to actively prosecute this effort. Work to this point has consisted of familiarization with the Nuclear Fuel Services plant, formulation of a few initial concepts, and initial work toward preparation of chemical flowsheets.

## II. FUEL MATERIAL PREPARATION

R. G. Wymer, R. E. Brooksbank, R. E. Leuze,  
J. P. McBride, W. D. Bond, P. A. Haas

### 1. CONVERSION STUDIES (R. E. Brooksbank)

In the LMFBR fuel cycle, it would be highly advantageous to convert the product solutions from the fuel reprocessing plants to solid fuel materials that are suitable both for shipping and for direct use in re-fabrication of fuel elements. Earlier fuel cycle studies have not necessarily optimized the conversion to meet both of these requirements. In order to meet both requirements, the solids must be in the desired chemical form with the necessary purity. In this study, we hope to determine the best method for accomplishing the desired conversion. Although the major emphasis will be placed on conversions to oxides, the conversion to advanced fuel forms (such as carbides, nitrides, and carbonitrides) will be included in our studies.

We are studying processes that are currently in use or under development; an economic evaluation is being made prior to undertaking extensive laboratory and engineering process studies. The conversion processes being evaluated include a variety of approaches, such as fluidized-bed conversion, flame denitration, sol-gel, and numerous precipitation processes.

#### 1.1 Sinterable Powder Preparation (W. D. Bond, P. A. Haas, R. E. Brooksbank)

Laboratory and engineering studies of the conversion of aqueous solutions of uranium and plutonium to powders will be initiated after our process evaluation studies (Sect. 1.2) have indicated which of the possible methods are the more promising.

#### 1.2 Process Evaluation

Currently plutonium is shipped from chemical processing plants as a nitrate solution. While this is satisfactory at present, safety considerations will probably dictate that the increased quantities of plutonium that will result from LMFBR fuel processing be shipped in a solid form. The objectives of this program are to define the most reasonable form for shipment to fabrication plants and to develop or adapt processes for this purpose. Processes currently used or being developed will be studied, and an economic evaluation will be made to establish the most promising approach. This work will, in turn, provide guidance for further experimental work. As a need for further developmental work is recognized, it will be reported.

The existing methods under study include those that are most likely to be used in production of first generation fast reactor fuel elements. They are: (1) dry powder blending of oxide powders for pelletizing,

(2) coprecipitation of plutonium and uranium to provide a mixed oxide for pelletizing, and (3) use of the sol-gel method to form either separate or blended  $UO_2$  and  $PuO_2$  microspheres or pelletizing stock. These are the most directly useful conversions, but if it appears desirable to convert to an intermediate solely for shipping purposes, this can also be considered.

#### 1.2.1 Chemical Conversion (F. E. Harrington, J. D. Sease, R. B. Pratt)

We are continuing the study of the costs involved in four alternative routes to the fuel preparation and fuel element fabrication for a specific LMFBR, as described earlier.<sup>1</sup> The plants being studied would produce oxide fuel elements (containing 500 kg of heavy metal core material per day) from depleted  $UF_6$  and  $Pu(NO_3)_4$  solution. The four alternative routes are: (1) mechanical blending to produce pellets, (2) coprecipitation to produce pellets, (3) sol-gel to produce pellets, and (4) sol-gel using the Sphere-Pac technique for rod fabrication.

In conversion-fabrication plants, "Safeguard" measures are somewhat comparable to three lines of defense: (1) controlled gates for the entrance and exit of fissile materials, (2) measurement of the flow of material at several strategic points within the plant, and (3) periodic plant inventories. Although these safeguard measures do not constitute a major fraction of the plant costs, they do represent a significant element both in plant investment and in operating costs.

The costs involved in safeguard measures will vary somewhat with the type of processing utilized. The amount of effort required to clean out equipment will increase as we progress from solution handling equipment through solids handling equipment to filters. Comparable plant strategic point flow and inventory checks can be performed with fewer check points in the sol-gel Sphere-Pac plant than in the three pellet plants studied. The degree of difficulty involved in cleanout and the number of samples required have a small (but real) effect on plant capital and operating costs. From these standpoints, the sol-gel Sphere-Pac would be the cheapest, the sol-gel pellet plant would be intermediate, and the remaining two pellet plants would be the most costly.

**Studies of annual requirements for process control, criticality control, and quality assurance indicate slight savings for the plants in the same order: Sphere-Pac the least expensive, followed by sol-gel pellets and then by the other two pellet plants.**

#### 1.2.2 Shipping and Storage (R. W. Horton)

The shipping and storage problems associated with the LMFBR fuel cycle are largely those of plutonium handling. There is a good background of experience in this area for a "once-through" plutonium cycle, but the

---

<sup>1</sup>LMFBR Fuel Cycle Studies Progress Report No. 5, ORNL-TM-2671 (August 1969), p. 38.

isotopic compositions to be handled in the LMFBR fuel cycle are sufficiently different to require a revision of past practice. In addition, the end use of the plutonium may call for different chemical treatments at either the reprocessing or fabricating plant to provide the purity and physical form needed.

The isotopic compositions under considerations are shown in Tables 2-1 and 2-2. The first of these shows calculated values (quantities, radioactivity, and thermal power) for plutonium recycled in light water reactors (thermal flux power reactors); the second table compares this same material with that resulting from plutonium recycled in LMFBR cores, and from mixed LMFBR core and blanket plutonium. Table 2-2 also shows the neutron source strength of these compositions, a factor to be considered in protection of shipments.

The totals shown in Table 2-1 can be expressed as a specific thermal energy of  $2.39 \times 10^{-3}$  cal sec<sup>-1</sup> g<sup>-1</sup> and a specific activity of 13.3 curies g<sup>-1</sup> at one year after discharge. An extensive study of plutonium shipping containers has been reported by The Dow Chemical Company, Rocky Flats Division.<sup>1-4</sup> These studies were based on a specific thermal energy of  $1.05 \times 10^{-3}$  cal sec<sup>-1</sup> g<sup>-1</sup> and a specific activity of 4.7 curies g<sup>-1</sup>. The difference between these two sets of values is sufficient to require revision of the shipping studies.

The Rocky Flats Division also reports on the conversion of plutonium nitrate to plutonium oxide suitable for shipment<sup>5</sup> and on the measurement methods suitable for nitrate and oxide shipments.<sup>6,7</sup> The conversion criteria were (1) safe shipping, (2) accurate plutonium measurement, and (3) solubility of the solid shipped. Properties of oxides prepared from oxalate, nitrate, hydroxide, and peroxide are reported.<sup>5,7</sup>

---

<sup>1</sup>J. D. Moseley, Study of Plutonium Oxide Heat Generation in a Wood Moderated Container, RFP-418, Rocky Flats Division, The Dow Chemical Co., Dec. 28, 1964.

<sup>2</sup>F. E. Adcock, et al, Plutonium Nitrate Shipping Packages, RFP-437, Rocky Flats Division, The Dow Chemical Co., Oct. 16, 1964.

<sup>3</sup>F. E. Adcock, et al, Plutonium Oxide Shipping Packages, RFP-501, Rocky Flats Division, The Dow Chemical Co., April 28, 1965.

<sup>4</sup>F. E. Adcock, W. F. Wackler, RFD Container - Model 1518 for Fissile Class II and Class III Shipments, RFP-1042, Rocky Flats Division, The Dow Chemical Co., April 8, 1968.

<sup>5</sup>J. D. Moseley, R. O. Wing, Properties of Plutonium Dioxide, RFP-503 Rocky Flats Division, The Dow Chemical Co., Aug. 24, 1965.

<sup>6</sup>J. T. Byrne, et al, Measurements of Plutonium Nitrate Shipping Solutions, RFP-436, Rocky Flats Div., The Dow Chemical Co., Oct. 1, 1964.

<sup>7</sup>J. T. Byrne, et al, Measurements Involved in Shipping Plutonium Oxide, RFP-502, Rocky Flats Div., The Dow Chemical Co., Aug. 10, 1965.

It is probable that plutonium shipped to a fabricator producing LMFBR core fuel should be in the form of a sinterable oxide of the proper particle size and chemical purity for direct use rather than in a form that necessitates dissolution. Hence, the chemical purification may have to be done in the fuel reprocessing plant, possibly as a precipitation that can serve both to purify and concentrate the product.<sup>1</sup>

The significant difference between the plutonium previously studied and the recycle plutonium is the large quantity of  $^{238}\text{Pu}$ . Two-thirds of the thermal energy of LMFBR plutonium comes from this source, resulting in 2.3 times the amount of thermal energy considered in the previous study. The total neutron flux is also nearly doubled, and probably will require more shielding for oxide shipments.

These characteristics, as well as the quantities involved (2700 kg of Pu for one AI Reference Core for the LMFBR) will have a considerable effect on fuel cycle economics. Plutonium shipments probably should be made as Class III shipments. Since the dilution with uranium that occurs in fabricating the fuel elements would ease the radiation and criticality problems greatly, some thought should be given to performing this step at the reprocessing plant in order to simplify shipping.

### 1.3 Advanced Fuel Studies (W. D. Bond)

Increasing demands on reactor fuels make the development of new or improved fuels important. Among the more promising advanced fuel materials for the LMFBR are the monocarbides, carbonitrides, and nitrides of plutonium and uranium. Sol-gel processes for the preparation of these materials are being developed on the laboratory scale. Stable, codispersed oxide-carbon sols are prepared by effecting dispersion of carbon black in  $\text{UO}_2$ ,  $\text{PuO}_2$ , or  $\text{PuO}_2\text{-UO}_2$  sols by ultrasonic agitation, and the oxide-carbon sols are then formed into gel microspheres or shards. After drying the gels to remove volatile materials, the gels are converted either to the monocarbide or to nitrides or carbonitrides, depending on the atmospheres used in carbothermic reduction. Monocarbides are formed when carbothermic reduction is effected under inert gas or vacuum atmospheres, whereas nitride or carbonitride conversion is effected under a nitrogen atmosphere.

Most of our work has been concerned with preparation of carbides. We had previously demonstrated the preparation of dense  $\text{ThC}_2$  and  $(\text{Th,U})\text{C}_2$  microspheres by sol-gel processes. In more recent work, laboratory-scale preparation of dense UC microspheres was demonstrated. Plutonium carbide microspheres have been prepared but the product characterization has not been completed. Work is now in progress on the preparation of uranium-plutonium carbide spheres and on uranium-plutonium carbonitride. Kinetic studies are being carried out on the carbothermic synthesis step to better understand the rate controlling mechanism.

---

<sup>1</sup>E. L. Christensen, W. J. Maraman, Plutonium Processing at The Los Alamos Scientific Laboratory, LA-3542, Los Alamos Scientific Laboratory of the U. of Cal., Los Alamos, N.M., April 1969.

Table 2-1. Isotopic Composition of Plutonium Product from a Light Water Reactor<sup>1</sup>

Nuclide	Concentrations (g/metric ton of fuel charged to reactor)			Radioactivity (curies/metric ton of fuel charged to reactor)			Thermal Power (watts/metric ton of fuel charged to reactor)		
	Time after Discharge from Reactor (days)			Time after Discharge from Reactor (days)			Time after Discharge from Reactor (days)		
	0	30	300	0	30	300	0	30	300
<sup>236</sup> Pu	0.10	0.10	0.08	5.32x10 <sup>1</sup>	5.21x10 <sup>1</sup>	4.35x10 <sup>1</sup>	1.85	1.81	1.52
<sup>238</sup> Pu	1.20x10 <sup>4</sup>	1.20x10 <sup>4</sup>	1.19x10 <sup>4</sup>	2.03x10 <sup>5</sup>	2.02x10 <sup>5</sup>	2.01x10 <sup>5</sup>	6.71x10 <sup>3</sup>	6.71x10 <sup>3</sup>	6.67x10 <sup>3</sup>
<sup>239</sup> Pu	5.92x10 <sup>5</sup>	5.92x10 <sup>5</sup>	5.92x10 <sup>5</sup>	3.63x10 <sup>4</sup>	3.63x10 <sup>4</sup>	3.63x10 <sup>4</sup>	1.13x10 <sup>3</sup>	1.13x10 <sup>3</sup>	1.13x10 <sup>3</sup>
<sup>240</sup> Pu	2.37x10 <sup>5</sup>	2.37x10 <sup>5</sup>	2.37x10 <sup>5</sup>	5.22x10 <sup>4</sup>	5.22x10 <sup>4</sup>	5.22x10 <sup>4</sup>	1.63x10 <sup>3</sup>	1.63x10 <sup>3</sup>	1.63x10 <sup>3</sup>
<sup>241</sup> Pu	1.19x10 <sup>5</sup>	1.18x10 <sup>5</sup>	1.14x10 <sup>5</sup>	1.36x10 <sup>7</sup>	1.35x10 <sup>7</sup>	1.30x10 <sup>7</sup>	5.64x10 <sup>2</sup>	5.61x10 <sup>2</sup>	5.40x10 <sup>2</sup>
<sup>242</sup> Pu	4.00x10 <sup>4</sup>	4.00x10 <sup>4</sup>	4.00x10 <sup>4</sup>	1.56x10 <sup>2</sup>	1.56x10 <sup>2</sup>	1.56x10 <sup>2</sup>	4.60	4.60	4.60
<sup>241</sup> Am	0.0	5.20x10 <sup>2</sup>	5.10x10 <sup>3</sup>	0.0	1.68x10 <sup>3</sup>	1.65x10 <sup>4</sup>	0.0	5.62x10 <sup>1</sup>	5.51x10 <sup>2</sup>
Total	1.00x10 <sup>6</sup>	1.00x10 <sup>6</sup>	1.00x10 <sup>6</sup>	1.39x10 <sup>7</sup>	1.38x10 <sup>7</sup>	1.33x10 <sup>7</sup>	1.00x10 <sup>4</sup>	1.01x10 <sup>4</sup>	1.05x10 <sup>4</sup>

<sup>1</sup> Aqueous Processing of LMFBR Fuels - Technical Assessment and Experimental Program Definition, ORNL-4436 (in preparation).

Table 2-2. Isotopic Content and Neutron Sources in PuO<sub>2</sub> Recycle Fuels<sup>1</sup>

	Isotope							Total
	<sup>238</sup> U	<sup>236</sup> Pu	<sup>238</sup> Pu	<sup>239</sup> Pu	<sup>240</sup> Pu	<sup>241</sup> Pu	<sup>242</sup> Pu	
<b>LMFBR Core<sup>a</sup></b>								
Isotope content, g/kg (U+Pu)	761.6	1.4x10 <sup>-6</sup>	1.7	163.4	50.8	13.9	8.5	
wt % in Pu	—	0.6x10 <sup>-6</sup>	0.72	68.57	21.30	5.83	3.58	
Neutrons/sec/kg (U+Pu)								
From SF			4,500	—	48,000	—	14,000	66,000
From α-n			42,000	11,000	12,000	3,500 <sup>d</sup>	33	69,000
Total								135,000
<b>LMFBR Core<sup>b</sup></b>								
Isotope content, g/kg (U+Pu)	769.8	2x10 <sup>-6</sup>	2.1	138.1	61.9	17.4	10.7	
wt % in Pu	—	0.9x10 <sup>-6</sup>	0.9	60.0	26.9	7.5	4.6	
Neutrons/sec/kg (U+Pu)								
From SF			5,500	—	59,000	—	18,000	82,000
From α-n			52,000		15,000	4,400 <sup>d</sup>	42	81,000
Total								163,000
<b>LMFBR Core<sup>c</sup></b>								
Isotope content, g/kg (U+Pu)	781.3	23x10 <sup>-6</sup>	2.6	129.5	51.8	26.0	8.76	
wt % in Pu	—	11x10 <sup>-6</sup>	1.2	59.2	23.7	11.9	4.0	
Neutrons/sec/kg (U+Pu)								
From SF			6,900	—	49,000	—	15,000	71,000
From α-n			65,000	8,700	13,000	6,600 <sup>d</sup>	34	93,000
Total								164,000
<b>LWR Pu Recycle Core<sup>c</sup></b>								
Isotope content, g/kg (U+Pu)	956.4	4.6x10 <sup>-6</sup>	0.52	25.8	10.3	5.2	1.7	
wt % in Pu	—	11x10 <sup>-6</sup>	1.2	59.2	23.7	11.9	4.0	
Neutrons/sec/kg (U+Pu)								
From SF			1,400	—	9,800	—	2,900	14,000
From α-n			13,000	1,700	2,500	1,300 <sup>d</sup>	6.6	19,000
Total								33,000

<sup>a</sup>Mixed Pu from LMFBR core-blanket recycle.

<sup>c</sup>Pu from LWR recycle.

<sup>b</sup>Pu from LMFBR core recycle.

<sup>d</sup>From <sup>241</sup>Am assuming 1 yr of post-separation decay.

<sup>1</sup>Aqueous Processing of LMFBR Fuels - Technical Assessment and Experimental Program Definition, ORNL-4436 (in preparation).

### 1.3.1 Sol-Gel Process Studies

Sol-gel process development studies include the preparation of oxide-carbon sols that are suitable for forming gel shards or microspheres, and the conversion of these gels to carbides, nitrides, or carbonitrides by carbothermic synthesis. This month our work was concerned with the preparation of uranium-plutonium carbides and carbonitrides, the preparation of uranium carbonitride microspheres, the preparation of ammonium diuranate-carbon precipitations for conversion studies, and studies of porous oxides by scanning electron microscopy.

Preparation of Uranium-Plutonium Carbides and Carbonitrides (R. G. Haire, L. G. Farrar). — As a result of the interest in carbides, nitrides and carbonitrides for LMFBR fuels, the preparation of these compounds by a sol-gel process is presently being investigated on a laboratory basis. The general procedure for preparing the materials uses the same three steps as previously reported for other metal oxide sol systems ( $\text{ThO}_2$ ,  $\text{UO}_2$ , etc.): (1) a stable  $\text{MO}_2\text{-C}$  (metal oxide-carbon) sol is prepared by ultrasonically blending carbon black in the  $\text{MO}_2$  sol; (2) the resulting  $\text{MO}_2\text{-C}$  sol is used to make gel microspheres, shards, or powder; and (3) the gel material is converted to the desired product at an elevated temperature. In the third step, volatile materials remaining in the gel are removed prior to the carbothermic reduction. The preparation of carbides, nitrides or carbonitrides differs only in the atmosphere used for the reduction step.

Work to date on the uranium-plutonium system (20 mole % plutonium) has shown that the system behaves similarly to  $\text{UO}_2\text{-C}$  mixture. The  $(\text{U,Pu})\text{O}_2\text{-C}$  sols show excellent fluidity and stability, although they show the same sensitivity to air oxidation as the  $\text{UO}_2\text{-C}$  sols. Both precipitated and CUSP type of urania sols have been used to mix with low-nitrate, large crystallite (80Å) plutonia sols. Metal concentration of the mixed sols have ranged from 1.0 to 1.4  $\underline{\text{M}}$ ; carbon black (Spheron-9) has been dispersed in the mixed sol to give  $\text{C/M}$  mole ratios of 2.2 to greater than 4.0. Gel microspheres were prepared from the sols by the standard ORNL technique, using 2-ethyl-1-hexanol (0.5%  $\text{H}_2\text{O}$ ,  $\sim 10^{-3}$   $\underline{\text{M}}$  in  $\text{HNO}_3$  and surfactants). The surfactant was Span 80 or a Span 80-Pluronic mixture to give 1 to 1.5% surfactant. Shards and powders were obtained by evaporation under argon. In addition to removing the volatile materials, a low-temperature calcination in argon-hydrogen was used to control the  $\text{O/M}$  ratio in order to preserve the proper  $\text{C/M}$  ratio for the reduction step.

Results to date have indicated that for the preparation of dense carbide microspheres, the carbothermic reaction can be done at approximately  $1600^\circ\text{C}$  and densification assured by a subsequent heating period at  $1800^\circ\text{C}$ . As expected, the mixed system has shown no indication of local segregation of plutonium and behaves as a solid solution. Although the results have indicated that there was a small decrease in the plutonium content in some of the products, we believe that this heating sequence will minimize the preferential loss of plutonium. Temperatures higher than  $1850^\circ\text{C}$  have resulted in distortion and sticking together of microspheres. Of the  $(\text{U,Pu})$  carbides and carbonitrides prepared, x-ray analyses of several samples indicate a pure product ( $\text{MO}_2$ ,  $\text{M}_2\text{C}_3$  and  $\text{MC}_2$  lines absent). Chemical analyses have given  $\text{C/M}$  mole ratios of 0.9 to 1.10 for **monocarbides** and  $\frac{\text{C} + \text{N}}{\text{M}}$  ratios of 0.97 to 1.2 for carbonitrides. Oxygen contents

were high, ranging from 2000 to 6000 ppm; these values may reflect handling problems, which should be reduced or eliminated in future operations. Preliminary metallography results indicate that dense products comparable to those obtained for uranium can be prepared. Future work will be directed toward improving both sample handling and process variables.

Preparation of U(C,N) Microspheres (K. J. Notz). — The preparation of dense U(C,N) microspheres by a process analogous to that used for UC is being studied. The present procedures differ from that used for UC in two ways: an effective C/U mole ratio of 2.2 to 2.8, rather than 3.0, is used in the starting material, and the carbothermic reduction is conducted under a nitrogen atmosphere instead of an inert atmosphere. The reaction is being conducted at 1500 to 1700°C under flowing nitrogen. Reaction times of about 1 hr are being used, and appear to be adequate for essentially complete reaction, as judged by the residual oxygen contents.

Preliminary work with shards having an initial C/U mole ratio of about 2.5 gave carbonitrides of compositions near UC<sub>0.5</sub>N<sub>0.5</sub>. The product compositions were determined by chemical analysis and also calculated from the x-ray lattice parameters; the two methods agreed within 8% or better. The oxygen contents of these samples varied between 900 and 1900 ppm. The total anion (C + H + O)-to-cation ratios were between 0.90 and 0.99. X-ray diffraction detected only U(C,N) phases, but for two samples there appeared to be two U(C,N) phases of different lattice parameters present in the products. Mercury penetration data obtained on one sample showed 19% porosity with pores about 1 μ in diameter; the final (penetrated) density of this sample was 13.2 g/cc, or 95% of the calculated theoretical density for UC<sub>0.5</sub>N<sub>0.5</sub>.

**Work done earlier with microspheres was limited to materials having an initial C/U mole ratio of nearly 3; the products have therefore had a low nitrogen content, of the order 5 to 10 anion %, and some UC<sub>2</sub> has been present in all but one sample. The residual oxygens have been between 130 and 390 ppm. These products have all been relatively dense and non-porous; mercury penetration data show only 1 to 4% measurable porosity, and final densities of 12.1 to 12.9 g/cc, or 89 to 95% of theoretical (for UC).**

Preparation of ADU-Carbon Mixtures (K. J. Notz, T. B. Lindemer). — Sol-gel derived mixtures of carbon black and UO<sub>2</sub> can be made to react very rapidly (to give carbides) under appropriate conditions because of the very small particle size of both the oxide and the carbon and because of the intimate contact between the reactants. A comparable degree of fineness and particle association might also be attained by a precipitation process in which ammonium diuranate (ADU), uranium peroxide, or uranium oxalate is precipitated in the presence of colloiddally dispersed carbon. Alternatively, a colloidal carbon dispersion could perhaps simply be added to a suitable uranium-bearing solid. Initial experiments with ADU and Spheron-9 carbon black suggest that such an approach may be successful, since the filtrates from several such mixtures have been completely, or nearly completely, free of carbon, indicating that the carbon and the ADU have become strongly enough bonded to each other to retain all of the carbon in the filter cake. Samples have been prepared by a normal precipitation

process, reverse strike precipitation (addition of uranyl nitrate to ammonia), and addition of carbon to previously precipitated ADU. The kinetic reactivity and physical properties of these samples is being evaluated.

Scanning Electron Microscopy (S.E.M.) of Sol-Gel Derived Porous Oxide (K. J. Notz). — A structural model of oxide-carbon gels consistent with observable properties has been previously proposed (ORNL-TM-1780). The results of S.E.M. of two porous  $\text{ThO}_2$  samples prepared by densification-burning of such gels provides further corroboration of the earlier data, and interpretation. Grains observed by S.E.M. ranged from 500 to 2000 Å, in agreement with an x-ray crystallite size of 850 Å. The size of pores as seen by S.E.M. varied between 250 and 400 Å; the carbon black, which was burned out to create these holes, consisted of 300-Å particles, and the BET surface area of this material gives a calculated pore size of 230 Å.

### 1.3.2 Kinetic Studies of Carbothermic Synthesis (T. B. Lindemer, K. J. Notz, R. L. Beatty)

Carbothermic synthesis of carbides, carbonitrides, and nitrides from oxide-carbon gels is an important process step in the preparation of these materials by the sol-gel process. An understanding of the rate-controlling mechanisms and kinetic equations of these carbothermic syntheses would be very useful for the determination of the best conditions for effecting these syntheses.

We are continuing the study of vacuum conversion of oxide-carbon materials, such as those produced by the sol-gel process.

A paper entitled "The Role of Carbon in Reactions in the U-C-O-N System," by T. B. Lindemer, J. M. Leitnaker, and K. E. Spear, was presented at an international conference on heterogeneous kinetics at elevated temperatures. This conference was held at the University of Pennsylvania in Philadelphia on September 8-10. The paper will be available soon as an ORNL-TM report.

## 2 - SOL-GEL PROCESSES FOR PREPARATION OF LMFBR RECYCLE FUEL (R. E. Leuze)

Sol-gel processes are ideally suited to the preparation of LMFBR recycle fuel since they can be readily adapted to continuous and remote operation for processing materials behind shielding. The processes under development prepare sols by controlled solvent extraction of nitrate from plutonium and uranium nitrate solutions, the products from fuel reprocessing plants. The sols are then converted to the desired ceramic forms, usually high density oxide microspheres, required for subsequent fabrication into recycle fuel elements. This section reports progress for all of the process development and demonstration, equipment design, and instrument development being carried out to obtain sufficient information for design of a full scale facility. Also included is the preparation of sol-gel materials required for testing and for use in other parts of the LMFBR fuel recycle program.

### 2.1 Urania Sol Process and Equipment Development (J. P. McBride)

Although the LMFBR recycle fuel under consideration is mixed urania-plutonia, study of urania sol preparation is important because urania is used as a fertile material in an LMFBR and is the major component in the mixed oxide. Urania sols are also useful for studying other phases of the program such as sphere forming and tray drying.

The CUSP process (Concentrated Urania Sol Preparation) developed at ORNL has been selected as the method for preparation of urania sols since it is most amenable to scale-up and consistently produces good sols with desirable characteristics.<sup>1,2</sup> This section of the report covers all aspects of CUSP sol preparation including uranous nitrate feed preparation, laboratory- and engineering-scale process development, sol preparation, and equipment design and instrumentation.

#### Characterization of CUSP Sols (W. L. Pattison, J. P. McBride)

Sols prepared in engineering equipment by the CUSP process have shown good reproducibility in their physical and chemical properties.<sup>3</sup>

<sup>1</sup>J. P. McBride, K. H. McCorkle, W. L. Pattison, and B. C. Finney, "Preparation of Concentrated, Crystalline Urania Sols by Solvent Extraction," presented at the 15th Annual Meeting of the American Nuclear Society, Seattle, Washington, June 15-19, 1969; summary published in Trans. Am. Nucl. Soc. 12, 206 (1969).

<sup>2</sup>J. P. McBride, K. H. McCorkle, and W. L. Pattison, LMFBR Fuel Cycle Studies Progress Report, No. 5, August (1969), ORNL-TM-2671, p. 52.

<sup>3</sup>B. C. Finney and W. L. Pattison, LMFBR Fuel Cycle Studies Progress Report, No. 6, September (1969), (in press).

However, some differences among sols have been indicated by sphere-forming experiments (Sect. 2.3) and by compatibility experiments with plutonia sols. In addition, while shelf-lives of several months at 1 M are characteristic of most CUSP sols, there are differences in shelf-life, and one sol unaccountably gelled in 2 months under an argon atmosphere. In an effort to find differences among sols, CUSP sols were dried at room temperature under argon, and the BET surface areas of the gels were determined as a function of out-gassing temperature. These data, as well as the weight losses of the gels on out-gassing, and the shelf-lives of the sols are listed in Table 2-1. A wide range of surface areas, 44 to

Table 2-1. Surface Areas of CUSP UO<sub>2</sub> Gels as a Function of Out-Gassing Temperature

CUSP Gel No.	Outgas Temp. °C	Surface Area m <sup>2</sup> /g					Wt. Loss (%) <sup>a</sup>	Aging time for a 1 M sol to gel (months)
	85°C	100°C	130°C	200°C	300°C	400°C		
ES -31	128	121	119	123	85	79	11.9	>3.0
ES -5	122	117	--	62	70	--	6.8	1.9 <sup>b</sup>
ES -21	121	122	110	107	82	80	9.3	>3.5
ES -45	121	114	113	88	80	79	10.5	>1.5
ES -10	119	115	114	80	76	--	11.5	3.0
ES -3	111	112	--	76	74	--	7.9	>6
PCS -1	110	111	115	78	74	64	7.8	>2
ES -46	106	107	107	74	71	64	7.4	>1.5
ES -11	101	95	96	65	66	--	7.6	>4
ES -9	92	94	--	63	60	--	6.8	4.0
ES -16	77	67	65	63	62	--	8.7	>3.5
ES -7	61	60	56	63	70	--	16.8	>4.5
ES -12	49	49	51	66	70	--	7.1	3.5
ES -8	44	46	45	57	63	--	5.4	2.0

<sup>a</sup>Based upon original weight of gel dried under argon at room temperature.

<sup>b</sup>Gelled because of high NH<sub>4</sub><sup>+</sup> content.

128 m<sup>2</sup>/g, were observed for gels out-gassed at 85-130°C. For gels out-gassed at 300°C, however, the surface areas were all between 60 and 85 m<sup>2</sup>/g with an average value of 72. No correlation was observed between shelf-life and the trend in surface areas at the lower out-gassing temperatures. The ES-3 sol, which gave a high surface area gel when out-gassed at 85-130°C, has apparently been more compatible with plutonia sols than ES-7 which yielded a low surface area gel. Differences in sphere-forming behavior were found between ES-31, ES-21, and PCS-1 (see Sect. 2.3) which dried to gels having surface areas of 128, 122, and 115 m<sup>2</sup>/g, respectively, with ES-31 being the best performer. Sol ES-46, giving a gel of 107 m<sup>2</sup>/g surface area, did not form well. Sol ES-8, which dried to the lowest surface area gel (46 m<sup>2</sup>/g for gel out-gassed at 100°C), had a shelf life of only 2 months. On the other hand, sol ES-7, which gave a gel with a surface area of only 61 m<sup>2</sup>/g when out-gassed at 85°C, is still very fluid after 4.5 months aging.

The wide range of surface areas observed at the lower out-gassing temperatures may result from variations in the oxidation state of the surface of the sol particles in the different sols. There is some reason to believe that oxidation of the surface of the sol particles results in a lower surface area for the gel. Surface oxidation can occur as a result of air-exposure or simple aging and may explain some of the variations observed in sol behavior. Efforts to measure and determine the significance of the surface oxidation states are continuing.

#### Extraction of Formic Acid from CUSP UO<sub>2</sub> Sols (W. L. Pattison)

Scouting tests made a number of years ago were partially successful in removing free formic acid from precipitation-type urania sols. We performed a similar test with a CUSP UO<sub>2</sub> sol under more carefully controlled conditions.

Anhydrous methanol was added to the urania sol at a ratio of 10 moles of methanol for each mole of formate ion. The urania sol was heated and stirred at 51 to 55°C for 30 min in an open beaker on a hot plate in a glove box having an argon atmosphere with about 400 ppm O<sub>2</sub>. (The formation of methyl formate, which has a boiling point of 31.8°C, was indicated in previous experiments by a distinctive, fruitlike odor.) At the end of the thirty-minute heating period, the sol was cooled; 2.5 volumes of anhydrous n-hexanol were added to each volume of sol, and the mixture was stirred at a temperature of 40°C for fifteen minutes. The aqueous phase was adjusted to approximately its original volume by addition of distilled water, and the phases were separated.

Analysis of the final sol showed that at least 15% of the formic acid in the original sol had been removed. Since the analytical techniques used for formic acid cannot distinguish between formic acid, formaldehyde, and methanol in the presence of colloidal UO<sub>2</sub>, it is quite possible that the apparent final HCOOH/uranium mole ratio of 0.34 may actually be lower and that a larger percentage of the formic acid was removed.

Some of the characteristics of this method for removing formic acid from CUSP sols are as follows:

- (1) The fluidity of the sol is not changed substantially at any point in the process.
- (2) There is essentially no change in the  $\text{NO}_3^-/\text{U}$  ratio in the sol.
- (3) No coagulation or precipitation of colloidal material occurs.
- (4) The micelle structure is disrupted by the treatment, and the sol particles are dispersed into the individual 40 Å crystallites.
- (5) It is not necessary to change the concentration of CUSP sols from their as-prepared concentration, although some increase in uranium concentration does occur during the process due to the heating for 30 min at  $55^\circ$  and the extraction of water by the anhydrous n-hexanol.

#### Equipment Development (F. G. Kitts, F. L. Daley, J. R. Parrott)

Development of equipment for forming urania sols by the CUSP process is in progress in the Pilot Plant. A reductor for preparing the U(IV) feed solution and equipment for CUSP and plutonia sol forming and mixing will be added to the existing Solex facility and used to prepare 80%  $\text{UO}_2$ -20%  $\text{PuO}_2$  in 1 kg batches.

Our development work has been restricted mainly to testing mixing devices which might be used as the CUSP contactor. A 1 in. ID glass column packed with 1/4 in. Berl saddles was operated satisfactorily with co-current flow either upward or downward; flow rates of both phases may be varied independently.

Before further runs were made, the equipment was modified to make it more representative of that being designed for installation in the  $\alpha$  enclosures. The 1 in. ID packed column contactor was shortened from 3 1/2 ft to 3 ft, and the 4 in. ID reservoir for phase separation was reduced from 46 in. to 36 in. The heating coil was removed from the bottom section of this vessel, and an external heat exchanger of the same capacity was added. The recirculating pump for the aqueous phase was made the low point in the system, and the piping was arranged so the system could be drained completely at the pump inlet. A differential pressure cell with integral orifice was substituted for the rotameter as the flow indicator of the aqueous phase.

Seven additional runs were made with co-current flows upward (aqueous phase continuous) through a 3 ft packed length at an aqueous phase rate of 750 cc/min and extractant (0.2 M Amberlite LA-2 in 75% DEB-25% n-paraffin) rates of 200-300 cc/min. The feed and product sol compositions for these runs are listed in Table 2-2. Operational variables, such as temperature, indicated conductivity, and flow rates, are quite reproducible from run to run although the sols have somewhat variable fluidities,  $\text{NO}_3^-$  and  $\text{U}^{4+}$  concentrations, and conductivities.

Table 2-2. Analyses of Feeds and the Resulting CUSP  
Sols Prepared in a Packed-Bed Contactor

		Run Number					
		PC-5	PC-7	PC-8	PC-9	PC-10	PC-11 <sup>a</sup>
<u>Feed</u>							
U	(M)	1.02	1.05	1.05	0.97	1.04	1.04
U <sup>4+</sup>	(%)	77.3	75.1	81.0	90.1	90.3	
NO <sub>3</sub> <sup>-</sup>	(M)	1.98	2.11	2.11	2.10	2.06	2.06
HCOO <sup>-</sup>	(M)	0.32	0.41	0.41	0.42	0.38	0.38
NH <sub>4</sub> <sup>+</sup>	(M)	0.001	0.002	0.002	<0.001	<0.001	<0.001
pH		1.08	1.32	1.32	1.18	1.13	1.13
Age	(days)	1	1	3	6	1	3
<u>Product Sol</u>							
U	(M)	0.93	1.00	0.90	0.93	1.07	
U <sup>4+</sup>	(%)	73.3	85.4	80.5	82.8	82.2	
NO <sub>3</sub> <sup>-</sup>	(M)	0.146	0.083	0.202	0.143	0.120	
HCOO <sup>-</sup>	(M)	0.29	0.43	0.40	0.30	0.37	
NH <sub>4</sub> <sup>+</sup>	(M)	0.005	0.004	<0.001	0.004	<0.002	
Density	(g/cc)	1.2345	1.2523	1.2041	1.2353	1.271	
pH		2.18	3.38	1.97	2.79	2.22	
Sp. Conduc.							
@ 25°C (μmho)		5490	2977	8875	3708	4237	3190

<sup>a</sup>Analyses for PC-11 not yet complete.

All of these sols had a semi-solid emulsion layer of varying thickness floating on them. Efforts will be made to minimize emulsion formation in future runs. Careful measurements of the uranium hold-up were made after runs PC-8 and PC-10 in order to determine the amount of uranium recycle which will occur during repeated operations in this equipment. Approximately 6.9% of the uranium remained in the equipment after draining, and 14.4% of the uranium was entrained in the solvent and in the solvent system.

## 2.2 Urania-Plutonia Sol Process and Equipment Development (R. E. Leuze)

This section of the report covers all aspects of mixed urania-plutonia sol preparation including preparation of high-nitrate plutonia sol, special treatment of CUSP sol prior to mixing with plutonia, techniques for mixing plutonia and urania sols, and treatments required to produce satisfactory mixed sol ready for subsequent processing into the desired ceramic form. Progress on equipment development and engineering-scale demonstration is also reported here.

All efforts at the present time are directed at setting process conditions and preparing equipment in order to demonstrate engineering-scale preparation of mixed  $\text{UO}_2$ - $\text{PuO}_2$  and to produce several kilograms of irradiation test material during the first half of FY-1970. In the process selected for this demonstration, CUSP urania sol is pretreated to remove excess formate and is then mixed with a high-nitrate plutonia sol prepared by an alcohol extraction process (APEX). The mixed sol is contacted with a secondary amine to extract excess nitrate and is subsequently formed into microspheres or shards which can be dried and calcined to dense oxide product. This procedure was selected because CUSP and APEX sols have exhibited improved compatibility after mixing. It is believed that the highly crystalline characteristics of these sols are at least partially responsible for the improved behavior.

### Preparation of Plutonium Polymers by Alcohol Extraction (L. E. Morse)

Studies of plutonium polymer preparation by alcohol extraction were continued. In this process,  $\text{HNO}_3$  is extracted into n-hexanol from an aqueous solution of  $\text{Pu}(\text{NO}_3)_4$ . As the nitric acid is removed, a sequence of reactions occurs which results in the formation of plutonium polymer. Plutonium polymers produced in this manner are intended for use in the preparation of mixed urania-plutonia sols which can be further processed into fuel forms for an LMFBR. The extraction studies are being made in an apparatus enclosed in a glove box for alpha containment. This apparatus, described in the previous LMFBR Fuel Cycle report, consists of two stirred contactors which are connected by solution transfer lines. In the first contactor,  $\text{HNO}_3$  is extracted from the aqueous  $\text{Pu}(\text{NO}_3)_4$  solution with n-hexanol which is then transported to the second contactor where the  $\text{HNO}_3$  is stripped from the alcohol into water. The alcohol is continuously recycled to the first contactor. Extraction is continued until the rate of  $\text{HNO}_3$  removal becomes so slow as to make further operation impractical. The progress of the extraction is monitored by a conductivity probe in the plutonium nitrate solution.

Based on the experience of the first run reported last month, it appeared that extending the individual extraction cycle beyond 2.5 hours was unrewarding in terms of  $\text{HNO}_3$  extraction. Consequently, in the second experiment it was decided that three extraction cycles, each of 2.0-2.5 hours duration, would be employed. That is, after the first extraction cycle was completed the water used to strip  $\text{HNO}_3$  from the

n-hexanol was replaced with fresh water, and a second extraction cycle was carried out. Finally, a third extraction cycle was made after again replacing the stripping water. No difficulties were encountered in the operation of the apparatus. Samples were taken at the conclusion of each extraction cycle for spectrophotometric determination of the plutonium valence states, but the results are not yet available. Plutonium concentrations were determined by gross alpha counting, and nitrate concentrations were determined by titration with 0.1 N NaOH to the phenolphthalein end point.

The plutonium polymer produced in the first experiment (APEX-1) had the following characteristics:

Total Pu =	0.077 <u>M</u>
Plutonium as polymer =	99.5%
Plutonium as ionic Pu(VI) =	0.5%
NO <sub>3</sub> <sup>-</sup> =	0.091 <u>M</u>
$\frac{\text{NO}_3^-}{\text{Pu}}$ mole ratio =	1.2
specific conductivity =	13.9 x 10 <sup>-3</sup> mhos/cm

The results of the second experiment (APEX-10) are summarized in Table 2-3. Analyses of the sol products from the two runs are essentially the same except for the somewhat greater plutonium concentration in the APEX-10 product, which resulted from the higher plutonium concentration in the feed solution.

It was found that the three-cycle process can be used to prepare essentially the same product in less time than the two-cycle process. Although the three-cycle process required a larger total volume of water for stripping HNO<sub>3</sub> from the alcohol, the water from the third cycle was so dilute in HNO<sub>3</sub> (0.018 M) that it could be used for the first cycle in a subsequent preparation of plutonium sol. Another result of a third extraction cycle was to reduce the HNO<sub>3</sub> concentration in the n-hexanol to a sufficiently low level so that the n-hexanol could be used in a subsequent plutonium sol preparation without further treatment.

As observed in the first experiment (APEX-1), increases in specific conductivity were noted when the aqueous feed was allowed to stand between extraction cycles. Preliminary spectrophotometric examination of all samples, except the polymer product, showed that the distribution of plutonium into the various valence states also changed with time.

#### Mixed Plutonia-Urania Sol Compatibility Studies (O. K. Tallent)

Microsphere cracking has been a recurring problem during most of the development work with mixed CUSP-APEX (UO<sub>2</sub>-PuO<sub>2</sub>) sols. This cracking

Table 2-3. Analyses of Pu Polymer Prepared by Alcohol Extraction  
in Run No. APEX-10

Feed: ~250 ml 0.104 M Pu(IV) - 1.24 M NO<sub>3</sub><sup>-</sup>  
 Strip: ~1500 ml H<sub>2</sub>O  
 Alcohol extractant: ~3000 ml n-hexanol  
 Extractant to aqueous phase  
 volume ratios:  
 Extraction contactor: ~4  
 Stripping contactor: ~0.8

Samples	Extraction Time (hr)	Specific Conductivity (mhos/cm)	Total Pu (M)	NO <sub>3</sub> <sup>-</sup> (M)	NO <sub>3</sub> <sup>-</sup> /Pu (mole ratio)
Aqueous feed	--	208.3 x 10 <sup>-3</sup>	0.104	1.24	11.9
1*	2.0	60.3 x 10 <sup>-3</sup>	0.09	0.38	4.1
2*	2.5	25.3 x 10 <sup>-3</sup>	0.08	0.17	2.0
3*	2.5	15.0 x 10 <sup>-3</sup>	0.085	0.10	1.2

88

\*All samples taken at the conclusion of the extraction cycle.

has been taken as one criterion of incompatibility of the mixed sols. Recent tests involving the preparation of a few grams of microspheres have shown that in some cases the cracking problems can be eliminated by making minor modifications in the microsphere forming and drying procedures. It was found that sparging the sphere-forming alcohol with argon and that limiting the contact time between the microspheres and the drying alcohol were both effective in decreasing or eliminating sphere-cracking.

The sol for these tests was made by mixing an APEX sol which was 1.02 M Pu and 0.61 M  $\text{NO}_3^-$  with a portion of CUSP-ES-44 sol which had been contacted with eight volumes of n-hexanol and which was 0.97 M U, 0.115 M  $\text{NO}_3^-$ , and  $\sim 0.42$  M  $\text{HCOO}^-$ . Microspheres  $>400$   $\mu$  dia were formed in 2-ethyl-1-hexanol containing 0.7 v/o Pluronic 92, 0.2 v/o Span 80, 0.5-1.5 v/o water, and was adjusted to pH 2.5 with  $\text{HNO}_3$ .

In each of eight tests made with the use of an argon sparge, the microspheres produced were crack-free. In each of four control tests made without the sparge, the microspheres produced were severely cracked. In these tests the microspheres were removed from the forming column, dried in air or argon, and calcined at 1150°C in Ar- $\text{H}_2$ . Microspheres which were crack-free after drying were crack-free after calcination. Microspheres which were cracked after drying were more severely cracked after calcination. Indications are that the forming and drying steps are more crucial than the calcination step in preventing cracking.

The importance of minimizing the contact time between microspheres and drying solvent was indicated by a series of control tests where cracking was induced into eleven batches of newly-formed, crack-free microspheres by soaking the microspheres in various alcohols for 16 hours. The order of decreasing cracking severity induced by dry alcohols was n-butanol > n-hexanol > 2-ethyl-1-hexanol. The presence of water or surfactants in the alcohols increased the severity of the cracking by an order of magnitude. Plans are to incorporate the above described modifications in larger batch-size tests in the immediate future.

### 2.3 Sphere Preparation (P. A. Haas)

Information concerning the conversion of urania and urania-plutonia sols into microspheres of the desired size and with the desired properties is reported here. This includes studies on sphere-forming, chemistry of the sphere-forming column, recycle of the drying alcohol, drying and firing of gel spheres, and classification of the fired particles. The latest information on adapting these process steps and equipment to remote operation is also included.

#### Sphere Forming Column Chemistry (W. D. Bond, A. B. Meservey)

Over 60 microsphere-forming tests were made with CUSP sols in a small column with 2-ethyl-1-hexanol (2EH). Comparisons were made between

four sols (ES-21, ES-31, ES-46, and PCS-1) which were formed into microspheres in 2EH containing 1.0 v/o water with surfactant (Ethomeen S/15 and Span 80) concentrations and pH of the 2EH (1.9 to 8.9) as variables. General results were as follows:

1. Clustering could be controlled either by high Span levels (such as 0.4%) in 2EH at pH 2 to 9, or by Ethomeen (0.1-0.5%) in 2EH which had been acidified to a pH of 2 to 3. Ammonium ion, introduced during pH adjustment, promoted clustering.
2. Pitting and wrinkling were severe when 2EH containing Span was acidified, the distortion being worse at higher Span concentrations and lower pH's. Span did not cause pitting at pH's of 8 to 9. Microspheres from all four sols were pit-free when formed in 2EH at pH 7.5 containing 0.1% Ethomeen but no Span; however, clustering was prohibitive. All sols formed pitted spheres, but only slight clustering occurred when the sols were formed in the same drying alcohol but at pH 2. At pH 2 with 0.5% Ethomeen, there was no clustering, but heavy pitting occurred for all sols except ES-31.
3. Unexplained differences between duplicate runs with the same sols made it evident that not all the experimental variables were under control.
4. Various mixtures of surfactants at varied pH gave puzzling results, the great majority of microspheres being clustered, wrinkled, pitted, or broken. However, a few test conditions were found to give good gel microspheres in the  $600 \pm 100 \mu$  size range. These are as follows:

<u>Sol</u>	<u>Conditions for Good Sphere Forming</u>
ES-21:	0.4% Span-0.1% Ethomeen at pH ~5 and ~8.5 (rough surfaces).
ES-31:	0.2% Span-0.1% Ethomeen at pH ~6.8 (slightly rough surfaces). Also 0.4% Span-0.1% Ethomeen at pH ~8.7, and 0.5% Ethomeen at pH 2.
PCS-1:	0.4% Span-0.1% Ethomeen at pH ~8.5.
ES-46:	None of the conditions tried so far have given satisfactory results.

5. The oxidation-cracking of gel beads in air (with Ethomeen at a low pH) reported previously has been confirmed.

The unexplained differences between duplicate runs, duplicate samples of the same sol, and between sol batches may be due chiefly to small, but important differences in the states of oxidation of the sols. In the

laboratory tests, air exclusion may not have been as rigorous as is necessary even though the forming column was blanketed under argon. No measurements of the oxygen content of the 2EH have been made. Slight differences in oxidation state between sols is common. If their importance is verified by experiments, we may have to standardize sol oxidation states very carefully in order to use uniform conditions in a sphere forming column.

#### Microsphere Preparation Development (P. A. Haas)

Tests of conditions to prepare  $UO_2$  gel spheres from CUSP sols were continued. A liquid-liquid separator made by the Selas Corporation was used on the 2EH leaving the caustic scrub system and appears to prevent entrainment of scrub-solution droplets into the still. This performance and the durability of the separation membranes will have to be demonstrated for longer periods of operation.

Firing, sieving, and analyses of the  $UO_2$  gel spheres from tests with CUSP sols during June and July are now complete. Additional generalizations from these results are as follows:

1. Products with high densities and low surface areas are generally obtained even for drying and firing conditions which are less refined than the optimum conditions defined in laboratory tests. Nearly all the microspheres formed in 2EH which was scrubbed with caustic had densities  $>10.3$  g/cm<sup>3</sup> and surface areas  $<0.01$  sq m/g.
2. Sphere-forming operations which gave  $>98\%$  yield of good gel spheres have nearly all been either from the first few hours of operation with virgin 2EH or with sols concentrated to 2-3 M  $UO_2$ .
3. When lower yields of good product were obtained, losses of 5 to 20 per cent resulted from raisin-type distortion and/or coalescence to give doublets, triplets, or larger clusters. Losses due to cracking have been much less significant. (Note: Samples removed and dried in air for immediate examination showed much more cracking).
4. The amount of coalescence and/or clustering increased with increasing accumulated-operating-time for a batch of 2EH, higher pH's of the 2EH, lower Span concentrations, or entrainment of NaOH or  $NH_4OH$  into the sphere forming column.
5. The amount of raisin-type distortion increased at higher Span concentrations or lower pH's of the 2EH.
6. The smooth dimple-type distortion (a hollow shell as the extreme as compared to the wrinkled surface for an extreme raisin distortion) was not noticed for any conditions tested.

## 2.4 Preparation of Sol-Gel Test Materials (W. T. McDuffee)

Preparation of sol-gel materials for use in other parts of the LMFBR fuel cycle program is reported here. This includes materials for irradiation capsules and for development of fuel fabrication techniques such as sphere-pac or pellet forming.

### PuO<sub>2</sub> Sol Preparation

Four lots of PuO<sub>2</sub> sol, each containing about 150 g of plutonium, were prepared during the last month. These will be mixed with urania sols to prepare Pu<sub>0.2</sub>U<sub>0.8</sub>O<sub>2</sub> for irradiation tests.

### Preparation of Microspheres from Mixed UO<sub>2</sub>-PuO<sub>2</sub> Sols

Pretreatment of a CUSP sol by contacting it with n-hexanol to remove formic acid was described last month. Portions of this pre-treated sol were blended with plutonia sols (prepared by the standard precipitation-peptization-baking process) and formed into gel microspheres which were then dried and fired to high density oxide spheres. A total of 750 g of 400-600 μ-diam microspheres and 210 g of small microspheres (<25-μ-diam) were prepared. Considerable cracking occurred in the larger spheres, with only about half of the material being round and free of cracks. The <25-μ-diam microspheres were easier to prepare, and the yield of good material was >90%. These products were transferred to personnel in the Metals and Ceramics Division for use in irradiation tests.

Microsphere forming conditions were varied throughout the preparation of this material in an attempt to improve the yield and the quality of the final product. During the first part of the sphere-forming, the drying alcohol was held at a pH of 3.0-3.5. A small amount of clustering (~5% of the column inventory) occurred, and some of the partially gelled spheres cracked. Upon drying the gel spheres, about 50% of them cracked; and after firing, about 60% of the spheres were cracked. After the initial operation at a pH of 3.0-3.5, the pH of the solvent was allowed to rise to 4.0-4.5 for the remainder of the run. The first product recovered under these operating conditions was of considerably higher quality; only about 15% of the gel spheres and about 25% of the fired oxide spheres were cracked. Product recovered toward the latter part of the run made at these same conditions was of much poorer quality. Although only ~15% of the gel spheres were cracked, 90% of the spheres cracked during firing.

## 2.5 Plutonium Storage Facility (J. R. Parrott, R. G. Nicol, W. A. Shannon)

A facility for safely storing and handling plutonium is being built in Building 3019 to meet the needs for developmental work

involving the sol-gel flowsheet for fast reactor fuels. This facility is located in the basement (room 501) adjacent to the Metals and Ceramics Division alpha laboratory. It will have a capacity of 100 kg of plutonium in a solid (fluoride) or a liquid (nitrate) form.

Preparation of this facility is still under way. The glove box off-gas system has been put into service.

### III. FUEL FABRICATION AND EVALUATION

(A. L. Lotts, C. M. Cox, J. D. Sease, and  
T. N. Washburn)

The primary emphasis of fuel fabrication and evaluation studies related to the fuel cycle for the liquid-metal fast breeder reactor is on oxide fuels. The objective of our program is to obtain an economically optimized (U,Pu)O<sub>2</sub> fuel cycle for a liquid-metal fast breeder reactor by extending the performance capability and advancing the fabrication technology of oxide fuels. These fuels have the most advanced technology and greatest potential for reliable operation in first-generation LMFBR's. They have been tested in fast-flux environments but as yet have not been exposed under actual prototypic conditions. Currently, the burnup and heat rate are limited to about 50,000 Mwd/metric ton and 16 kw/ft, respectively, based on irradiation experiments with fuels that are not necessarily optimized for thermal, chemical, and mechanical performance.

The capability of oxide fuels can possibly be improved by adjusting structures or void distribution in the fuels. We emphasize irradiating fuels derived from the sol-gel process with thoroughly characterized structures and void distributions different from those of the oxide fuels irradiated heretofore. These include fuels fabricated by Sphere-Pac, vibratory compaction, extrusion, and pelletization. We compare the performance of these with the performance of reference fuels such as pellets derived from mechanically blended powders and coprecipitated material. The development of computer programs to assist in the analysis of test results and the development of a mathematical model to predict the performance of a fuel rod are integrated with the test program.

#### 1. FABRICATION DEVELOPMENT

(J. D. Sease)

The purpose of our fabrication development work is to provide suitable fabrication processes for sol-gel-derived materials and to fabricate irradiation test specimens and capsules for a variety of irradiation tests.

##### 1.1 Process Development

(R. A. Bradley, W. L. Moore)

This work is currently concerned with the engineering-scale development of the Sphere-Pac process and the development of sol-gel pelletization techniques for the fabrication of irradiation test specimens.

### 1.1.1 Sphere-Pac

Sphere-Pac is a technique for loading a fuel rod with graded microspheres. Our objective is to investigate the parameters that will allow the utilization of the Sphere-Pac process in the design of a production facility.

During the past month we completed a cursory investigation of variation of the time to infiltrate fine microspheres into a coarse bed of microspheres. The results showed that the infiltration time of a coarse bed, determined about every other day for a month, averaged 9.3 min with a standard deviation of 2.0 min. The same 0.245-in.-OD  $\times$  16-in.-long coarse bed had in previous experiments been infiltrated in 6.5 min with a range of  $\pm 0.5$  min. Therefore, this month we set up an experiment to determine the cause of the variation in loading time.

The test consisted of daily loading of a 0.245 in.  $\times$  16-in. bed of thoria microspheres, which had a normal size distribution of 510 to 600  $\mu$ . The Syntron vibrational amplitude was run at a high level of 100 and a low level of 70 setting. The stainless steel pin was vertically clamped at its top to the Syntron vibrator which was inclined 45° to the test pin. After loading of the coarse bed, the distance from the tube top to the top of the bed was measured as a check of consistent bed density. Fine thoria microspheres with a normal size distribution of 5 to 45  $\mu$  were then infiltrated into the coarse bed through a funnel with a screen soldered on the bottom. Runs were made with screens of 149- $\mu$  and 297- $\mu$  openings. Infiltration of the fines was accomplished at Syntron settings of 70 and 100. All fine microspheres were loaded without the aid of a follower rod. However, toward the completion of an infiltration run, when the fine microspheres remained in only the stem of the funnel, a follower rod was used to detect when all of the fine microspheres were out of the funnel. The infiltration was considered complete when the follower rod contacted the screen. Both the fine and coarse microsphere fractions were stored in open containers. A sample of the fines which loaded slowly was sent for moisture and CO<sub>2</sub> determinations.

The average coarse bed density for loadings at Syntron settings of 70 was 58.9% T.D. and at Syntron settings of 100 was 59.6%. The results of the various infiltration times at the Syntron setting of 70 and 100 with 149 and 297- $\mu$  screen funnels are shown in Table 1. The infiltration times at Syntron settings of both 100 and 70 took less time with 297- $\mu$  screens than with the 149- $\mu$  screen. Apparently the smaller screen opening is more conducive to causing bridging, therefore restricting the infiltration of the fines. With either the 149- $\mu$  screen or the 297- $\mu$  screen, infiltration times were shorter and less varied when the fines were infiltrated at a Syntron setting of 70. The reason that infiltration times are longer at Syntron settings of 100 is that with the higher amplitude of vibration, considerable upward energy is put into the coarse bed. Results of moisture and CO<sub>2</sub> analysis will be reported next month.

Table 1. Fine Fraction Infiltration Times with Syntron Settings  
of 70 and 100 with 149- $\mu$  and 297- $\mu$  Screen Funnels

Infiltrations with 149- $\mu$ Screen				Infiltrations with 297- $\mu$ Screen			
Syntron Setting		Infiltration Time		Syntron Setting		Infiltration Time	
Coarse	Fine	Average (min/sec)	Range (sec)	Coarse	Fine	Average (min/sec)	Range (sec)
70	70	3/53	5	70	70	2/15	16
100	100	5/25	125	100	100	4/26	100
				100	70	2/35	13

### 1.1.2 Pelletization of Sol-Gel Urania-Plutonia

The fabrication of the  $(U,Pu)O_2$  pellets for the ORR SG-3 capsule was described in last month's report. We adjusted the O/M of these to 1.99 by heat treating in Ar-4%  $H_2$  at 1300°C with a Ta foil getter.

We prepared a 1300-g batch of  $(Pu_{0.20},U_{0.80})O_2$  powder for use in making pellets for the ETR 43-120 through 43-123 series of irradiation capsules. We are presently calcining this powder. A test sinter run indicated that the powder would be suitable for making both the 84% dense pellets required for ETR and the 87.6% dense pellets for GR-1 (on the GCFR program).

The preparation of approximately 3 kg of  $(Pu_{0.20},U_{0.80})O_2$  (93% enriched U) is under way. Due to criticality limitations, the material must be prepared in 10 batches. The blending and drying will require about four weeks.

## 1.2 Capsule Fabrication

(E. J. Manthos, W. L. Moore,  
M. K. Preston, R. B. Pratt)

Two instrumented TREAT capsules (TREAT I and II) are awaiting shipment to the TREAT Reactor. The fuel portion of the ORR capsule SG-3 was fabricated. Planning for the fabrication of the EBR-II, Series II fuel rods continued.

### 1.2.1 TREAT Capsule Fabrication

The two TREAT capsules completed last month were temporarily stored in the Nuclear Materials Storage Area. The instrument plugs and cables for each capsule were thoroughly checked out. Resistance measurements were made for each wire and recorded for checkout purposes at the TREAT Reactor site.

Compilation of all data sheets, certification paper for materials, inspection reports, and x-ray radiographs is essentially complete. Checking of all the data is not complete. Photography of the assembly sequence and capsule hardware for future reference and for inclusion in the assembly report is complete.

Arrangements for shipping the TREAT capsules are nearly complete. The shipping container is ready, and the shipping container's protective package is due at ORNL October 1. The DOT approval for shipment of fissile material and alkali metal in the same container was received.

### 1.2.2 ORR Capsules

The fuel element portions of ORR instrumented capsule SG-3 were fabricated and are ready for insertion into the irradiation capsule. The fuel elements for the ORR capsule consist of two 3-in.-long fueled annuli clad in 3/8-in.-OD Ti-modified type 304 stainless steel with a 1/8-in.-diam central thermocouple well of W-25% Re. The fuel used in fuel pin SG-3A was TREAT microspheres from fuel lot 103, which contained a nominal  $(U_{0.8}, Pu_{0.2})O_2$  with an O/M of 1.987. The fuel was loaded by the Sphere-Pac process to a smear density of 82.1% of theoretical. Fuel pin SG-3B contained  $(U_{0.8}, Pu_{0.2})O_2$  pellets with an average density of 83.5. When the 0.0025-in. diametral gap is taken into account, this is equivalent to a smear density of 82.2. The O/M of these pellets was 1.992. The elements were fabricated with no difficulty.

### 1.2.3. EBR-II, Series II Unencapsulated Fuel Rods

We are currently analyzing requirements for fabricating 19 unencapsulated fuel rods which will be irradiated in a shared 37-rod subassembly in the EBR-II Reactor.

## 2. FUEL EVALUATION

(C. M. Cox, T. N. Washburn,  
J. M. Leitnaker)

The fuel evaluation work involves both out-of-reactor and in-reactor tests to characterize the fuels of interest and to determine performance limits of the fuels.

### 2.1 Characterization of Fuels

The development of sol-gel fuel fabrication requires characterization of the material to control the process and to determine which properties are important to irradiation behavior. Characterization requires determining both the chemical composition and the physical properties. Thermodynamic studies contribute to the development of the process for the fuel and aid in predicting fuel performance for both irradiation testing and model studies.

#### 2.1.1 Analytical Chemistry (W. H. Pechin)

A specification was prepared for the  $UO_2$  blanket pellets to be used in the EBR II, Series II irradiation tests. The analyses and limits covered by this specification are listed in Table 2. Specifications for the  $ThO_2$  insulator pellets and the  $(U, Pu)O_2$  fuel pellets are in preparation.

The finished blanket pellets shall conform to the following analyses:

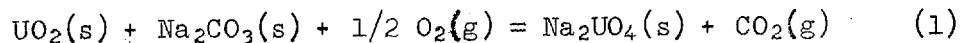
Table 2. Summary of Specification  
for UO<sub>2</sub> Blanket Pellets

Analysis	Limit
Total uranium	not less than 88.0 wt %
Carbon	100 ppm maximum
Nitrogen	100 ppm maximum
Chloride	20 ppm maximum
Fluoride	20 ppm maximum
Iron	100 ppm maximum
Sum of calcium, silicon, and aluminum	300 ppm maximum
Oxygen-to-uranium ratio	not greater than 2.002
Moisture	30 ppm maximum
Gas release	The volume of gas at STP released to vacuum when whole pellets are heated to 1200°C shall not exceed 0.05 cm <sup>3</sup> /g of UO <sub>2</sub> .

2.1.2 Alkali Metals - Uranium-Oxygen Investigations (J. M. Leitnaker,  
K. E. Spear)

Interaction of alkali metals with UO<sub>2</sub> is of interest for two reasons. First, the coolant proposed for liquid metal fast breeder reactors is sodium. Pin holes in the clad may allow sodium to diffuse into the fuel pin, driven by the reaction of sodium with the fuel. Second, since cesium is a prominent fission product, the extent to which the cesium reacts with the fuel, clad, and other fission products is important in interpreting the results of in-reactor tests. Our immediate efforts are on the Na-U-O system, but work on the Cs-U-O; Na-U,Pu-O; and Cs-U,Pu-O systems is contemplated.

We have previously discussed<sup>1</sup> our attempted study of the reaction



and the fact that the Na<sub>2</sub>UO<sub>4</sub> was not as stable as predicted. That is,

<sup>1</sup> J. M. Leitnaker, K. E. Spear, "Fuel-Cladding Compatibility Studies for Gas-Cooled Fast Breeder Reactors," Fuel Cycle Technology Monthly Report for Month Ending August 1969, pp. 38-40.

we observed that  $\text{Na}_2\text{UO}_4$  did not form from  $\text{UO}_2$  and  $\text{Na}_2\text{CO}_3$  under conditions predicted by data given in the literature. We also noted that by heating  $\text{Na}_2\text{CO}_3\text{-UO}_2$  in a 100:1  $\text{CO}_2/\text{CO}$  mixture produced a new phase.

During the present reporting period we have run several additional experiments to determine the conditions of stability and the composition of this new compound. Heating the  $\text{Na}_2\text{CO}_3\text{-UO}_2$  mixture under a 10:1  $\text{CO}_2/\text{CO}$  mixture at  $900^\circ\text{C}$  also produced the new phase while a 1:1  $\text{CO}_2/\text{CO}$  mixture seemed to reverse the reaction. (There is some question about this last point; a 1:1 mixture may be very close to the equilibrium composition gas mixture.) Additional experiments should let us establish the stability of the new phase, the composition of which is still unknown. We have done a number of experiments to try to prepare well crystallized samples and to establish the composition. We attempted to measure weight losses of powdered samples and deduce the composition from this information plus x-ray examination. However, the hygroscopic nature of  $\text{Na}_2\text{CO}_3$  plus a lack of atmosphere control when handling powdered samples caused this approach to be unsuccessful. However, samples of 2:1 (mole ratio)  $\text{UO}_2\text{-Na}_2\text{CO}_3$ , which had been heated at approximately  $1000^\circ\text{C}$  in a 9:1  $\text{CO}_2/\text{CO}$  ratio, revealed by metallographic examination two phases:  $\text{Na}_2\text{CO}_3$  and the new phase. Thus, the new phase has at least one U per Na and is probably richer in U than this. Either polarized light or sensitive tint is capable of revealing the diphasic character of the mixture.

By using a large excess of  $\text{Na}_2\text{CO}_3$ , we hoped to produce a single crystal of the compound from the  $\text{Na}_2\text{CO}_3$  melt. However, our early experiments did not produce good results, although some crystal growth was revealed. We attempted to remove the  $\text{Na}_2\text{CO}_3$  by melting, but the material was too viscous. Finally, heating to above  $1600^\circ\text{C}$  in vacuum in the induction furnace removed most of the  $\text{Na}_2\text{CO}_3$  by volatilization, but also caused vaporization of  $\text{Na}_2\text{O}$ , leaving  $\text{UO}_2$ .

Several samples of the  $\text{Na}_2\text{CO}_3 + \text{UO}_2$  were mixed together, pelletized, and heated in an oxidizing atmosphere. Conditions and results are tabulated in Table 3.

In the first four samples of Table 3, metallography appeared to reveal several phases; the x-ray patterns were quite similar. However, the high temperature may be causing a phase change from other phases and on cooling, imperfect crystallization results. Sample 42-1 appears single-phase by x ray. The x-ray lines are sharp and clear. According to the nominal composition, a previously unknown compound has been prepared. However, we do not see extra  $\text{Na}_2\text{CO}_3$  in our x rays because of a difference in mass absorption coefficient. Since 42-2 is two-phase, however, it appears that indeed we may have seen a new material. (The known sodium uranates are:  $\text{Na}_2\text{UO}_4$ ,  $\text{Na}_2\text{U}_2\text{O}_7$ ,  $\text{Na}_2\text{U}_3\text{O}_{10}$ ,  $\text{Na}_2\text{U}_4\text{O}_{13}$ ,  $\text{Na}_2\text{U}_6\text{O}_{19}$ , and  $\text{Na}_2\text{U}_7\text{O}_{22}$ . Sample 42-1 has four mole of Na to one of U.) Clearly, further effort will be necessary to identify the phases.

A particularly interesting facet of the metallography is that when the samples stand after being polished, they react with the atmosphere, resulting in the growth of white—or clear—crystals on

Table 3. Results of Heating  $\text{Na}_2\text{CO}_3\text{-UO}_2$  Pelletized Mixtures in Air<sup>a</sup>

Number	Mixture (moles) <sup>b</sup>		Color	X ray	Metallography
	$\text{UO}_2$	$\text{Na}_2\text{CO}_3$			
35-1	2	0.85	Dark brown	Diffuse, phases not clear	Diphasic under polarized light. Bright yellow phase is minor. Dark phase is anisotropic.
35-2	2	0.95	Light brown	Diffuse, phases not clear	Under polarized light, sample is nearly all orange—see little second phase—very faint trace of the dark phase of 35-1.
35-3	2	1.05	Dark orange	Diffuse, phases not clear	See another anisotropic phase—not same as the 35-1, plus the material of 35-2.
35-4	2	1.15	Dark orange	Diffuse, phases not clear	Similar to 35-3 except more of the anisotropic phase seen in 35-3.
42-1	1	2	Bright orange	Sharp, 1 phase	Could see little difference in these samples by metallography except density increases from 1 through 4. There may be a light second phase ( $\text{Na}_2\text{CO}_3$ ?).
42-2	1.4	2	Bright orange	Sharp, 2 phases	
42-3	1.6	2	Bright orange	Sharp, 2 phases	
42-4	1.8	2	Bright orange..	Sharp, 2 phases	

<sup>a</sup>Samples 35-1, 35-2, 35-3, and 35-4 were heated over a weekend in oxygen at  $850^\circ\text{C}$  and then overnight in air at  $1100^\circ\text{C}$ . Samples 42-1 through 42-4 were heated twice overnight at  $850^\circ\text{C}$  in air. All samples were pelletized between heatings.

<sup>b</sup>There is some uncertainty about the quantity of moisture in the  $\text{Na}_2\text{CO}_3$ .

top of the sample. The growth is particularly impressive (over a period of a couple of weeks) if the sample has been ground in water instead of oil. This growth is quite similar in appearance to a growth seen by hot-cell personnel in irradiated samples and suggests a similar mechanism. This phenomenon needs further study.

### 2.1.3 Chemical Effects of Nuclear Burnup on (U,Pu)O<sub>2</sub> Fuels (J. M. Leitnaker, K. E. Spear)

Previously reported calculations<sup>2</sup> have shown that the manner in which rare earths take up oxygen (either as RE<sub>2</sub>O<sub>3</sub> or REO<sub>2</sub>) in their dissolution in (U,Pu)O<sub>2</sub> fuels can be important in determining the effect of burnup on oxygen potential of the fuel. Furthermore, the effect of this dissolution is important on the swelling of the fuel. Our experiments are designed to gain an understanding of these kinds of behavior in (U,Pu)O<sub>2</sub> fuels. Our work last month seemed to indicate that Eu<sup>+3</sup> was oxidized to a state, effectively, between +3 and +4 in the solid solution.

One of the problems reported last month was that obtaining equilibrium between physically mixed oxides is difficult. We continued work in this regard on Eu<sub>2</sub>O<sub>3</sub>-UO<sub>2</sub> mixtures and began similar studies with CeO<sub>2</sub>-UO<sub>2</sub> mixtures. Our initial approach was heating in vacuum in a W crucible to higher temperatures, which are attainable in our induction furnace. This procedure works and equilibrium—as detected by x-ray diffraction—is attained. However, weight losses of several milligrams are observed from the sample in the one to two hours required. Since a great deal of effort would be required to determine what is being lost, we are seeking different approaches.

One technique which seems promising is to co-precipitate the Ce<sup>+4</sup> and U<sup>+6</sup> materials from acid solutions in NH<sub>4</sub>OH. By gentle heating in H<sub>2</sub>, the unwanted material, NH<sub>4</sub>OH, NH<sub>4</sub>NO<sub>3</sub>, and H<sub>2</sub>O, could be vaporized, leaving only submicron-scale mixture of CeO<sub>2</sub>-UO<sub>2</sub> (with some extra water and oxygen, perhaps). Further heating at 1200°C in 10:1 CO/CO<sub>2</sub> mixture does indeed produce a clear, sharp x-ray pattern.

Further efforts will be directed toward quantitative precipitation of known quantities of U<sup>+6</sup> and Ce<sup>+8</sup> (and other rare earth ions), reduction to something near the +4 state for the U, and further equilibration in CO/CO<sub>2</sub> mixtures. This procedure will, hopefully, result in mixtures from which the lattice parameters can be determined precisely.

---

<sup>2</sup> Leitnaker, op.cit.

## 2.2 Irradiation of Fuels

(C. M. Cox, T. N. Washburn,  
E. L. Long, Jr., H. C. McCurdy)

The final evaluation of (U,Pu)O<sub>2</sub> fuels will be based upon their irradiation performance. The irradiation testing program is concentrating on comparative tests of three fabrication forms: Sphere-Pac, pellets, and extrusions. The program includes thermal-flux irradiations that permit use of instrumented capsules and achievement of high burnup levels in relatively short times. These tests will provide supplemental information essential to the analysis of the fast-flux irradiation tests, in which the radial fission-rate distribution and cladding damage are more typical of anticipated LMFBR operating conditions. The test program also includes power transient tests to investigate fuel performance under abnormal operating conditions. The development of mathematical models to predict fuel behavior and of computer programs for analyzing fuel performance are integral parts of the irradiation test program.

### 2.2.1 Uninstrumented ETR Tests (A. R. Olsen, D. R. Cuneo)

The status of the tests in this series is given in Table 4. There have been no significant changes in the status of the first six capsules.

The last four capsules, 43-116 through 43-119 as reported previously<sup>3</sup> are being irradiated to provide fuel containing short half-life fission products for processing studies. No detailed postirradiation examination of these rods is planned. The first of these capsules contained Sphere-Pac (U-15% Pu)O<sub>2</sub> fuel irradiated to over 1% FIMA burnup. At the request of the AEC, we now plan to concentrate on Fast Flux Test Reactor (FTR) fuel for these studies. Consequently, fuel made to FTR reference specifications has been ordered and will be irradiated instead of the originally planned sol-gel Sphere-Pac fuel in experiments 43-117, 43-118, and 43-119. We have on hand type 316 stainless steel tubing of 0.230-in. OD × 0.015-in. wall thickness fabricated to FTR specifications for these test rods.

### 2.2.2 Instrumented ETR Tests (C. F. Sanders)

Four instrumented ETR capsules are being constructed to determine the effects of high cladding temperatures, high fission gas retention, and long fuel columns on fuel element performance. We completed design of the capsules, and engineering drawings were issued. The

---

<sup>3</sup> A. R. Olsen, C. M. Cox, and R. B. Fitts, "Uninstrumented Thermal Flux Irradiation Tests," Fuels and Materials Development Program Quart. Progr. Rept. March 31, 1969, ORNL-4420, pp. 25-29.

Table 4. Noninstrumented Thermal Flux Tests of  
(U,Pu)O<sub>2</sub> Fuels

Experiment Number	Fuel		Number of Rods	Peak Burnup (% FIMA) <sup>a</sup>	Peak Linear Heat Rate (w/cm)	Peak Cladding Inner Surface Temperature (°C)	Status September 1969
	Form	Composition					
43-99	Sphere-Pac	( <sup>235</sup> U <sub>0.80</sub> ,Pu <sub>0.20</sub> )O <sub>2.00</sub>	2	1.5 <sup>b</sup>	1640 <sup>b</sup>	1000	Examined
43-100	Sphere-Pac	( <sup>235</sup> U <sub>0.80</sub> ,Pu <sub>0.20</sub> )O <sub>2.00</sub>	2	1.4 <sup>b</sup>	1470 <sup>b</sup>	900	Examined
43-103	Sphere-Pac Pellet	UO <sub>2.02</sub> (20% <sup>235</sup> U)	3	5	690	530	Being examined
		UO <sub>2.00</sub> (20% <sup>235</sup> U)	1				
43-112	Sphere-Pac	( <sup>238</sup> U <sub>0.85</sub> ,Pu <sub>0.15</sub> )O <sub>1.97</sub>	3	0.7	500	360	Being examined
		UO <sub>2.02</sub> (20% <sup>235</sup> U)	1				
43-113	Sphere-Pac	( <sup>238</sup> U <sub>0.85</sub> ,Pu <sub>0.15</sub> )O <sub>1.97</sub>	3	10 <sup>c</sup>	500 <sup>c</sup>	380 <sup>c</sup>	In-reactor, ≥ 7.5% FIMA
		UO <sub>2.02</sub> (20% <sup>235</sup> U)	1				
43-115	Sphere-Pac	( <sup>238</sup> U <sub>0.85</sub> ,Pu <sub>0.15</sub> )O <sub>1.97</sub>	3	5 <sup>c</sup>	600 <sup>c</sup>	460 <sup>c</sup>	Being examined
		UO <sub>2.02</sub> (20% <sup>235</sup> U)	1				
43-116	Sphere-Pac	( <sup>238</sup> U <sub>0.85</sub> ,Pu <sub>0.15</sub> )O <sub>1.97</sub>	4	1.5 <sup>c</sup>	600 <sup>c</sup>	460 <sup>c</sup>	Being examined
43-117 } 43-118 } 43-119 }	Ref. FTR Pellets	( <sup>238</sup> U,Pu )O <sub>1.98</sub>	4	1.5 <sup>d</sup>	600 <sup>c</sup>	460 <sup>c</sup>	In preparation

<sup>a</sup>FIMA is fissions per initial actinide metal atom.

<sup>b</sup>Rods failed in reactor from overpowering.

<sup>c</sup>These are target design values.

<sup>d</sup>This is an approximate level. Test will be irradiated for two FTR cycles to produce fuel for reprocessing studies.

design parameter data are listed in Table 5. Fabrication of the hardware was started, the capsule tubing was inspected, and the fuel cladding is being inspected. All of the capsule material is on hand except the 5/8-in.-OD tubing for the sleeves, and it is expected shortly. A request was submitted to the Idaho Nuclear Corporation for the checkout and installation of the instrumentation needed for this series of tests.

### 2.2.3 ORR Instrumented Tests (R. B. Fitts, D. R. Cuneo, V. A. DeCarlo)

The ORR instrumented tests are designed to study the thermal performance of experimental fuel rods. The first series of tests is designed for studying sol-gel-derived (U,Pu)O<sub>2</sub> fuels.

Capsule SG-2 is undergoing postirradiation examination. The external visual inspection of the capsule and fuel rods, the dimensional characterization of the fuel rods, and the collection of the gases contained in the rods are completed. All of these observations were normal except that one gas sample was lost due to an improper cut made on the fuel rod during disassembly. Since the fuel rods were identical, this is not believed to be an important loss. We have found no significant external changes in the fuel rods. They are presently being sectioned for metallography.

Fabrication of capsule SG-3 is essentially complete. This test will contain (U<sub>0.8</sub>,Pu<sub>0.2</sub>)O<sub>1.98</sub> fuel at 81% smear density. The upper rod contains Sphere-Pac fuel and the lower rod contains pellet fuel. The fuel centerline thermocouple in each rod will permit a direct comparison of the performance of these two fuel forms. The irradiation test is scheduled to commence in October.

### 2.2.4 TREAT Reactor Tests (C. M. Cox, R. E. Adams, E. J. Manthos)

The Series I TREAT experiments will compare the transient behavior of unirradiated sol-gel-derived Sphere-Pac and pelletized (U<sub>0.8</sub>,Pu<sub>0.2</sub>)O<sub>2</sub> fuels. The hazards analysis, test specifications, and operating manual have been submitted to the TREAT staff and accepted with minor revisions. Approval has been obtained to ship the first two capsules to TREAT on October 1, 1969.

A procedure for the disassembly and examination of the first two TREAT capsules in the hot cells is being written.

### 2.2.5 Fast-Flux Irradiation Tests (A. R. Olsen)

The Series I encapsulated tests described previously<sup>4,5</sup> are continuing their irradiation in Subassembly XO50. The exposure as of

<sup>4</sup> A. R. Olsen, Experimental Description and Hazards Evaluation for the Series I ORNL Oxide Fuels Irradiation in EBR-II, ORNL-TM-2635, in press

<sup>5</sup> A. R. Olsen, C. M. Cox, and J. D. Jenkins, "Fast-Flux Irradiation Tests," Fuels and Materials Development Program Quart. Progr. Rept. for Period Ending March 31, 1968, ORNL-4420, pp. 33-34.

Table 5. Design Parameters for ETR Instrumented Capsules

Capsule Identification	43-120 and 43-121	43-122 and 43-123
Composite fuel composition	(0.2 Pu-0.8 U) <sub>01.98</sub>	(0.2 Pu-0.8 U) <sub>01.98</sub>
Fuel length, in.	20	3
Cladding dimension, in.	0.250 × 0.016 wall	0.250 × 0.016 wall
Fuel-to-clad bond	He	He
Peak linear heat rate, kw/ft	19	15.5
Max cladding outer surface temp, °C	600	500
Max cladding inner surface temp, °C	660	550
Max fuel surface temp, °C	820	590
Max fuel center temp, °C	2340	1980
Capsule dimensions, in.	1.000 OD × 0.065 wall	1.000 OD × 0.065 wall
Sleeve dimensions, in.	0.625 OD × 0.035 wall	0.625 OD × 0.035 wall
Cladding capsule bond	NaK-44	NaK-44
Fuel pins per capsule	1	4
Insulator composition	UO <sub>2</sub>	ThO <sub>2</sub>
No. of Sphere-Pac pins per capsule	1	2
No. of pellet pins per capsule	0	2
Composition of coarse microspheres	(0.27 Pu-0.73 U) <sub>01.98</sub>	(0.2 Pu-0.8 U) <sub>01.98</sub>
Composition of fine microspheres	UO <sub>2.00</sub>	(0.2 Pu-0.8 U) <sub>01.98</sub>
Max. burnup	43-120 - 5% FIMA 43-121 - 10% FIMA	43-122 - 5% FIMA 43-123 - 10% FIMA

August 30 (the end of EBR-II, Run 37) was 5906 Mwd of operation. The current calculated peak burnup for the highest heat rate rod in this series is 3.1% FIMA or approximately 63% of the currently scheduled burnup. Because of the current EBR-II experimental operation at power levels above 50 Mw, Subassembly X050, as well as other experimental fuel subassemblies, was removed at the start of Run 38. Continued exposure is proposed toward the end of Run 38. Since the test exposure to be accumulated during this run is unknown, the discharge schedule for the subassembly is in doubt. The earliest discharge will be after Run 39 in January 1970; however, exposure during Run 40 is a possibility.

The proposal for "Approval-in-Principle" for the Series II unencapsulated tests was submitted to the AEC. This proposal involves a 37-pin subassembly to be shared with the Babcock and Wilcox Company. The pin allocations have been subdivided so that 18 positions will be used by B & W and 19 positions by ORNL. The two experimental programs have been coordinated to provide complementary fuel performance data. Each site will be responsible for the fabrication, inspection, shipping, and postirradiation examination of its own pins; but a single safety analysis will be prepared for the subassembly.

Tables 6 and 7 define the fuel varieties and burnup levels proposed for irradiation by each of the sites. The ORNL test pins will concentrate on pelletized and Sphere-Pac sol-gel-derived fuel.

Although we have not proceeded with specific designs for the fuel pins, pending preliminary approval, we currently propose to use a fuel pin with a 0.250-in. OD  $\times$  0.016-in. wall type 316 stainless steel cladding. The cladding material has been obtained from Pacific Northwest Laboratories. The fuel column length will be 13.5 in., and the balance of the pin interior will contain features similar to the ORNL Series I test rods. The B & W pin design will be similar, but may differ in detail. The pin end fittings will be designed to fit a Mark J subassembly. Since we are interested in performing these tests with peak cladding temperatures in the 550 to 650°C temperature range, we have contacted the EBR-II project on the possibilities of revising the Mark J subassembly to accommodate 37 pins with a 0.250-in.-OD cladding.

#### 2.2.6 Irradiation Test Calculations (A. R. Olsen, R. B. Fitts, C. M. Cox)

A series of calculations was made using computer codes developed over the past two years to describe various features of fuel irradiations. The results of these calculations were incorporated into a paper presented recently.<sup>6</sup>

---

<sup>6</sup> A. R. Olsen, R. B. Fitts, and C. M. Cox, "Analysis of the Validity of Fast Reactor Fuel Tests in Existing Test Reactors," Paper presented at the National Symposium on Developments in Irradiation Testing Technology, NASA, Lewis Research Center, Sandusky, Ohio, Sept. 9-11, 1969. To be published in the proceedings; also ORNL-TM-2716.

Table 6. Proposed B &amp; W Program

18 Allotted Positions in the  
37-pin Subassembly

Material <sup>a</sup>	Bundle Burnup, Mwd/T $\times 10^{-3}$				
	0	25	50	75	100
Vi-Pac	Pin 1				Pin 38
Vi-Pac	Pin 2				Pin 39
Sphere-Pac	Pin 3				Pin 40
Sphere-Pac	Pin 4				Pin 41
Sphere-Pac	Pin 5				Pin 42
Pellets	Pin 6				Pin 43
Pellets	Pin 7				Pin 44
Vi-Pac	Pin 8			Pin 45	
Sphere-Pac	Pin 9			Pin 46	
Pellet	Pin 10			Pin 47	
Vi-Pac			Pin 11		
Vi-Pac			Pin 12		
Vi-Pac			Pin 13		
Sphere-Pac			Pin 14		
Sphere-Pac			Pin 15		
Sphere-Pac			Pin 16		
Pellet			Pin 17		
Pellet			Pin 18		

<sup>a</sup>All types of fuel will be irradiated with a smear density of  $82 \pm 1\%$  of theoretical.

Table 7. Proposed ORNL Series II EBR-II Irradiation Tests  
 19 Allotted Positions in the  
 37-pin Subassembly

Material <sup>a</sup>	Smear Density (% T.D.)	Bundle Burnup, Mwd/T × 10 <sup>-3</sup>				
		0	25	50	75	100
SP	80		Pin 19		Pin 48	
SP	80		Pin 20			
SP	85		Pin 21		Pin 49	
SP	85		Pin 22			
SP	85		Pin 23		Pin 50	
SP	85		Pin 24			
SPL	80		Pin 25		Pin 51	
SPL	80		Pin 26			
SPL	85		Pin 27		Pin 52	
SPL	85		Pin 28			
SP	85		Pin 29		Pin 53	
SP	85		Pin 30		Pin 54	
PEL	85		Pin 31		Pin 55	
PEL	85		Pin 32			
PEL	90		Pin 33		Pin 56	
PEL	90		Pin 34			
PELL	80		Pin 35		Pin 57	
PELL	80		Pin 36			
PELL	85		Pin 37		Pin 58	

<sup>a</sup> SP = Sol-gel Sphere-Pac with O/M of 1.98  
 SPL = Sol-gel Sphere-Pac with O/M of 1.94  
 PEL = Sol-gel Pellets with O/M of 1.98  
 PELL = Sol-gel Pellets with O/M of 1.94



## INTERNAL DISTRIBUTION

1. R. D. Ackley
2. R. E. Adams
3. G. M. Adamson, Jr.
4. L. G. Alexander
5. E. D. Arnold
6. M. J. Bell
7. M. R. Bennett
8. R. L. Bennett
9. R. E. Blanco
10. J. O. Blomeke
11. E. S. Bomar
12. W. D. Bond
13. G. E. Boyd
14. R. A. Bradley
15. R. E. Brooksbank
16. K. B. Brown
17. F. R. Bruce
18. W. D. Burch
19. W. H. Carr
20. W. L. Carter
21. G. I. Cathers
22. J. M. Chandler
23. S. D. Clinton
24. H. E. Cochran
25. C. F. Coleman
26. J. H. Coobs
27. C. M. Cox
28. R. L. Cox
29. D. J. Crouse
30. F. L. Culler, Jr.
31. J. E. Cunningham
32. F. C. Davis
33. W. Davis, Jr.
34. H. G. Duggan
35. J. H. Evans
36. D. E. Ferguson
37. L. M. Ferris
38. B. C. Finney
39. R. B. Fitts
40. J. D. Flynn
41. M. H. Fontana
42. E. J. Frederick
43. J. H. Frye, Jr.
44. W. Fulkerson
45. F. J. Furman
46. H. W. Godbee
47. H. E. Goeller
48. J. H. Goode
49. A. T. Gresky
50. W. R. Grimes
51. W. S. Groenier
52. P. A. Haas
53. R. G. Haire
54. R. L. Hamner
55. W. O. Harms
56. F. E. Harrington
57. C. C. Haws, Jr.
58. M. R. Hill
59. N. W. Hill
60. F. J. Homan
61. D. E. Horner
62. F. J. Hurst
63. A. R. Irvine
64. F. A. Kappelmann
65. P. R. Kasten
66. A. H. Kibbey
67. F. G. Kitts
68. B. B. Klima
69. J. M. Leitnaker
70. C. S. Lisser
71. R. E. Leuze
72. M. H. Lloyd
73. J. T. Long
74. A. L. Lotts
75. R. S. Lowrie
76. H. G. MacPherson
77. R. E. MacPherson, Jr.
78. S. Mann
79. E. J. Manthos
80. C. D. Martin, Jr.
81. J. P. McBride
82. R. W. McClung
83. K. H. McCorkle
84. W. T. McDuffee
85. A. B. Meservey
86. J. G. Moore
87. W. L. Moore
88. L. E. Morse
89. C. A. Mossman
90. J. P. Nichols
91. E. L. Nicholson
92. K. J. Notz
93. C. H. Odom
94. A. R. Olsen
95. J. R. Parrott
96. W. A. Pate
97. P. Patriarca
98. W. L. Pattison

99. W. H. Pechin
100. J. W. Prados
101. R. B. Pratt
102. R. H. Rainey
103. J. M. Robbins
104. J. T. Roberts
105. J. D. Rollins
106. A. D. Ryon
107. C. F. Sanders
108. J. M. Schmitt
109. J. L. Scott
110. J. D. Sease
111. L. B. Shappert
112. Moshe Siman-Tov
113. J. W. Snider
114. H. F. Soard
115. W. G. Stockdale
116. W. C. T. Stoddart
117. J. C. Suddath
118. O. K. Tallent
119. E. H. Taylor
120. R. E. Thoma
121. R. E. Toucey
122. D. B. Trauger
- 123-124. W. E. Unger
125. V. C. A. Vaughen
126. T. N. Washburn
127. D. C. Watkin
128. C. D. Watson
129. A. M. Weinberg
130. J. R. Weir
131. G. A. West
132. M. E. Whatley
133. W. M. Woods
134. E. I. Wroblewski
- 135-136. R. G. Wymer
137. O. O. Yarbro
138. H. C. Young
- 139-140. Central Research Library
141. Document Reference Section
- 142-151. Laboratory Records
152. Laboratory Records-RC
153. ORNL Patent Office
154. Nuclear Safety Information Center

## EXTERNAL DISTRIBUTION

## AEC, Washington

- 155. R. W. Barker
- 156. P. Clark
- 157. J. Crawford
- 158. G. W. Cunningham
- 159. A. Van Echo
- 160. J. S. Griffio
- 161. N. Habeman
- 162. J. A. McBride
- 163. T. McIntosh
- 164-173. W. H. McVey
- 174. H. Schneider
- 175-178. J. M. Simmons
- 179. E. E. Sinclair
- 180. A. N. Tardiff
- 181. W. R. Voigt
- 182. M. J. Whitman

AEC - ANL, USAEC, 9800 S. Cass Avenue, Argonne, Illinois 60439

- 183. M. E. Jackson, RDT Senior Site Representative

AEC - Canoga Park Area Office, USAEC, P. O. Box 591, Canoga Park, California 91305

- 184. C. W. Richards

AEC - Gulf General Atomic, P. O. Box 2325, San Diego, Calif. 92112

- 185. R. H. Ball, RDT Senior Site Representative

AEC - IDO, P. O. Box 2108, Idaho Falls, Idaho 83401

- 186. K. K. Kennedy, Idaho Operations Office

AEC - ORNL RDT Site Office

- 187. D. F. Cope, RDT Senior Site Representative
- 188. R. L. Philippone

AEC - ORO, Oak Ridge, Tennessee 37830

- 189-203. DTIE
- 204. Laboratory and University Division

AEC - Richland Operations Office, USAEC, P. O. Box 550, Richland, Washington 99352

- 205. W. Devine, Jr., Director, Production Reactor Division
- 206. P. H. Holsted, RDT Senior Site Representative, PNL
- 207. J. Morabito, FFTF Project Manager, RDT
- 208. J. Shirley, FFTF Project Administrator, RL

Allied Chemical Nuclear Products, Inc., Gen. Chem. Div., Box 35,  
Florham Park, N. J. 07932

- 209. R. I. Newman
- 210. E. M. Shank

ANL, 9700 South Cass Avenue, Argonne, Illinois 60439

- 211. A. Amorosi, IMFBR Program Office
- 212. Leslie Burris, Jr., Associate Director of Chemical  
Engineering Division
- 213. S. Lawroski
- 214. W. J. Mecham
- 215. M. Nevitt, Director, Metallurgy Division
- 216. W. B. Seefeldt
- 217. C. E. Stevenson
- 218. R. C. Vogel
- 219. D. S. Webster

Atlantic Richfield Hanford Co., Attention: Document Control, P. O.  
Box 250, Richland, Washington 99352

- 220. G. C. Oberg
- 221. Milt Szulinski
- 222. R. E. Tomlinson

Atomics International, Div. of North American Aviation, Inc., P. O.  
Box 309, Canoga Park, California 91305

- 223. R. Aronstein
- 224-227. Simcha Golan
- 228. C. A. Trilling

Babcock & Wilcox, Research and Development Div., P. O. Box 1260,  
Lynchburg, Virginia 24505

- 229. E. M. Croft
- 230. E. W. Dewell
- 231. David Mars

Battelle Pacific Northwest Laboratory, P. O. Box 999, Richland,  
Washington 99352

- 232. E. R. Astley
- 233. D. C. Boyd
- 234. C. R. Cooley
- 235. Director, PNL
- 236. E. D. Grazzini
- 237. D. R. de Halas
- 238. A. M. Platt

BNL, Upton, New York 11973

- 239. W. E. Winche

Combustion Engineering, Inc., Nuclear Power Dept., P. O. Box 500,  
Windsor, Connecticut 06095

- 240-241. W. P. Staker

E. I. du Pont de Nemours & Co., Savannah River Laboratory, Aiken,  
South Carolina 29801

- 242. L. H. Meyer
- 243. D. A. Orth
- 244. E. B. Sheldon

General Electric Company, 283 Brokaw Rd., Santa Clara, Calif. 95050

- 245. R. G. Barnes
- 246. A. S. Gibson
- 247. W. H. Reas

Gulf General Atomic, P. O. Box 608, San Diego, California 92112

- 248. Stanley Donelson
- 249. A. J. Goodjohn
- 250-251. R. H. Graham
- 252. A. R. Matheson
- 253. R. E. Norman
- 254. J. N. Siltanen
- 255. K. B. Steyer

Idaho Nuclear Corporation, P. O. Box 1845, Idaho Falls, Idaho 83401

- 256. J. A. Buckham
- 257. W. J. Maeck

Massachusetts Institute of Technology, Cambridge, Massachusetts 02139

- 258. Manson Benedict

National Lead Company of Ohio, Cincinnati, Ohio

- 259. S. Marshall

National Lead, New Projects Dept., 11 Broadway, New York, N. Y. 10000

- 260. S. H. Brown

Nuclear Fuel Services, Inc., Wheaton, Maryland 20902

- 261. W. H. Lewis, Vice President

Nuclear Materials and Equipment Corp., Apollo, Pennsylvania 15613

- 262. C. S. Caldwell
- 263. W. J. Ross
- 264. M. Selman

Westinghouse Electric Corp., P. O. Box 355, Pittsburgh, Pa. 15230

- 265. E. F. Beckett
- 266. C. E. Guthrie

Westinghouse Electric Corp., P. O. Box 158, Madison, Pa. 15663

- 267. Robert Markley
- 268. W. C. Ritz